博士論文

Agarwood leaf methanolic extract as corrosion inhibitor of mild steel in HCl solution

(塩酸水溶液中の軟鉄腐食に対する反応抑制材としての沈香葉メタノール抽出物)

長岡技術科学大学大学院工学研究科
エネルギー・環境工学専攻

HELEN LEE YUN SIN

Acknowledgements

This thesis is first and most importantly dedicated to God for empowering me and granting me with His Grace through this journey of completing this doctoral thesis. Without His Will, all efforts would have been futile.

To Prof. Umeda who is also my supervisor. This thesis would have been impossible without his guidance, patience and support. To Assoc. Prof. Shironita, the journey through the completion of this thesis has been smoother with her help and advice. Also to Prof. Uchida, Prof. Sato, Prof. Saito, and Prof. Imakubo as my examiners who gave very thoughtful inputs through the defence of this thesis.

Also not to be forgotten is my supervisor from Universiti Sains Malaysia (USM), Prof. Afidah. To her I am forever grateful for her reassurance, guidance and for introducing me to this Double Degree Program. To my co-supervisor Prof. Bahruddin for the useful input and help especially concerning the analytical chemistry.

To my family, especially my parents who had provided me with the much needed moral support, for being understanding of my needs and for the prayers.

I am also thankful to the assistance of the other staffs from NUT and USM, especially Dr. Hazwan, Prof. Jain and Mr. Ali for their friendliness and help whenever I would need.

Last but never the least, I am also grateful to the members of the laboratory for all the fun we had, the friendship and the extra hand needed.

Helen Lee Yun Sin

Table of Content

Preface

Corrosion is a serious problem faced that cost many industries billions of dollars. Corrosion inhibitors were thus developed to overcome the corrosion problem. The leaf extract of an agarwood producing tree (*Aquilaria malaccensis*) was obtained and studied as corrosion inhibitors for mild steel in HCl solution. The chemical content of the extract was studied using a Quadruple time-of-flight liquid chromatography mass spectrometer (Q-TOF LC/MS) and Fourier transform infra-red spectrometer. Adenosine was discovered to be one of the compounds existing in the extract. The anti-corrosion behaviors of the leaf extract and adenosine were studied using the weight loss method, electrochemical impedance spectroscopy (EIS) and potentiodynamic polarization measurement and both the extract and adenosine were found to be excellent corrosion inhibitors for mild steel in HCl solution. Adenosine was also studied using the Electrochemical quartz crystal microbalance (EQCM) measurement and the corrosion inhibition mechanism of adenosine was discussed.

In **chapter 1**, the overview of the corrosion process and the problems were shown and the usage of corrosion inhibitors was introduced. Mild steel and the agarwood leaf sample used were also introduced. Along with these, the anti-corrosion, chemical analyses and surface morphology analyses was also included in this chapter. Finally, the purpose of the thesis was shown.

In **chapter 2**, the experimental methods such as the weight loss study, the electrochemical studies used for this study were elaborated.

In **chapter 3**, the anti-corrosion behavior of the *Aquilaria malaccensis* leaf extract was studied using the weight loss measurement, EIS and potentiodynamic polarization

method. The leaf extract was found to inhibit corrosion up to over 90 % at the concentration of 1500 ppm. The data obtained from the anti-corrosion analysis was fitted into the Langmuir adsorption isotherm model and the leaf was found to adsorb by a mix-type mechanism.

In **chapter 4**, the leaf extract content analysis was shown. From the Q-TOF LC/ MS study, there were five compounds discovered including adenosine. The FTIR study revealed that the extract had desirable functional groups that could possibly contribute to the good corrosion inhibition activity of the leaf extract.

In **chapter 5**, the anti-corrosion behavior of adenosine was studied using the weight loss method and then the stagnant and hydrodynamic electrochemical methods. It was found that adenosine was an excellent inhibitor with over 70 % inhibition efficiency at the concentration of 1 mmol dm^{-3} in stagnant condition. Adenosine inhibited corrosion less efficiently in the hydrodynamic solution. The data obtained from the anti-corrosion analysis were fitted into the Langmuir adsorption isotherm model and adenosine was found to adsorb by the mixed-type adsorption mechanism.

In **chapter 6**, the surface morphology of the corrosion of mild steel immersed in the HCl solution with and without the extract or adenosine was shown using the laser scanning microscope (LSM). The presence of the extract or adenosine improved the surface as it was smoother than the mild steel immersed without the inhibitors. Quantum chemical study was performed for adenosine in an attempt to explain the adsorption of the adenosine on the surface of the mild steel for the anti-corrosion activity. The EQCM study was also shown to support the proposed mechanism of the adsorption of adenosine on the surface of the mild steel.

In **chapter 7**, the thesis was concluded.

1. INTRODUCTION

1.1. Iron and mild steel

Iron is a largely used base material for constructions and automobiles due to its malleability and strength, thus making it a very versatile material. However, the problem faced by pure iron is corrosion, as pure iron is highly unstable and it has a tendency to oxidize to a more stable form such as iron oxides, sulfides, silicates, carbonates or metal ores. This tendency to form a more stable compound is a natural formation and the extraction of pure iron from their ores requires high energy of around 1773 K for temperature.

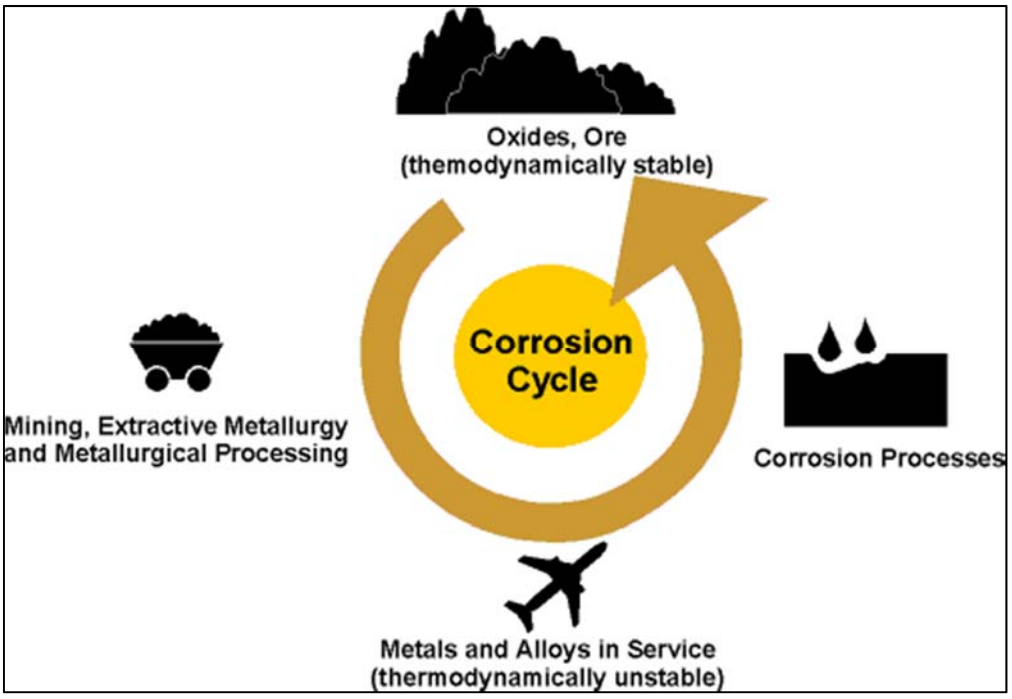

Figure 1.1. The corrosion cycle of metals [1].

To overcome the tendency of the extracted iron to revert into that of the ore, the iron can be mixed with a small percentage of non-iron elements to make it more stable than the extracted iron. This process is called alloying (Figure 1.1).

There are many types of alloys produced from iron and one of it is mild steel. Mild steels are iron alloys with an addition of a very low percentage of carbon element (0.05 to 0.25 %), and as such, retains much of its flexibility, as higher carbon contents could increase the hardness of the iron alloys. Mild steels have densities of approximately 7.85 g cm^{-3} and Young's modulus of about 200 GPa.

Among the applications of mild steels are everyday objects such as motorcycle frames, automobile chassis and cookware.

Mild steels are useful materials for the construction due to their high flexibility and compressive strength. It is also lighter, more durable and ductile. Due to the high flexibility (low brittleness), mild steels are easier to shape and weld for structural forms compared to other high carbon steels which can break. The composition of mild steel allows for electrical currents to travel through it without damaging the makeup of the material. Additionally, it is also a low cost material. However, mild steels are vulnerable to corrosion in an acidic environment, and as such, corrosion protection methods should be applied to retard the corrosion activity of mild steels exposed to acidic media and to prolong the lifetime of the mild steel.

1.2.Corrosion

Corrosion of metal is a natural phenomenon which is a gradual attack on the metal, usually as a result of chemical or electrochemical interactions between the metal and the

environment. It is not to be confused with deterioration caused by physical causes as that would be described as erosion, galling or wear. It is a reaction that causes metals to revert to their original form. This inevitable phenomenon works to a disadvantage to many industries and causes negative impacts. There are three main motivations on the current researches into corrosion which are [2]:

- **Economy**

  This is a primary motive for many current researches into corrosion as the interest of industries is to maximise profit. The study of corrosion can reduce direct losses and indirect losses due to the problems of corrosion. Examples of direct losses are costs of replacing corroded structures and machineries, and also the labor needed for the replacement of the structures and machineries. Indirect loses are such as the profit lost due to the shutdown of the machinery during the replacement process, loss of products from leaking (corroded) pipelines, contamination of products due to corrosion, loss of efficiency of the machinery.

- **Safety**

  As corrosion can affect the quality of the structure of iron and steel, a corroded steel or iron structure is weakened and can be dangerous. Safety is a prime consideration for the designing of equipment.

- **Conservation**

  The world's supply of iron and steel is limited therefore the effort to conserve iron and steel is important to avoid wastage. Conservation is also important in other related aspects such as water, energy and human effort into the production and fabrication for the iron and steel structures and machineries. Table 1.1 shows the

estimated supply of each metal left in year 1975 and 1995. Although the figures provided were estimations and the figures could change with new discoveries of suitable mining sites, it is hard to deny the fact that the supplies will continuously deplete as the demand for the raw materials increase especially with the advancement of technology.

Also, an additional factor to consider is the impact of environmental pollution onto other metal works such as national landmarks, works of art and historical artefacts. With the increase in the pollution incidents, there is a critical concern to conserve structures from the effects of pollution, such as exposure to the acid rain which can corrode the mentioned structures in a long run.

Table 1.1. 1975 and 1995 estimates of the global conserve of various metals [3].

	1975 Estimate of years of supply [4]	**1995 Estimate years of supply [5]**
Aluminium	185	162
Iron	110	77
Nickel	100	43
Molybdenum	90	-
Chromium	64	-
Copper	45	22
Zinc	23	16

1.3. Acid as a corrosive medium

Due to the extensive usage of iron and steels such as in the oil and gas exploration industry, acid is used for industrial processes such as acid cleaning, pickling, descaling, drilling, and this exposes the iron and steels to the corrosive acid environment.

Among many acids used, hydrochloric acid (HCl) is among acids that are highly corrosive towards iron and steel. It is corrosive towards iron and steels even when used in small concentrations. This could be problematic given that iron and steels (including mild steels) are extensively used for many important purposes, including structural and construction. The prolonged exposure of irons and steels to acidic environment is bound to weaken the structure and quality of the iron and steels and might even cause danger in situations when it collapses or breaks, especially if it is poorly maintained or not regularly replaced.

1.4. Corrosion as an electrochemical reaction

As corrosion is an electrochemical process, the processes of corrosion can be described by half-cell reactions. Half-cell reactions are the equations, usually involving electron on either side of the equation which when combined with other suitable half-cell reactions would describe a complete reaction taking place. For the purpose of this thesis, the half-cell reaction of a mild steel in HCl solution will be described.

1.4.1. Anodic reaction

The main anodic reaction of steel in acidic solution can be summarized as the metal dissolution:

$$Fe(s) \longrightarrow Fe^{2+}(aq) + 2e^{-} \quad (1)$$

A typical anodic reaction involves the oxidation process and in the corrosion process of a mild steel (main component is Fe) in acidic solution, Fe oxidizes into Fe^{2+} ions and dissolves into the solution. This can be observed as the mild steel increasingly becomes thinner when exposed to acidic solution in a long period.

1.4.2. Cathodic reaction

The main cathodic reaction of steel in acidic solution can be summarized as the hydrogen evolution:

$$2H^{+}(aq) + 2e^{-} \longrightarrow H_2(g) \quad (2)$$

A typical cathodic reaction involves the reduction process and in the corrosion process of a mild steel in acidic solution, H^{+} in the solution reduces to become H_2 gas which eventually escapes from the solution. This can be observed as bubbles on the surface of the mild steel that is in contact with the acidic solution.

1.4.3. Coupled electrochemical reactions

On a surface of mild steel exposed to the HCl solution without any influence of electric, the surface of mild steel experiences both the anodic and cathodic reaction simultaneously and freely. At certain sites, the anodic reaction occurs, Fe is oxidized to Fe^{2+} and passes the electron to other sites where the cathodic reaction occurs, hydrogen gas is formed (Figure 1.2). The reason that the same surface of mild steel can have both reactions happening is due to the inhomogeneous nature of the surface from impure atoms (other

additional elements in the mild steel such as carbon), adsorbed ions from the solution, missing atom from the surface of the mild steel, grain boundaries and other shape differences on the surface of mild steel.

The coupled electrochemical reaction can thus be summarized as the following equation:

$$Fe(s) + 2H^{+}(aq) \longrightarrow Fe^{2+}(aq) + H_2(g) \quad (3)$$

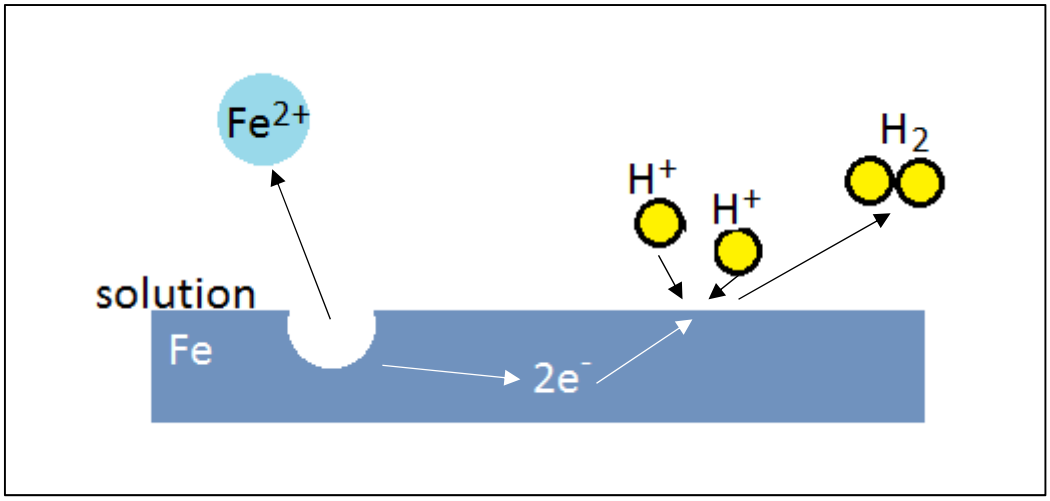

Figure 1.2. Coupled electrochemical reaction taking place for Fe in acidic solution.

1.5. Corrosion inhibitors

Research are thus geared towards methods of retarding the corrosion process in the hope of protecting the metal or to the least, prolonging the lifetime of the metal. Modern corrosion science has since begun from the 20th century using the local cell model proposed by Evans and the corrosion potential model proposed by Wagner and Traud. The two models are then joined to describe corrosion as a coupled electrochemical reaction consisting of anodic metal oxidation and cathodic oxidant reduction [6].

Currently, there are many ways to counter the corrosion problem. The methods of corrosion prevention can basically be put as [7, 8]:

- **Materials selection and design**
- **Protective coatings**
- **Cathodic and anodic protection**
- **Corrosion inhibition**

Among all other methods of corrosion control and prevention, corrosion inhibitors are popular due to the ease in application and the advantage of *in-situ* application without disruption of the process [9], aside from being cost effective. Recent studies estimate that the United States' demand for corrosion will increase to USD 25 billion in 2017. In 2012, the estimated market demand for inhibitors were 26.6 % to refining petroleum, 16.9 % utilities, 16,7 % gas and oil production, 15.3 % chemical, 9.5 % metals, 7.1 % pulp and paper, 8.0 & others (as cited from Dariva and Galio, adapted from www.pfonline.com/news/us-demand-for-corrosion-inhibitors-to-reach-25-billion-in-2017) [10]. Corrosion inhibitors are substances which when added in small concentrations to the corrosive media will decrease or prevent the reaction of the metal with the media. The primary *modus operandi* of organic corrosion inhibitors is the adsorption of some kind onto the surface of the metals thus preventing the interaction of the corrosive medium [11-13] as adapted by [10]:

- The inhibitor adsorbs onto the surface to form a protective thin film or by combination between inhibitor ions and the surface of metal.
- The inhibitor forms a film by oxide protection of the metal.
- The inhibitor forms a complex with the corrosive component.

Thus, the ability of the inhibitor's molecules to adsorb onto the surface of the metal plays the key role. It has been known that organic molecules containing nitrogen, sulphur or oxygen atoms can adsorb at the metal-solution interface and thus inhibits the corrosion of the metal [14, 15].

1.6. Natural corrosion inhibitors

The development of corrosion inhibitors were thus focused on synthesizing inhibitors containing the desired functional groups with good adsorption properties. Though many synthetic corrosion inhibitors showed good anti-corrosion activity, the issue lies in the toxicity of the said inhibitors towards humans and the environment. Many of these synthetic inhibitors can cause damage, either reversible or irreversible, to the organ system during the process of synthesizing the inhibitors or application [16]. Thus the current trend is to develop corrosion inhibitors that are safe, cost effective, easily available, environmental-friendly and effective in preventing corrosion. This being so, there have been extensive researches that are dedicated to the development of corrosion inhibitors that are more environmentally friendly. The term 'green corrosion inhibitors' becomes a popular term to refer to corrosion inhibitors that are environmentally friendly and/or derived from plant extracts [17]. Table 1.3 lists some examples of corrosion inhibitors that has been studied and reported as green corrosion inhibitors in HCl as a corrosive medium.

From the pursuit of discovering more green corrosion inhibitors, many of the inhibitors were naturally derived, especially from waste materials of the plant parts. The development of corrosion inhibitors from waste materials is sustainable as the wastes are being reused instead of being discarded. The waste materials such as fruit peels, seeds

and hulls has high antioxidant properties and are rich in phytochemicals that are useful as corrosion inhibitors. Examples of plant waste materials that has shown to have good corrosion inhibition properties are argan hulls extract, fruit peels extracts, garlic peel extract, guava seed extract and coconut coir dust extract [18-22].

In general, the said plants extracts contributed to corrosion inhibition due to the presence of many compounds in the extracts that worked synergistically to produce a corrosion retardation effect [23-27]. Mostly, the corrosion inhibition effect was believed to be actively contributed by the compounds that belong to the phytochemical groups which are also good antioxidants such as alkaloids, flavonoids, and tannins [28]. Extensive studies on known molecules have been done and it was discovered that inhibitor molecules with the presence of bond-forming, electron-rich groups/atoms are known to be responsible for the corrosion inhibition properties [29-32]. The widely accepted explanation of corrosion inhibition by these plant extracts is the adsorption of the inhibitors' molecules on the surface of a metal forming a barrier between the metal and corrosive substance, thus preventing corrosion [33-37].

Table 1.3. List of several studied green corrosion inhibitors with HCl as corrosive medium [38].

Green corrosion inhibitor	Type of inhibitor	Type of corrosive medium	Type of metal	Maximum inhibition efficiency	Adsorption mechanism
Crude methanolic extract of	Mixed	HCl (1.0 M)	Mild Steel	96	Adsorption due to Fe-inhibitor complex at iron oxide layer
Artemisia pallens (Asteraceae)	-	-	-	-	-
Bark of Ochrosia oppositifolia (OOB)	Mixed	HCl (1.0 M)	Mild Steel	96	Adsorption due to the formation of protective
	-	-	-	-	layer of corrosion inhibitor
2-((5-mercapto-1,3,4-thiadiazol-2-ylimino) methyl) phenol	Cathodic	HCl (0.5 M)	Mild Steel	97	Chemisorption
	-	-	-	-	-
(NE)-N-(thiophen-3-ylmethylidene	Mixed	HCl (1.0 M)	Mil Steel	88.9	Chemisorption
	-	-	-	-	-
Osmanthus fragran leaves extract (OFLE)	Mixed	HCl (1.0 M)	Carbon Steel	96.8	Physical Adsorption
Bis-Schiff bases of isatin	Mixed	HCl (1.0 M)	Mil Steel	-	Physical/Chemical Adsorption
Pyridine derivate	Mixed	HCl (1.0 M)	Mil Steel	-	Physisorption/Chemisorption
Pyridine-2-thiol (P2T)	-	-	-	98.3	-
2-Pyridyl disulfide (2PD)	-	-	-	98.1	-
Alkaloid extracts	Mixed	HCl (1.0 M)	Mil Steel	95.3	Adsorption of extract and aniline onto the
Aniba roosa eodora plant	-	-	-	-	steel surface blocking its active sites
Murraya koenigii leaves extract	Mixed	HCl (1.0 M)	Mil Steel	97.02	Adsorption of inhibitor molecules
					due to protonation of amino group
Sulfa drugs compounds	Cathodic	-	-	-	Adsorption of sulfa compounds on solid substrate
(sulfaguanidine, sulfamethazine, sulfamethoxazole and sulfadiazine)		HCl (1.0 M)	Mil Steel	66.3-94.9	-
fast green dyes	Cathodic	HCl (0.5 M)	Mil Steel	98	Adsorption of large and flat inhibitor molecules by blocking
	-	-	-	-	the surface area of mild steel and adsorbed electrostatically
Bamboo leaf extract	Mixed	HCl (1.0 M)	Cold Rolled Steel (CRS)	90.3	Adsorption id due to both physisorption and chemisorption
Olive leaves extract (Olea europaea)	Mixed	HCl (2.0 M)	Carbon Steel		Strong physical adsorption of olive leaf extracts
		-	-		components onto the steel surface
(mango, orange, passion, cashew) peel	-	HCl (1.0 M)	Carbon Steel	80-95	Extracts in organic compounds adsorbed
		-	-		at the electrode active sites
Black pepper extract	-	HCl (1.0 M)	C38 Steel	95.8	Chemisorption at solid surface
Ananas sativum leaves extract	-	HCl (1.0 M)	Aluminum	96.09	Chemisorption of phytochemical constituents of the extract
		-	-	-	on the metal surface by blocking active sites
Pactin terrestrial plants	-	HCl (2.0 M)	Aluminum	91	Physisorption
Vernonia amygdalina (bitter leaf extract)	-	HCl (0.1 M)	2S Al Alloy	38.4- 49.5	chemisorption
Triazole derivatives	Cathodic	HCl (0.5 M)	Copper	-	Adsorption of Triazole derivatives on electrode surface
4-amino-4H-1,2,4-triazole-3thiol (ATT)		-	-	98.44	involve Physisorption and Chemisorption
4-amino-5-methyl-4H-1,2,4-triazole-3thiol (AMTT)		-	-	99.1	-
4-amino-5-methyl-4H-1,2,4-triazole-3thiol (AMTT)		-	-	99.06	-
Aloe vera extract	-	HCl (2.0 M)	Zinc	67	The adsorption of organic compounds in the extract
					on zinc surface to the attack of aggressive ions

1.7.Agarwood trees

Agarwood is also known as karas, gaharu, oud, agar, eaglewood and aloeswood. Agarwood is a resin-containing heartwood produced by Aquilaria and Gynops trees.

Examples of Aquilaria species that produces agarwood includes *Aquilaria malaccensis, Aquilaria subintegra, Aquilaria sinensis, Aquilaria rostrata* and *Aquilaria filarial.* Currently, it is commercially planted for harvesting the resin which can be processed to obtain the agarwood essential oil. The pure agarwood essential oil has a high value of up to 30 thousand US dollars per kilogram in year 1999 [39].

The high price of the agarwood essential oil could be due to its chemical content which can be difficult to synthesize and mimic to produce the distinguished fragrance. The extraction process of agarwood oil (Figure 1.3) yields a rather limited one L for every 100 to 150 kg agarwood [40]. Also, the growth of agarwood is not a process that naturally occurs on every agarwood tree, making it rarer. The growth of agarwood resin is usually caused by injury (from animals) or infections to the woody parts such as the trunk, roots and branches. Thus, the growth of agarwood is due to a self-defense mechanism. Farmed trees undergo inoculation processes to induce the tree to develop agarwood (Figure 1.4.). Inoculation methods include chemical methods, i.e.: chemical suspension, and physical methods, i.e.: nailing the tree with iron, bamboo sticks and scrapping off the bark. Such methods could create stress to the trees and thus induce the production of agarwood.

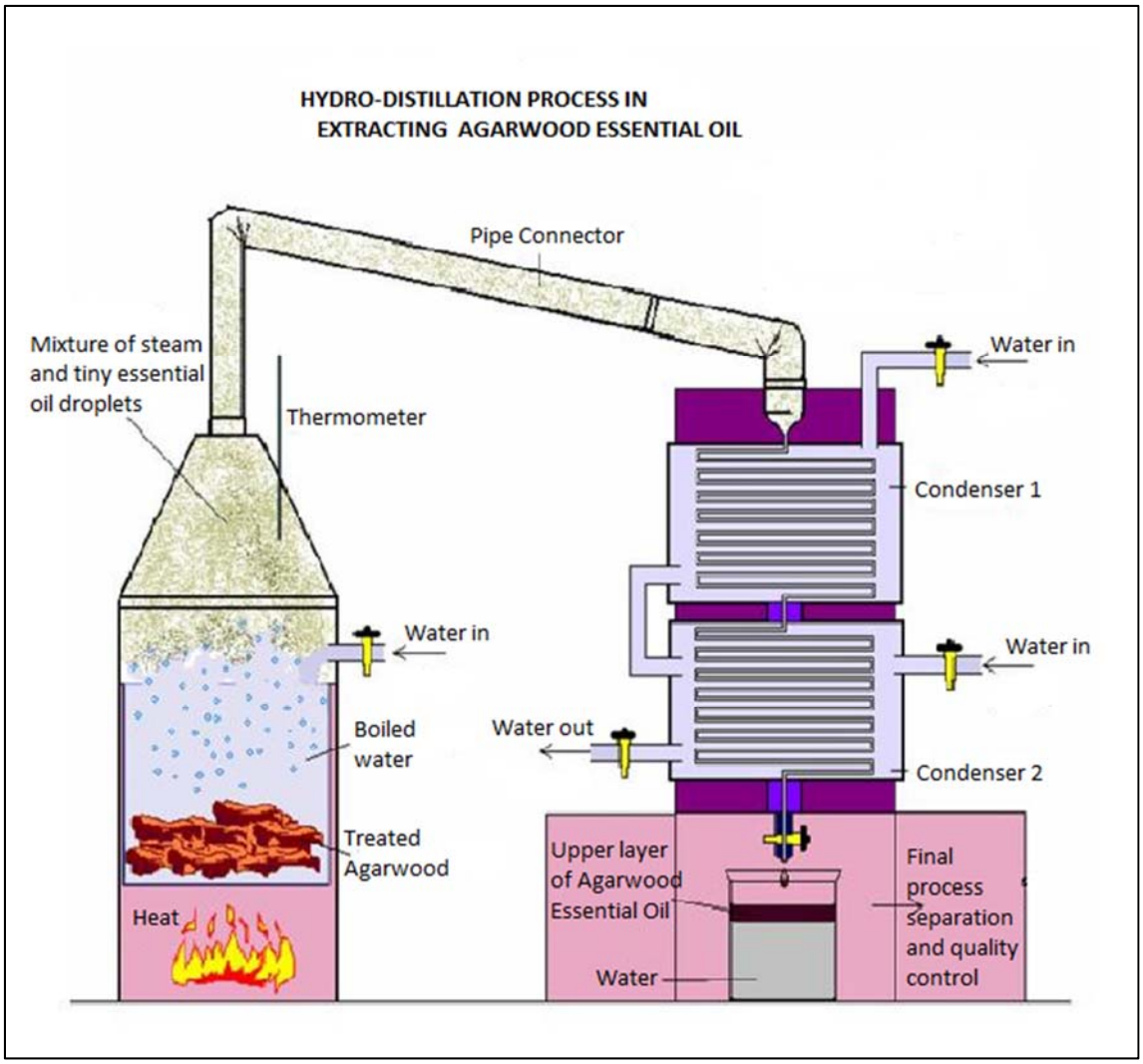

Figure 1.3. Agarwood distillation process to obtain the essential oil (Hafizmuar at English Wikipedia /CC-BY-SA-3.0).

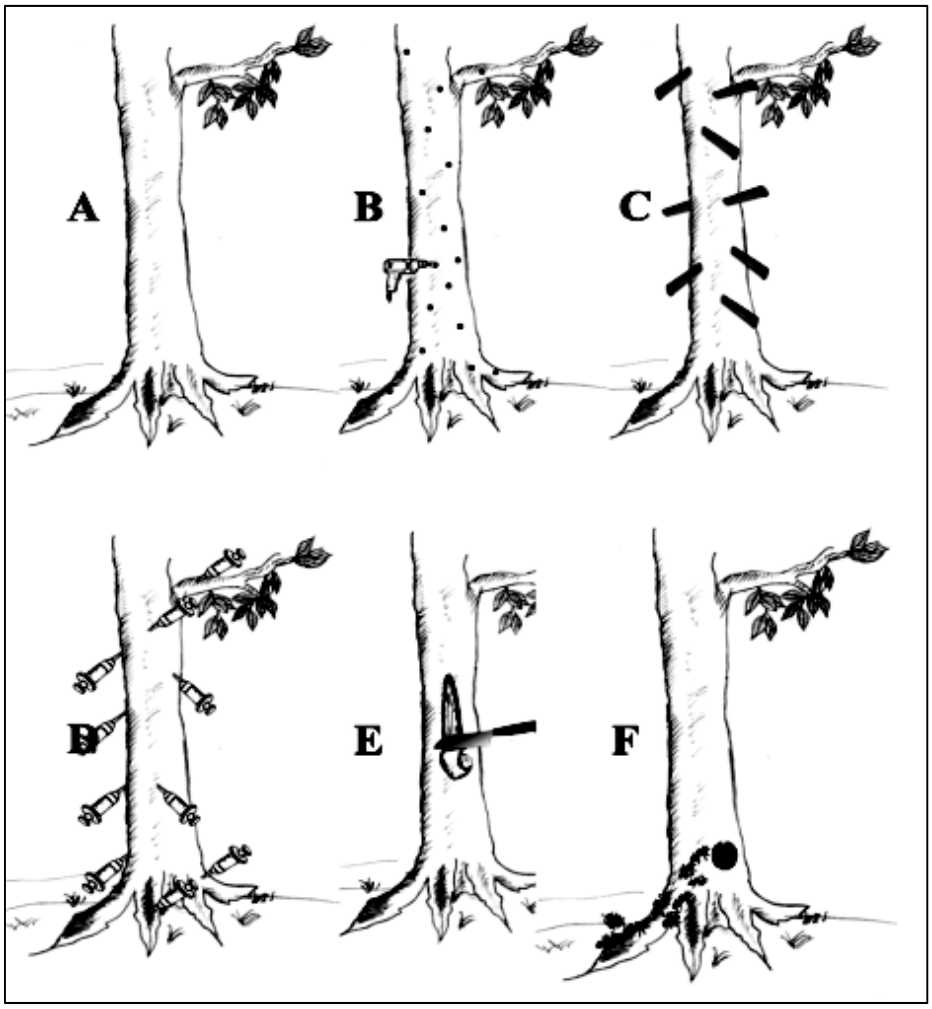

Figure 1.4. Illustration of induction methods commonly used in agarwood formation: (A) no induction/injury made for natural maturation process, (B) drilling the stems, roots and large branches, (C) Installation of foreign objects (metal, PVC) into pores, (D) inserting syringes, (E) peeling off the barks and (F) digging a hole to facilitate hatching of ants and snails in the tree [41].

While the resin and also wood segments are valued, the leaves are relatively of no value and are usually discarded as waste after the extraction of the resin-containing parts. To a small extent, the leaves have been processed and marketed as 'health teas' in Taiwan and in Southeast Asia. The leaves are also used as a sedative, analgesic and as a digestive ailment in traditional medicine [42]. The leaves has been researched on for laxative

properties, antihyperglycemic activity, anti-bacterial and anti-inflammatory properties [43-46]. The agarwood leaves also reported good antioxidant activity and the presence of polyphenols and other phenolic compounds [47-50].

1.8. *Aquilaria malaccensis*

Aquilaria malaccensis (Latin word for "from Malacca", a place in Malaysia) (Figure 1.5) is from the Thymelaeaceae family and it is a type of agarwood producing tree. The tree is a large evergreen tree growing over 15 to 30 m tall and 1.5 to 2.4 m in diameter with white flowers [51].

The leaves are described to grow alternately with a petiole of 4-6 mm long, shiny on both sides curving upwards to the margin with veins of 12 to 16 pairs, of elliptical oblong to oblong lanceolate shape of the size 7.5 to 12 × 2.5 to 5.5 cm [52].

Aquilaria malaccensis trees are widely distributed in south and south-east Asia. It is found in Bangladesh, Bhutan, Iran, Indonesia, Malaysia, Myanmar, Philippines, Singapore and Thailand [10]. Aquilaria species has adapted to live in various habitats including areas that are rocky, sandy, well-drained slopes and ridges and land near swamps. They typically grow in locations with average daily temperatures of 293 to 295 K [53-55].

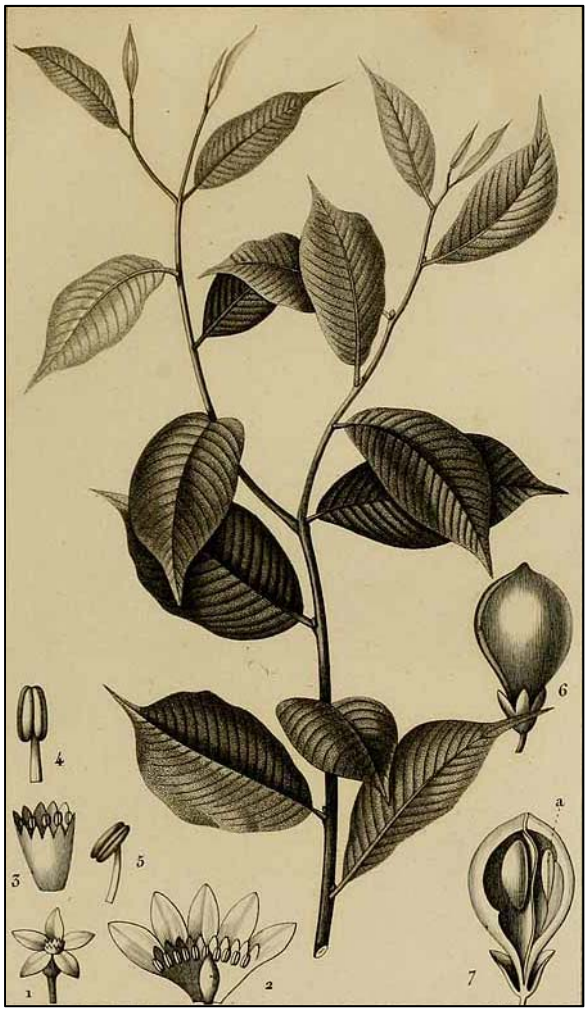

Figure 1.5. *Agarwood malaccensis* illustration by P.J. F. Turpin [56].

Considering the fact that there are tens of thousands of Aquilaria trees harvested annually (as of reported by Soehartono et al. in 2002) for the production of agarwood oil [57], the supply for the leaves would be large too as most of the leaves were thrown away and not used for the agarwood oil extraction. Thus, there would be supplies for the raw material for the production of agarwood leaves as corrosion inhibitors for market. Aside from the advantage of using plant materials as a form of a more environmentally safe corrosion

inhibitor, the idea of developing good corrosion inhibitors from waste materials is also more sustainable.

The extract was obtained from the leaf (Figure 1.6) and it was applied as a corrosion inhibitor of mild steel in acidic medium. Investigations of corrosion inhibition potential of the agarwood leaf extract has shown promising results of the anticorrosion properties with inhibition efficiency of over 90 % at 1500 ppm. The corrosion inhibition properties of the extract can be attributed to the anti-oxidant properties of the leaf, along with the presence of phenolic compounds that possibly have good adsorption properties.

Figure 1.6. Agarwood leaves used for the experiments.

1.9. *Aquilaria malaccensis* leaf extract as corrosion inhibitor of mild steel in HCl

The efficiency of *Aquilaria malaccensis* leaf extract as an inhibitor of the corrosion process can be evaluated by several methods. The methods are briefly introduced as following:

- **Weight loss method**

The weight loss method is a simple and reliable method that determines the corrosion inhibition efficiency of the inhibitor by comparing the rate of mass loss of the specimen due to corrosion for the blank solution and the solution with inhibitor. Lower mass loss would indicate better corrosion inhibition.

- **Electrochemical impedance spectroscopy (EIS) analysis**

The EIS analysis is a type of electrochemical method that determines the corrosion inhibition efficiency by measuring the resistance of the cell (with the specimen as a working electrode) in the solution of with and without the inhibitor. Higher resistance for charge transfer would indicate better corrosion inhibition.

- **Potentiodynamic polarization measurement**

The potentiodynamic polarization measurement is also an electrochemical method to determine the corrosion inhibition efficiency. This measurement measures the current density of the cell (with the specimen as a working electrode) in the solution of with and without inhibitor. Lower current density would indicate better corrosion inhibition.

- **EIS analysis with hydrodynamic condition**

The EIS analysis can be conducted with a cell with a controlled flow of solution (hydrodynamic condition) to test for the corrosion inhibition activity in the presence of flowing condition.

- **Adsorption studies**

The adsorption studies are conducted to understand the mechanism of the adsorption of the inhibitor molecules onto the surface of the specimen.

- **Quantum chemical studies**

The mechanism of adsorption would be further supported by the quantum chemical studies.

1.10. Purpose of thesis

Thus, this thesis is prepared to fulfill several purposes:

- To obtain extract from the leaf of *Aquilaria malaccensis* and to determine the corrosion inhibition activity of the extract.
- To conduct chemical analysis and to identify the compounds present in the agarwood leaf extract.
- To study the corrosion inhibition mechanism of the best identified compound (adenosine).
- To discuss on the adsorption of the extracts and the identified compound (adenosine) by using the data obtained from the corrosion inhibition studies and to possibly relate the inhibition efficiency of the extract and the identified compound (adenosine) to the chemical analysis data.

References

[1] M. G. Fontana, Corrosion engineering, Tata McGraw-Hill Education, 2005.

[2] H. H. Uhlig, R. W. Revie, Corrosion and Corrosion Control Second Edition, John Wiley and Sons, Inc., United States of America, 1985.

[3] E. McCafferty, Introduction to corrosion science, Springer Science & Business Media, 2010.

[4] S. Mufson, Washington Post, Washington, DC, (2006).

[5] Fairfax J., (1991) A5.

[6] N. Sato, Basics of Corrosion Chemistry, in: Green Corrosion Chemistry and Engineering, Wiley-VCH Verlag GmbH & Co. KGaA, 2011, pp. 1-32.

[7] M. Fontana, N. Greene, in, McGraw-Hill, 1986.

[8] K. A. Chandler, D. A. Bayliss, (1985).

[9] G. H. Koch, M. P. Brongers, N. Thomson, Y. Virmanio, J. H. Payer, M. Kutz, Handbook of environmental degradation of materials, (2005) 3-24.

[10] C. G. Dariva, A. F. Galio, Developments in Corrosion Protection, InTech, (2014).

[11] V. GENTIL, LTC: Rio de Janeiro, (2003).

[12] H. Ju, Z.-P. Kai, Y. Li, Corrosion Science, 50 (2008) 865-871.

[13] L. V. Ramanathan, in: Corrosão e seu controle, São Paulo: Hemus, 1988.

[14] I. A. Aiad, A. Hafiz, M. El-Awady, A. Habib, Journal of surfactants and detergents, 13 (2010) 247-254.

[15] B.-Y. Liu, Z. Liu, G.-C. Han, Y.-H. Li, Thin Solid Films, 519 (2011) 7836-7844.

[16] P. B. Raja, M. G. Sethuraman, Materials Letters, 62 (2008) 113-116.

[17] D. Kesavan, M. Gopiraman, N. Sulochana, Chem. Sci. Rev. Lett, 1 (2012) 1-8.

[18] L. Afia, R. Salghi, E. H. Bazzi, A. Zarrouk, B. Hammouti, M. Bouri, H. Zarrouk, L. Bazzi, L. Bammou, Research on Chemical Intermediates, 38 (2012) 1707-1717.

[19] J. C. da Rocha, J. A. d. C. P. Gomes, E. D'Elia, Corrosion Science, 52 (2010) 2341-2348.

[20] S. S. de Assunção Araújo Pereira, M. M. Pêgas, T. L. Fernández, M. Magalhães, T. G. Schöntag, D. C. Lago, L. F. de Senna, E. D'Elia, Corrosion Science, 65 (2012) 360-366.

[21] K. P. V. Kumar, M. S. N. Pillai, G. R. Thusnavis, Journal of Materials Science & Technology, 27 (2011) 1143-1149.

[22] S. Umoren, U. Eduok, A. Israel, I. Obot, M. Solomon, Green Chemistry Letters and Reviews, 5 (2012) 303-313.

[23] A. S. Yaro, A. A. Khadom, R. K. Wael, Alexandria Engineering Journal, 52 (2013) 129-135.

[24] A. Bouyanzer, B. Hammouti, L. Majidi, Materials Letters, 60 (2006) 2840-2843.

[25] N. Odewunmi, S. Umoren, Z. Gasem, Journal of Industrial and Engineering Chemistry, 21 (2015) 239-247.

[26] M. Deyab, Journal of Industrial and Engineering Chemistry, 22 (2015) 384-389.

[27] G. O. Avwiri, F. Igho, Materials Letters, 57 (2003) 3705-3711.

[28] N. M'hiri, D. Veys-Renaux, E. Rocca, I. Ioannou, N. M. Boudhrioua, M. Ghoul, Corrosion Science, 102 (2016) 55-62.

[29] S. Şafak, B. Duran, A. Yurt, G. Türkoğlu, Corrosion Science, 54 (2012) 251-259.

[30] P. Morales-Gil, G. Negrón-Silva, M. Romero-Romo, C. Ángeles-Chávez, M. Palomar-Pardavé, Electrochimica Acta, 49 (2004) 4733-4741.

[31] H. Hamani, T. Douadi, M. Al-Noaimi, S. Issaadi, D. Daoud, S. Chafaa, Corrosion Science, 88 (2014) 234-245.

[32] K. Ansari, M. Quraishi, A. Singh, Corrosion Science, 79 (2014) 5-15.

[33] V. Rajeswari, D. Kesavan, M. Gopiraman, P. Viswanathamurthi, K. Poonkuzhali, T. Palvannan, Applied Surface Science, 314 (2014) 537-545.

[34] M. Benabdellah, M. Benkaddour, B. Hammouti, M. Bendahhou, A. Aouniti, Applied Surface Science, 252 (2006) 6212-6217.

[35] A. Hamdy, N. S. El-Gendy, Egyptian Journal of Petroleum, 22 (2013) 17-25.

[36] H. Zhang, D. Wang, F. Wang, X. Jin, T. Yang, Z. Cai, J. Zhang, Desalination, 372 (2015) 57-66.

[37] M. Wahdan, A. Hermas, M. Morad, Materials Chemistry and Physics, 76 (2002) 111-118.

[38] G. Khan, K. M. S. Newaz, W. J. Basirun, H. B. M. Ali, F. L. Faraj, G. M. Khan, International Journal of Electrochemical Science, 10 (2015) 6120-6134.

[39] A. Barden, N. A. Anak, T. Mulliken, M. Song, Heart of the matter: agarwood use and trade and CITES implementation for Aquilaria malaccensis, Traffic International Cambridge, 2000.

[40] G. A. PERsOOn, (2007).

[41] S. Akter, M. T. Islam, M. Zulkefeli, S. I. Khan, International Journal of Pharmaceutical and Life Sciences, 2 (2013) 22-32.

[42] M. Kakino, S. Tazawa, H. Maruyama, K. Tsuruma, Y. Araki, M. Shimazawa, H. Hara, BMC complementary and alternative medicine, 10 (2010) 1.

[43] H. Hara, Y. Ise, N. Morimoto, M. Shimazawa, K. Ichihashi, M. Ohyama, M. Iinuma, Bioscience, biotechnology, and biochemistry, 72 (2008) 335-345.

[44] R. Pranakhon, P. Pannangpetch, C. Aromdee, Sonklanakarin Journal of Science and Technology, 33 (2011) 405.

[45] H. Rahman, K. Vakati, M. C. Eswaraiah, International Journal of Basic Medical Sciences and Pharmacy (IJBMSP), 2 (2012).

[46] S. Kamonwannasit, N. Nantapong, P. Kumkrai, P. Luecha, S. Kupittayanant, N. Chudapongse, Annals of clinical microbiology and antimicrobials, 12 (2013) 1.

[47] A. Huda, M. Munira, S. Fitrya, M. Salmah, Pharmacognosy Research, 1 (2009) 270.

[48] T. Ito, M. Kakino, S. Tazawa, T. Watarai, M. Oyama, H. Maruyama, Y. Araki, H. Hara, M. Iinuma, Journal of nutritional science and vitaminology, 58 (2012) 136-142.

[49] T. Ito, M. Kakino, S. Tazawa, M. Oyama, H. Maruyama, Y. Araki, H. Hara, M. Iinuma, Food Science and Technology Research, 18 (2012) 259-262.

[50] J. Sattayasai, J. Bantadkit, C. Aromdee, E. Lattmann, W. Airarat, Journal of Ayurveda and integrative medicine, 3 (2012) 175.

[51] A. Barden, N. A. Anak, T. Mulliken, M. Song, TRAFFIC International, Cambridge, UK, (2000).

[52] L. Oyen, N. X. Dung, Plant resources of South-East Asia, Backhuys Publ., 1999.

[53] Afifi, in: Lokakarya Pengusahaan Hasil Hutan Non Kayu (Rotan, Gaharu, dan Tanaman Obat), Department Kehutanan, Indonesia-UK Tropical Forest Management Programme, Surabaya, Indonesia, 1995.

[54] P. Kessler, K. Sidiyasa, Tropenbos series (7) Show all parts in this series, (1994).

[55] H. Wiriadinata, in: Lokakarya Pengusahaan Hasil Hutan Non Kayu (Rotan, Gaharu, dan Tanaman Obat), Departemen Kehutanan. Indonesia-UK Tropical Forest Management PRogramme, Surabaya, Indonesia, 1995.

[56] P. J. F. Turpin, in, pp. 1816-1830.

[57] T. Soehartono, A. Newton, A. Mardiastuti, Journal of Tropical Forest Science, (2002) 364-378.

2. METHODOLOGY

The following experimental was conducted to fulfill the purpose of the thesis and each introduction to the experimental methods are as follows:

2.1. Weight loss method

This is a gravimetric method and it is one of the simplest method to analyze the anti-corrosion activity of the inhibitors. The pre-corroded specimens (in this case is mild steel) are immersed in the selected medium with and without the inhibitors for a specific period of time. Then, the weight change (difference in weight before and after the immersion) of the specimens was compared. In highly acidic solutions such as 1 mol dm^{-3} HCl, the specimens immersed in corrosive medium spiked with inhibitors typically has less weight change (weight loss) compared to the specimen immersed in the corrosive medium only. The lesser weight loss indicates a successful inhibitor. The setup for the weight loss study is as shown in Figure 2.1.

Figure 2.1. Weight loss method experimental setup.

2.2. Electrochemical method

The electrochemical method allows for the analysis of the corrosion inhibition activity with the influence of electric. The data can be analyzed to understand the behavior of the corrosion inhibition of the inhibitors. There are two main electrochemical methods that will be focused on in this thesis which is the electrochemical impedance spectroscopy (EIS) and the potentiodynamic polarization. A cell for the electrochemical analysis consists of a working electrode (specimen), a reference electrode, a counter electrode, corrosive medium with/without the inhibitor and a potentiostat connected to the computer (Figure 2.2). The conditions of the electrical influence can be controlled by the computer and executed by the potentiostat. A successful corrosion inhibition by the corrosive medium containing the inhibitor will have a higher resistance (for EIS) and lower corrosion current density (for potentiodynamic polarization) than the specimen analyzed in the corrosive medium only (blank).

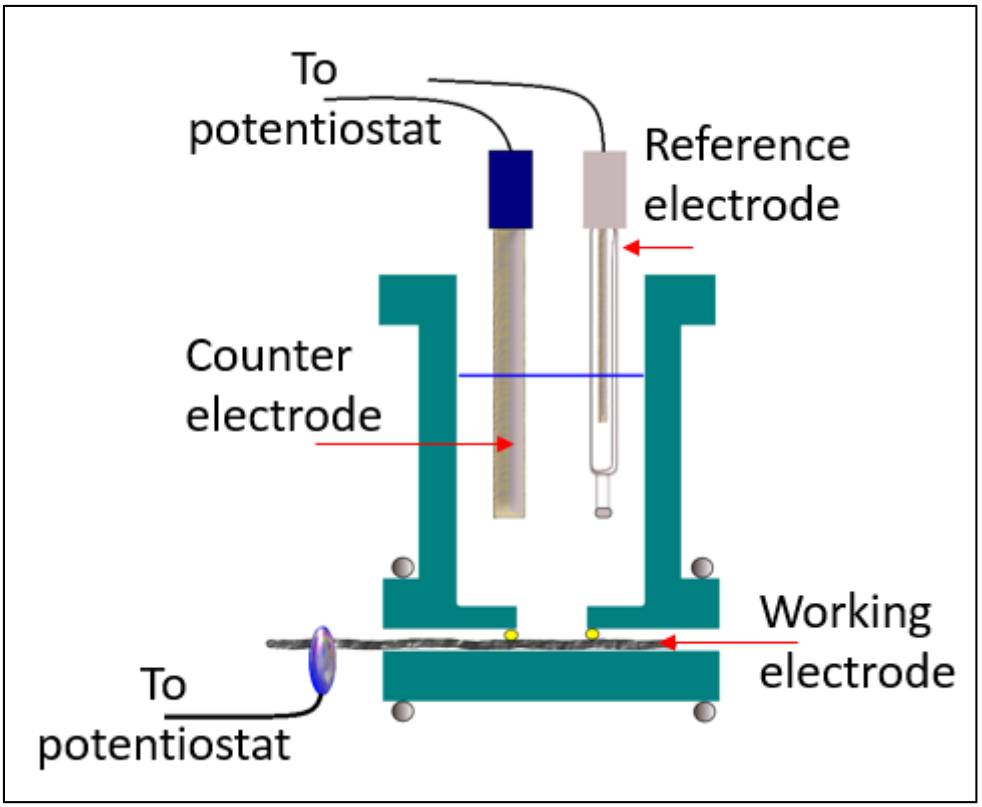

Figure 2.2. Electrochemical cell setup.

2.2.1. Electrochemical impedance spectroscopy (EIS) analysis

Dielectric spectroscopy/ AC impedance spectroscopy/ electrochemical impedance spectroscopy (EIS) is a commonly used method for the purpose of corrosion evaluations. As the name suggests, an AC impedance measurement is a determination of electrical impedance of the metal specimen to electrolyte interface at various alternating current (AC) frequencies [1]. All three components of resistance, capacitance and inductance results in the blockage of current flow:

$$E=IZ \qquad (1)$$

Where E is the potential (V), I is the current (A) and Z is the magnitude of impedance containing elements of an equivalent circuit (for example capacitor and inductor).

The impedance measurement is made of the imaginary component (resistance) and the real component (capacitance and inductance). A result of such measurement is the Bodes plot or Nyquist plot, both of which represents the same result in a different perspective: the correlation of the imaginary impedance to the real impedance (Nyquist) or the correlation of the impedance magnitude to log frequency and phase angle (Bodes). For the purpose of this thesis, the Nyquist plot (Figure 2.3.) is further elaborated.

The shape of the Nyquist plot can be fitted into equivalent circuits to further describe the mechanism of the reaction. Components such as the constant phase element (CPE), capacitor, solution resistance (R_s) and charge transfer resistance (R_{ct}) were used to build an equivalent circuit that best fits the shape of the Nyquist plot obtained from the corrosion analysis. A typical equivalent circuit used to describe many corrosion inhibition studies of mild steel in HCl is shown as Figure 2.4. From the fit of the Nyquist plot to the equivalent circuit, the values of the equivalent components were then obtained. In general, the increase in the R_{ct} indicates a successful corrosion inhibition. The CPE describes the behavior of the electric double-layer.

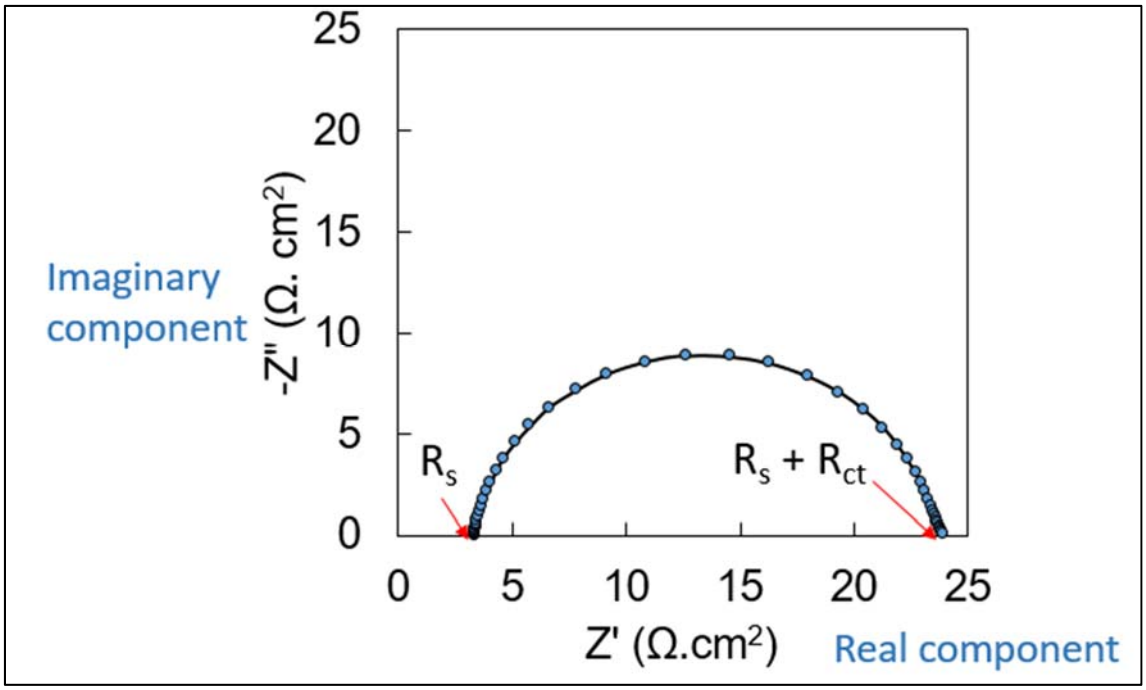

Figure 2.3. An example of a Nyquist plot.

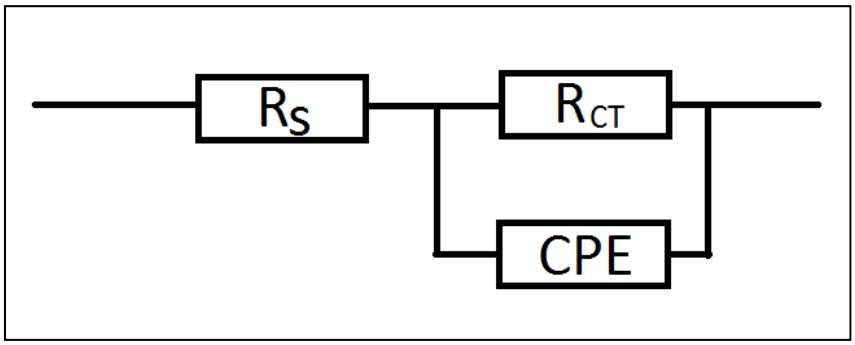

Figure 2.4. An example of an equivalent circuit (Randles type).

2.2.2. Potentiodynamic polarization measurement

The potentiodynamic polarization is another commonly applied technique for corrosion studies. As the name suggests, the techniques involves polarizing the potential to a certain

range from the corrosion potential, E_{corr}. This would provide the potential-current relationship which would then be used to calculate the corrosion rate and also to understand the behavior of the electrochemical cell at its separate anodic and cathodic reaction. The potential-log current relationship can be represented as a Tafel plot as Figure 2.5. While E_{corr} is the potential where the rate of the anodic reaction equals to that of the cathodic reaction, polarizing the cell to more negative potentials would obtain the cathodic curve, which is the potential-log current relationship of the cathodic reaction of the electrochemical cell. Likewise, polarizing the cell to more positive potentials would obtain the anodic curve, which is the potential-log current relationship of the anodic reaction of the electrochemical cell. The slopes from the cathodic and anodic curves when extrapolated and intersected with the E_{corr} would provide for another parameter: the corrosion current density (I_{corr}). In general, a decrease in the I_{corr} would indicate a successful corrosion inhibition. The shift of the E_{corr} can impart the details of the inhibitor being an anodic type inhibitor, a cathodic type inhibitor or mixed type inhibitor. In general, mild steel in a low pH medium undergoes metal dissolution for the anodic reaction while the cathodic reaction is the hydrogen gas evolution.

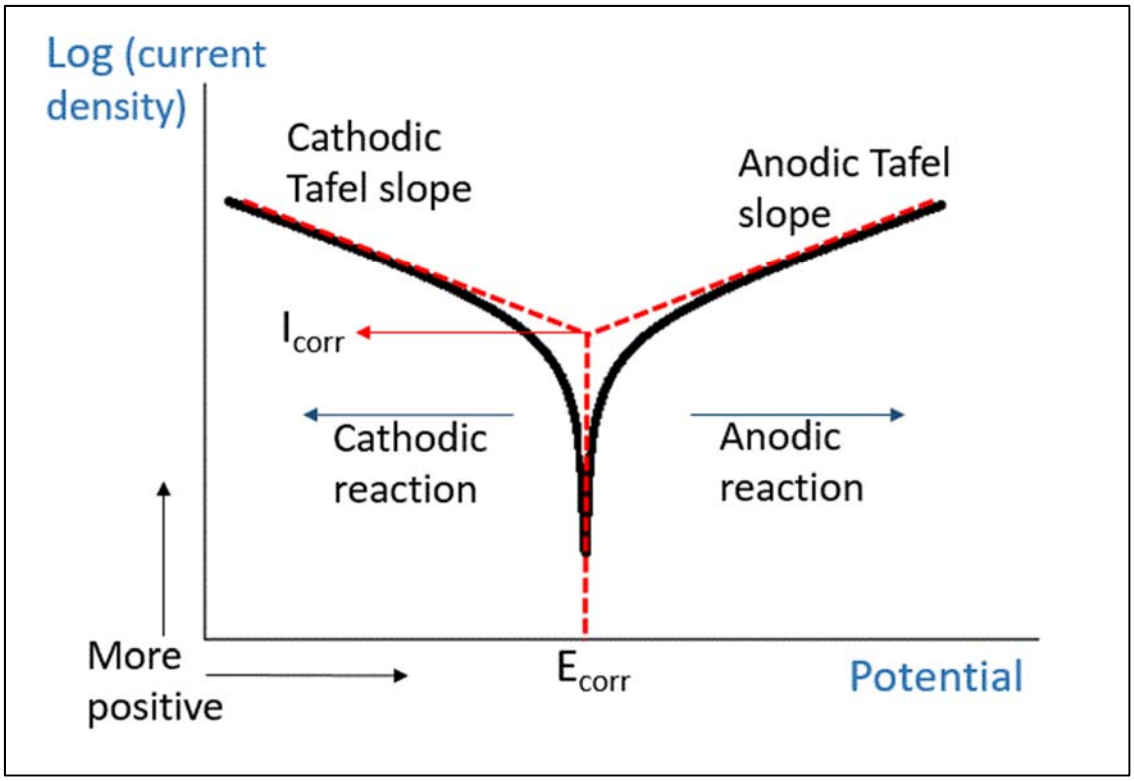

Figure 2.5. An example of a Tafel plot.

2.2.3. Hydrodynamic condition

Aside from electrochemical measurements using a beaker shaped cell (Figure 2.2) which limits the flow of the cell, the electrochemical measurements can also be conducted using the channel flow cell (Figure 2.6), which allows for measurement in the hydrodynamic condition. This will allow for the study of the corrosion inhibition behavior from a flowing cell.

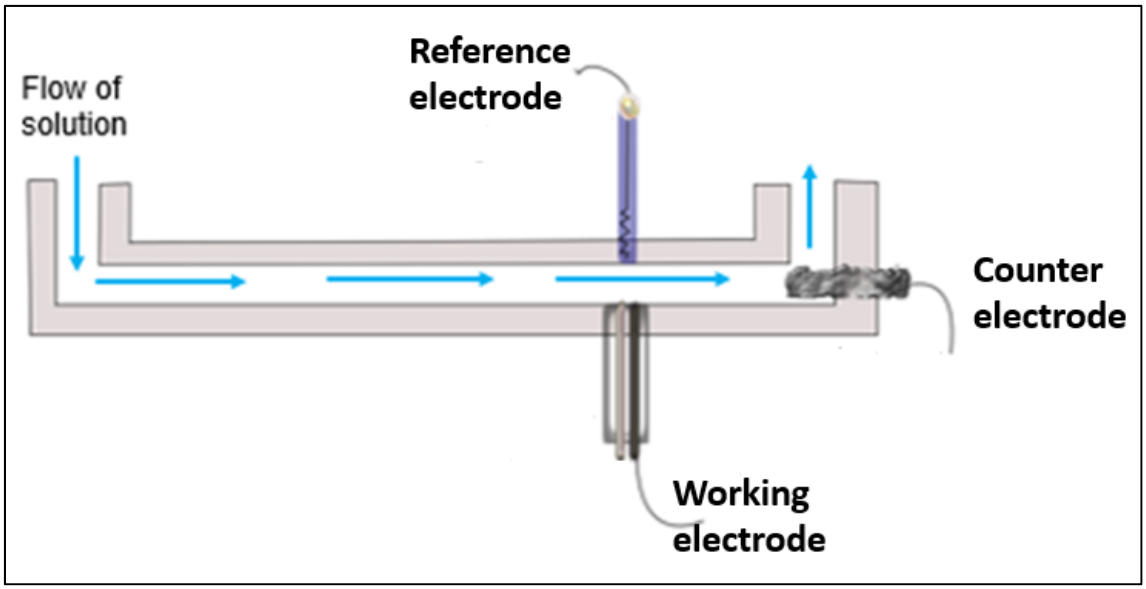

Figure 2.6. Channel-flow cell setup.

2.2.4. Electrochemical quartz crystal microbalance (EQCM)

Also, the beaker cell for static electrochemical measurement can be combined with the quartz crystal microbalance (QCM) to form the electrochemical quartz microbalance (EQCM). A QCM can simultaneously measure the frequency change response of the electrochemical cell. The frequency response can be calculated to obtain the mass change response of the surface of the working electrode during the electrochemical measurement. The setup for the EQCM studies is similar to the setup for an electrochemical studies in Figure 2.2, but with the QCM attached to the working electrode as well. The setup is shown as Figure 2.7.

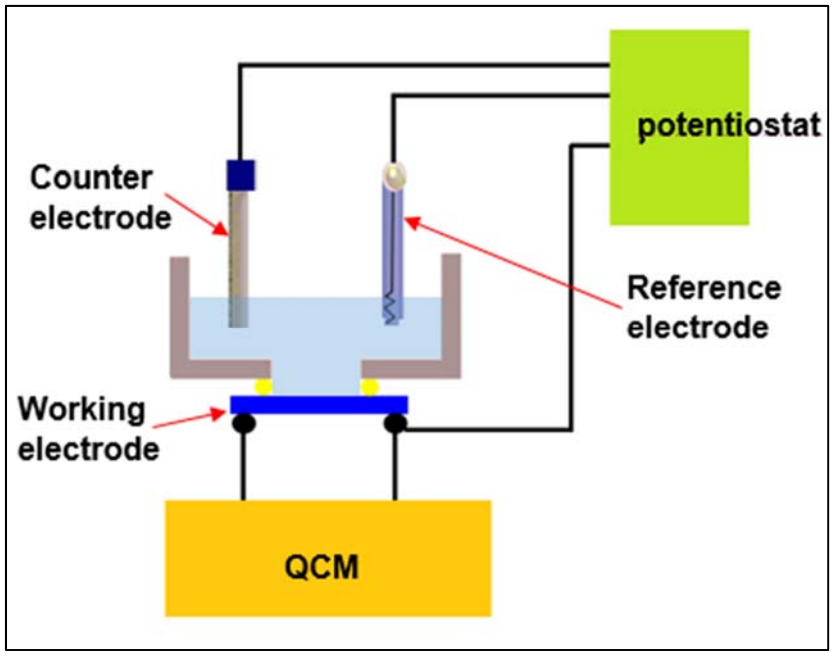

Figure 2.7. EQCM setup.

2.3. Adsorption studies

The data obtained from the corrosion studies can be extracted for secondary data to describe the adsorption behavior of the inhibitor. This can be done by fitting the data from the corrosion studies into several adsorption isotherm models and finding the best fit [2]. The model that best fits the data will then be used to describe the adsorption of the inhibitor onto the specimen during the corrosion inhibition process. The information that can be obtained from such model fittings are the type of adsorption of the molecules (chemisorption, physisorption) and to describe the interaction of the molecules to each other.

Physisorption is a non-specific loose binding, such as via Van der Waals interaction or electrostatic interaction between the charged inhibitor and the charged metal surface. This interaction is considered as weaker and can be easier disrupted than the chemisorption.

Chemisorption is a formation of chemical bond between the inhibitor molecule and the empty d-orbital of the Fe.

Both types of adsorption can be determined by calculating the Gibbs free energy value at a single temperature. Typically, Gibbs free energy of more negative than -40 kJ mol^{-1} defines the inhibitor as adsorbing by the chemisorption process while Gibbs free energy of more positive than -20 kJ mol^{-1} defines the inhibitor as adsorbing by the physisorption process [3]. There can be instances when the inhibitor has a calculated Gibbs free energy value that is in between those mentioned values and thus the inhibitor is defined as absorbing by both the processes of chemisorption and physisorption.

Langmuir adsorption isotherm model describes the adsorption of the inhibitor onto the surface of metal with three assumptions:

- The surface has specific number of sites where solute molecules can adsorb on to.
- The adsorption is of a monolayer of inhibitor molecules onto the surface of metal.
- The surface of the metal is in contact with the solution with inhibitor which is strongly attracted to the surface of metal.

The Langmuir isotherm is given by the equation [3]:

$$\frac{\theta}{1-\theta} = K_{ads}C \quad (1)$$

Which can be rearranged as:

$$\frac{C}{\theta} = \frac{1}{K_{ads}} + C \quad (2)$$

Where C is concentration of the inhibitor, Θ is the surface coverage and K_{ads} is the adsorption equilibrium constant.

2.4. Chemical analyses

The chemical analysis for the content of the extracts is important to understand the mechanism better. The chemical analyses were done to identify the type of functional groups present in the extracts and to identify the compounds present in the extracts. These will provide a better understanding of the contents of the agarwood leaf extracts and the possible mechanism of corrosion inhibition from the compounds present. The identified compounds can then be individually tested for the corrosion inhibition behavior on mild steel in HCl solution. The best individual compound will then be used for further anti-corrosion tests and adsorption studies. Two types of chemical analyses that were conducted were Fourier transform infrared (FTIR) spectroscopy and the quadrupole-tandem of flight liquid chromatography/ mass spectrometry (Q-TOF LC/MS).

2.4.1. Fourier transform infrared (FTIR) spectroscopy analysis

Fourier transform infrared (FTIR) spectroscopy is a useful method to understand the types of functional groups and types of bonding that can exist in a sample. Radiation containing the IR wavelengths is split into two beams, one which is a fixed length and the other a variable length. The constructive and destructive interference (due to the varying distance) produces varying intensities (an interferogram). The Fourier transform then converts this from time domain to frequency domain. The analysis of one broad banded pass of radiation through the sample gives rise to the complete IR spectrum [4]. The IR spectrum obtained for a sample, in which radiation absorption is affected by the types of bonds present in the sample. The FTIR analysis has advantages of simultaneous analysis for a broad spectrum and also high resolution.

2.4.2. Quadrupole-time of flight liquid chromatography/ mass spectrometry (Q-TOF LC/MS) analysis

This analysis combines the method of separation from the liquid chromatography and mass identification of a mass spectrometry. This is a useful method for the identification of compounds in natural products. The mass analyzer used for this equipment, as indicated by the name, is the quadrupole-time of flight (Q-TOF). The time of flight (TOF) is a method of mass spectrometry where the ion's mass-to-charge-ratio is determined from the time taken for an accelerated ion to reach a detector at a known distance. The resultant mass–to-charge spectrum can then be matched with a known standard, or through libraries to identify the present compound.

References

[1] P. A. Schweitzer, Corrosion of Linings & Coatings: Cathodic and Inhibitor Protection and Corrosion Monitoring, CRC press, 2006.

[2] I. Ahamad, R. Prasad, M. Quraishi, Corrosion Science, 52 (2010) 1472-1481.

[3] I. Ahamad, R. Prasad, M. A. Quraishi, Corrosion Science, 52 (2010) 3033-3041.

[4] R. M. Silverstein, F. X. Webster, Spectrometric Identificatiom of Organic Compounds Sixth Edition, John Wiley and Sons, Inc, New York, 1998.

3. ANTI-CORROSION BEHAVIOUR OF *AQUILARIA MALACCENSIS* LEAF EXTRACT ON MILD STEEL IN HCl

3.1. Introduction

There are several trees from the Aquilaria family that are farmed for harvesting the agarwood resin. *Aquilaria malaccensis* is an agarwood-producing tree naturally distributed in South and Southeast Asia [1]. These farmed trees are usually induced to produce the agarwood resin by inoculation, and the resin can be harvested from the woody parts of the tree such as the trunk, roots and the branches. The leaves have minor uses such as being sold as traditional teas for stomach ailments [2], but the leaves are usually thrown away in abundance as it is less profitable compared to the highly-prized resin.

Corrosion inhibitors are amongst the more popular methods for corrosion protection due to their cost-effectiveness. Although many effective synthetic inhibitors have been developed [3-7], the movement of the corrosion inhibition research has been geared towards greener approaches such as using waste materials, especially from plants [8-10]. Aside from the likelihood that such inhibitors will be less toxic, it is also a more cost-saving approach as it is making use of waste materials as raw materials. The most acceptable mechanism of the corrosion inhibition from the plants is the adsorption of the extract's molecules, forming a protective thin film over the metals to create a barrier from the corrosive medium [11-1]. Many of the plants were reported to contain compounds that are helpful for the adsorption by physisorption (Van der Waals attraction), chemisorption (bond sharing) or a mix of both processes. The structure of the compounds mostly resembles those of the conventional organic inhibitors [13] with functional groups that are bond-sharing and/or electron-donating [14-17].

Aquilaria malaccensis has been previously reported for its good antioxidant properties and the existence of phytochemicals that could be beneficial as a corrosion inhibitor [18, 19]. Some agarwood leaf extracts have also been shown to successfully inhibit corrosion [20, 21]. The purpose of this chapter is to clarify the corrosion inhibition mechanism of *Aquilaria malaccensis* for mild steel in 1 mol dm^{-3} HCl. The corrosion inhibition was studied by gravimetric and electrochemical methods and the adsorption isotherm model was used to explain the adsorption process.

3.2. Methodology

3.2.1. Extraction

The *Aquilaria malaccensis* leaf was obtained from Telok Kumbar, Penang Island, Malaysia. The collected mature leaves were wiped clean, air-dried, powdered and extracted. The powdered leaf was exhaustively extracted with methanol at room temperature (300 ± 2 K) and concentrated using a rotary evaporator at 313 K into a paste form. The paste was dried in an oven at 308 K until no change in mass was observed.

3.2.2. Corrosion inhibition study

3.2.2.1. Solution and specimen

The 1 mol dm^{-3} HCl was prepared by diluting 37 % concentrated HCl (AR grade) in double distilled water. For solutions with the leaf extract, the leaf extract was diluted to specific concentrations (50 to 1500 ppm) using the prepared HCl solution then 50 mL of the solution was used for each specimen. Mild steel with the composition of: Fe; 99.146 %, C; 0.205%, Mn; 0.55%, Si; 0.06% and P; 0.039%, with the dimensions of 1 × 3 × 0.06

cm was used for the weight loss study while mild steel with an exposure area of 3.142 cm^2 was used for the electrochemical studies. The surface of the mild steel was successively polished with emery papers of grades from 200 to 1200 then degreased with acetone before it was rinsed with double distilled water. It was then lightly towel dried and left to dry at room temperature before it was used.

3.2.2.2. Weight loss method

The initial weight of the mild steel was measured, then the mild steel was immersed into the HCl solutions with and without the presence of the leaf extract at various concentrations for 24 hours. It was then removed, rinsed with distilled water and dried before the final weight was measured. All the concentrations were evaluated in triplicate and the result was the mean of the triplicates. The experiment was performed at room temperature of 300 ± 2 K [21]. The inhibition efficiency (IE %) of the leaf extract was calculated using the following equation:

$$\text{IE } \% = \left(\frac{W_2 - W_1}{W_2}\right) \times 100 \quad (1)$$

where W_1 is the weight loss of the specimen immersed with the leaf extract (g) and W_2 is the weight loss of the blank specimen (g).

3.2.2.3. Electrochemical methods

All the electrochemical measurements were carried out using a potentiostat/ galvanostat/ ZRA Reference 600 (Gamry Instruments) with a three-electrode cell. Platinum was used as the counter electrode, a saturated calomel electrode (SCE) was used as the reference

electrode and the mild steel was used as the working electrode. The open circuit potential (OCP) measurement was observed for 30 minutes before the electrochemical measurements were conducted. All the experiments were conducted at a temperature of 300 ± 2 K [21].

3.2.2.3.1. Potentiodynamic polarization measurement

The measurement was conducted at the scan rate of 1 mVs^{-1} at an overpotential of ± 300 mV with reference to the corrosion potential (E_{corr}). The linear segments of the anodic and cathodic curves were extrapolated to E_{corr} to obtain the corrosion current densities (I_{corr}). The IE % of the leaf extract was calculated using the following equation:

$$IE\ \% = \left(\frac{I_2 - I_1}{I_2}\right) \times 100 \quad (2)$$

where I_1 is the current density of the specimen with the leaf extract (μA cm^{-2}) and I_2 is the current density of the blank specimen (μA cm^{-2})

3.2.2.3.2. Electrochemical impedance spectroscopy (EIS) measurement

The measurement was conducted at the frequencies from 100 000 to 0.1 Hz at the amplitude of 10 mV and the scan rate of 10 points per decade. The fitting of the curves and the parameters were obtained using the Echem Analyst by Gamry. The IE % was calculated using the following equation:

$$IE\ \% = \frac{R_{ct(1)} - R_{ct(2)}}{R_{ct(1)}} \times 100 \quad (3)$$

where $R_{ct(1)}$ is the charge transfer resistance of the specimen with the leaf extract ($\Omega.cm^2$) and $R_{ct(2)}$ is the charge transfer resistance of the blank specimen ($\Omega.cm^2$)

3.3. Results and discussion

3.3.1. Weight loss method

From Figure 3.1, it was apparent that the increase in the concentration increased the inhibition efficiency of the leaf extract. The IE % increased until the concentration was 500 ppm, then the shape of the curve became a plateau at greater than 500 ppm. This indicated that the optimum IE % was reached at the concentration of 500 ppm or higher for the weight loss method. The IE % continued to minimally increase after 500 ppm (91.33 %) until 1500 ppm (94.49 %).

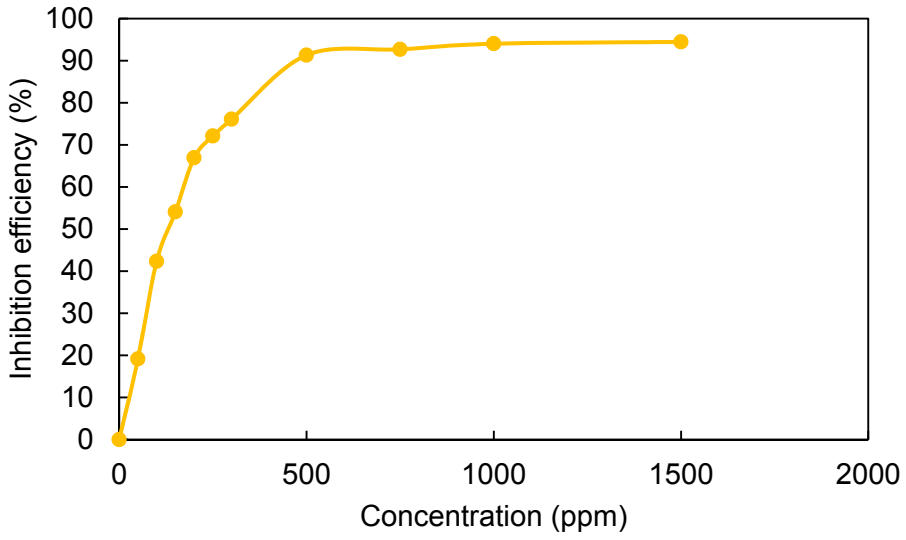

Figure 3.1. Weight loss measurement for mild steel in 1 mol dm^{-3} HCl with and without agarwood leaf extract.

3.3.2. Potentiodynamic polarization measurement

The potentiodynamic polarization measurement was realized in the OCP ± 300 mV range from a cathodic-to-anodic sweep and represented as Tafel plots in this chapter. The obtained parameters listed are in Table 3.1. From Figure 3.2, the current density (I_{corr}) of the Tafel curves decreased with the increase in the concentration of the leaf extract. The highest recorded IE % was 91 % at the concentration of 1500 ppm. The reaction when the cell was polarized to the cathodic region (more negative region) to the OCP is hydrogen evolution, the reaction of which can be simplified by the following ionic equation [22]:

$$2H^+ + 2e^- \longrightarrow H_2 \quad (5)$$

while the reaction when the cell was polarized to the anodic region (more positive region) to the OCP is metal dissolution, the reaction of which can be simplified by the following ionic equation [22]:

$$Fe \longrightarrow Fe^{2+} + 2e^- \quad (6)$$

While the leaf extract inhibited the cathodic reaction at all the tested concentrations, the anodic reaction was not inhibited at the lower concentrations. However, the leaf extract successfully inhibited the anodic process at 750 ppm and higher as the current density was lowered in the anodic region. This indicated that the trigger for the inhibition effect happens at different concentrations of the leaf extract for the anodic and cathodic reactions. Both the anodic slope (B_a) and cathodic slope (B_c) were almost the same until 750 ppm then changed at higher than 750 ppm. This indicated a change in the metal dissolution and hydrogen evolution at higher than 750 ppm. The E_{corr} of the leaf extract did not shift much from the E_{corr} of the blank specimen, indicating that the leaf extract

acted as a mixed-type inhibitor at all concentrations [23]. However, since the current densities from the cathodic region were much lower than the anodic region, therefore, the leaf extract acted as a mixed-type but predominantly cathodic inhibitor.

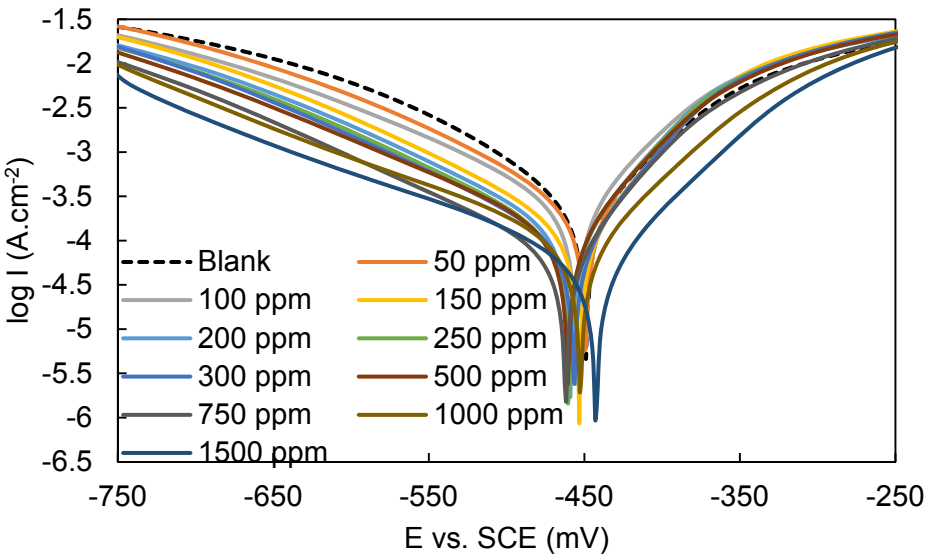

Figure 3.2. Tafel plot for mild steel in 1 mol dm^{-3} HCl with and without agarwood leaf extract.

Table 3.1. Parameters obtained from Tafel plot for mild steel in 1 mol dm^{-3} HCl with and without leaf extract.

Concentration (ppm)	I_{corr} **(μA/cm²)**	E_{corr} **(mV)**	B_a **(mV/decade)**	$-B_c$ **(mV/ decade)**	***IE %***
blank	282	-449	75	117	-
50	200	-450	60	100	29
100	195	-456	56	113	31
150	126	-453	53	107	55
200	100	-459	41	101	65
250	89	-461	51	106	68
300	79	-456	51	109	72
500	76	-461	51	104	73
750	63	-462	52	118	78
1000	45	-453	58	137	84
1500	25	-443	63	147	91

3.3.3. Electrochemical impedance spectroscopy (EIS) measurement

The EIS measurements are represented by Nyquist plots in this chapter (Figure 3.3). For the EIS analysis, the curve had the shape of a single capacitive loop thus indicating the corrosion process to be mainly charge-transfer controlled for the metal dissolution. Supporting this fact are the slight changes in the *n* values with or without the presence of the leaf extract [24, 25]. The *n* values decreased with the increase in the concentration due to the adsorption of the extract molecules, thus increasing the nonhomogeneity of the surface [26, 27]. The curves appear to be in the shape of depressed semicircles, which is a deviation from the ideal capacitor behavior. Such deviations are characteristics of the dispersion in frequency due to the surface roughness and nonhomogeneities [28, 29].

Thus the Randles-CPE type equivalent circuit (Figure 3.3 inset) was used to better fit the processes.

The impedance of CPE is expressed by:

$$Z_{CPE} = \frac{1}{Y_o(j\omega)^n} \quad (7)$$

where Y_o is the frequency dependent magnitude of the pseudo-capacitance, j is $-1^{1/2}$, ω is the angular frequency and $-1 \leq n \leq 1$.

The parameters obtained from the Nyquist plot fitted into the Randles equation are listed in Table 3.2. While the solution resistance (R_s) values indicated slight changes, the charge transfer resistance (R_{ct}) values evidently increased with the increase in the concentration. The R_{ct} was used to calculate the IE% using formula (3) and the leaf extract showed an increasingly successful corrosion inhibition with the increase in the concentration. The increase in the R_{ct} signifies a slow corroding system, and according to several papers, this is attributed to the adsorption of the leaf extract molecules that displace water molecules and other ions originally adsorbed on the surface of the mild steel, thus reducing the area of the active sites at which the corrosion takes place [24, 30, 31]. This may cause the formation of a protective thin film on the surface of the mild steel.

The lower CPE values for the leaf extract compared to the blank specimen could be caused by the reduction in the local dielectric constant and/or increase in the thickness of the electrical double layer. This could be due to the adsorption of the leaf extract molecules at the metal/solution interface [32].

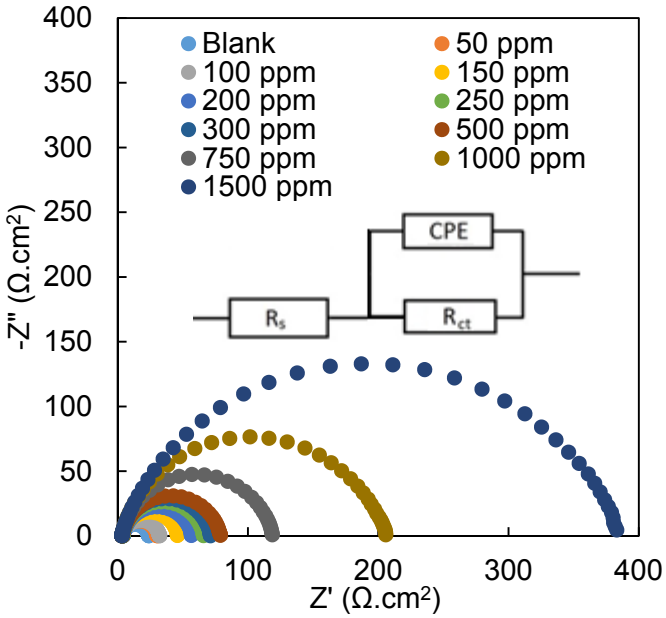

Figure 3.3. Nyquist plot for mild steel in 1 mol dm^{-3} HCl with and without agarwood leaf extract, inset: Randles equivalent circuit model.

Table 3.2. Parameters obtained from Nyquist plot for mild steel in 1 mol dm^{-3} HCl with and without leaf extract.

Concentration (ppm)	R_{ct} **(Ω.cm²)**	R_s **(Ω.cm²)**	**CPE (μF/cm²)**	***n***	***IE %***
Blank	22.03	3.752	1326	0.920	-
50	26.96	3.208	1178	0.912	11.31
100	28.22	3.814	1049	0.904	15.27
150	42.45	3.384	971	0.911	43.68
200	52.41	4.166	836	0.906	54.38
250	61.93	3.777	748	0.905	67.08
300	67.87	3.189	732	0.904	64.77
500	75.13	3.506	757	0.888	68.17
750	114.56	3.550	547	0.894	79.13
1000	199.39	3.214	657	0.855	88.01
1500	372.96	3.035	895	0.813	93.59

3.3.4. Adsorption isotherm model

The corrosion retarding effect observed for all the corrosion measurements was due to the adsorption of the inhibitor molecules on the surface in the form of a protective thin film from the aggressive acid solution while the exposed areas of the surface of the mild steel undergo the corrosion process. Thus, the assumption is made that the inhibition efficiency is directly related to the surface of the mild steel that is 'covered'/adsorbed by the inhibitor's molecules [33]. To understand the type of adsorption by the leaf extracts' molecules on the surface of the mild steel, the surface coverage (Θ) calculated from the different corrosion measurement methods (Θ = IE %/100) was fitted into several adsorption isotherm models. The Langmuir adsorption isotherm was the best fit with a coefficient of determination (R^2) value of close to unity.

The Langmuir adsorption isotherm model assumes that the adsorbed molecules form a monolayer of film, only occupy one site and do not interact with other molecules [34, 35]:

$$\frac{c}{\theta} = \frac{1}{K_{ads}} + c \qquad (8)$$

where C is the concentration, Θ is the surface coverage, and K_{ads} is the adsorption constant

Plotting C/Θ versus C yields Figure 3.4.

The K_{ads} value is related to the Gibbs free energy [36]:

$$\Delta G_{ads} = -RT \ln (K_{ads} \times A) \qquad (9)$$

where ΔG_{ads} is the change in the Gibbs free energy/standard adsorption free energy, R is the universal gas constant (8.314 J K^{-1} mol^{-1}), T is the absolute temperature (K), and A is the density of water (1000 g L^{-1})

There are two main types of adsorptions: i.e., physisorption and chemisorption. The physisorption process, which is indicated by the values of ΔG_{ads} less negative than -20 kJ mol^{-1}, is attributed to the electrostatic interaction between a charged surface of the substrate and the ions in the medium. The chemisorption process, which is indicated by the values of ΔG_{ads} more negative than -40 kJ mol^{-1}, is attributed to the charge transfer from the molecule or electron sharing between the substrate and other molecules [37]. The calculated parameter from the Langmuir adsorption isotherm fitting (Table 3.3) indicated the leaf extract to be a mixed-type inhibitor but mainly a physisorption process. This indicated that the extract contained molecules that can adsorb onto the surface of the mild steel by physisorption and chemisorption.

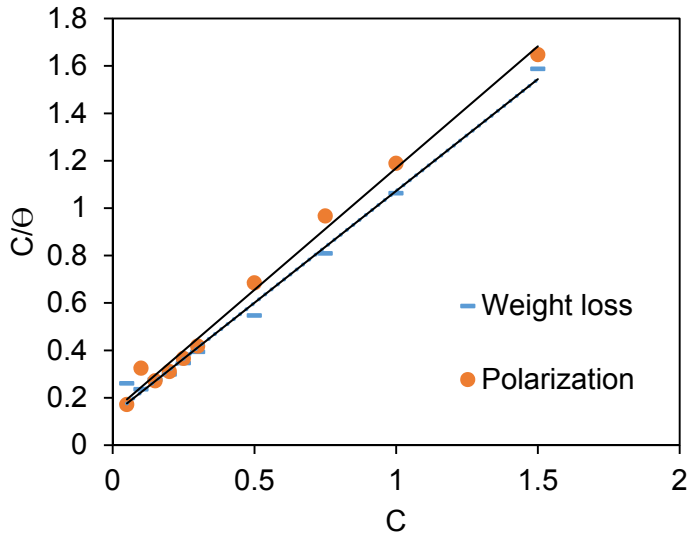

Figure 3.4. Relationship of C/Θ and C for weight loss method and potentiodynamic polarization measurement.

Table 3.3. Langmuir adsorption isotherm model parameters for agarwood leaf extract in 1 mol dm^{-3} HCl for different anti-corrosion measurements.

Method	R^2	**Y-axis intersection**	K_{ads}	ΔG_{ads} (kJ mol^{-1})
Weight loss	0.9922	0.1292	7.73	-22.33
Polarization	0.9922	0.1417	7.05	-22.10
EIS	0.9159	0.3023	3.31	-20.21

3.4. Conclusions

- The *Aquilaria malaccensis* leaf extract successfully inhibited the corrosion of mild steel in 1 mol dm^{-3} HCl up to 94.49 % at the concentration of 1500 ppm.
- The leaf extract acted as a mixed-type, but predominantly cathodic inhibitor based on the potentiodynamic polarization measurement.
- The leaf extract best fits the Langmuir adsorption isotherm and was adsorbed by a mixed-type, but predominantly physisorption process based on the Gibbs free energy calculation.

References

[1] S. Oldfield, C. Lusty, A. MacKinven, The world list of threatened trees, World Conservation Press, 1998.

[2] M. Kakino, S. Tazawa, H. Maruyama, K. Tsuruma, Y. Araki, M. Shimazawa, H. Hara, BMC complementary and alternative medicine, 10 (2010) 1.

[3] S. L. Li, Y. G. Wang, S. H. Chen, R. Yu, S. B. Lei, H. Y. Ma, D. X. Liu, Corrosion Science, 41 (1999) 1769-1782.

[4] A. Braig, Progress in Organic Coatings, 34 (1998) 13-20.

[5] E. E. F. El Sherbini, Materials Chemistry and Physics, 61 (1999) 223-228.

[6] P. Mutombo, L. Pospíšil, J. Fiedler, J. Čejka, J. Karhan, J. Vošta, Journal of Electroanalytical Chemistry, 405 (1996) 223-226.

[7] B. A. Abd-El-Nabey, A. El-Toukhy, M. El-Gamal, F. Mahgoob, Surface and Coatings Technology, 27 (1986) 325-334.

[8] A. Khadraoui, A. Khelifa, K. Hachama, R. Mehdaoui, Journal of Molecular Liquids, 214 (2016) 293-297.

[9] A. N. Grassino, J. Halambek, S. Djaković, S. Rimac Brnčić, M. Dent, Z. Grabarić, Food Hydrocolloids, 52 (2016) 265-274.

[10] S. Africa, African Journal of Pure and Applied Chemistry, 2 (2008) 046-054.

[11] K. Rose, B.-S. Kim, K. Rajagopal, S. Arumugam, K. Devarayan, Journal of Molecular Liquids, 214 (2016) 111-116.

[12] N. El Hamdani, R. Fdil, M. Tourabi, C. Jama, F. Bentiss, Applied Surface Science, 357, Part A (2015) 1294-1305.

[13] N. Soltani, N. Tavakkoli, M. Khayat Kashani, A. Mosavizadeh, E. E. Oguzie, M. R. Jalali, Journal of Industrial and Engineering Chemistry, 20 (2014) 3217-3227.

[14] M. Mehdipour, B. Ramezanzadeh, S. Y. Arman, Journal of Industrial and Engineering Chemistry, 21 (2015) 318-327.

[15] O. A. Abdullatef, Egyptian Journal of Petroleum, 24 (2015) 505-511.

[16] A. Y. El-Etre, M. Abdallah, Z. E. El-Tantawy, Corrosion Science, 47 (2005) 385-395.

[17] H. Gerengi, H. I. Sahin, Industrial & Engineering Chemistry Research, 51 (2011) 780-787.s.

[18] A. Huda, M. Munira, S. Fitrya, M. Salmah, Pharmacog. Res., 1 (2009) 270

[19] A. Khalil, A. Rahim, K. Taha, K. Abdallah, Journal of Applied and Industrial Sciences, 1 (2013) 78-88.

[20] H. L. Y. Sin, A. A. Rahim, B. Saad, M. I. Saleh, P. B. Raja, Int. J. Electrochem. Sci, 9 (2014) 830-846.

[21] H. L. Y. Sin, A. A. Rahim, C. Y. Gan, B. Saad, M. I. Salleh, M. Umeda, in: Measurement, (submitted) 2016.

[22] N. Kıcır, G. Tansuğ, M. Erbil, T. Tüken, Corrosion Science.

[23] E. S. Ferreira, C. Giacomelli, F. C. Giacomelli, A. Spinelli, Materials Chemistry and Physics, 83 (2004) 129-134.

[24] K. Boumhara, M. Tabyaoui, C. Jama, F. Bentiss, Journal of Industrial and Engineering Chemistry, 29 (2015) 146-155.

[25] F. Bentiss, M. Traisnel, L. Gengembre, M. Lagrenée, Applied Surface Science, 152 (1999) 237-249.

[26] A. Popova, E. Sokolova, S. Raicheva, M. Christov, Corrosion Science, 45 (2003) 33-58.

[27] W.-h. Li, Q. He, S.-t. Zhang, C.-l. Pei, B.-r. Hou, Journal of Applied Electrochemistry, 38 (2007) 289-295.

[28] S. Martinez, M. Metikoš-Huković, Journal of Applied Electrochemistry, 33 (2003) 1137-1142.

[29] H. Shih, F. Mansfeld, Corrosion Science, 29 (1989) 1235-1240.

[30] F. Growcock, R. Jasinski, Journal of the Electrochemical Society, 136 (1989) 2310-2314.

[31] S. Muralidharan, M. A. Quraishi, S. V. K. Iyer, Corrosion Science, 37 (1995) 1739-1750.

[32] A. Döner, G. Kardaş, Corrosion Science, 53 (2011) 4223-4232.

[33] E. E. Oguzie, Corrosion Science, 49 (2007) 1527-1539.

[34] A. J. Bard, L. R. Faulkner, J. Leddy, C. G. Zoski, Electrochemical methods: fundamentals and applications, Wiley New York, 1980.

[35] M. Lebrini, F. Bentiss, H. Vezin, M. Lagrenée, Corrosion Science, 48 (2006) 1279-1291.

[36] T. F. Tadros, Applied surfactants: principles and applications, John Wiley & Sons, 2006.

[37] E. A. Noor, A. H. Al-Moubaraki, Materials Chemistry and Physics, 110 (2008) 145-154.

4. *AQUILARIA MALACCENSIS* LEAF EXTRACT CONTENT ANALYSIS

4.1. Introduction

Due to the concerns of negative impacts on the environment and human health by certain synthetic inhibitors, there has been a surge in the interest of developing safer alternatives [1] which has led to the discovery of the usage of the extracts from various parts of plants as excellent corrosion inhibitors. More recently, there has been an increasing interest in corrosion inhibition studies utilizing plant waste materials such as extracts from banana peels, coconut coir dust, discarded marigold flowers and palm oil fronds as a more environmentally sustainable approach [2-6]. In general, the said plants extracts contributed to corrosion inhibition due to the presence of many compuonds in the extracts that worked synergistically to produce a corrosion retardation effect [7-11]. Mostly, the corrosion inhibition effect was believed to be actively contributed by the compounds that belong to the phytochemical groups which are also good antioxidants such as alkaloids, flavonoids, steroids, flavones and tannins [12, 13]. Extensive studies on known molecules have been done and it was discovered that inhibitor molecules with the presence of bond-forming, electron-rich groups/atoms are known to be responsible for the corrosion inhibition properties [14-17]. The widely accepted explanation of corrosion inhibition by these plant extracts is the adsorption of the inhibitors' molecules on the surface of a metal forming a barrier between the metal and corrosive substance, thus preventing corrosion [18-22].

Agarwood trees produce fragrant resins that are the most sought after among the resinous woods. They are also used in digestive, sedative and antiemetic drugs aside from producing fragrant products [23]. The leaves are relatively valueless, usually thrown away and are considered a waste product. From several studies, the agarwood leaf extracts

such as *Aquilaria malaccensis*, which is an agarwood-producing tree has been shown to contain antioxidants and phytochemicals which could be beneficial for the corrosion inhibition of mild steel in an acidic medium [24-26].

From chapter 3, the leaf extract of *Aquilaria malaccensis* was shown to be an excellent corrosion inhibitor of mild steel in HCl solution at low concentrations of 1000 ppm. However, the functional groups and the present compounds in the extract that could have contributed to the understanding of the corrosion inhibition ability of the extract should be further explored. Thus, in this chapter, the chemical functional groups (types of bonds) and the chemical compounds that are present in the *Aquilaria malaccensis* leaf extract was explored using the Fourier transform infrared (FTIR) analysis and Quadrupole-time-of-flight liquid chromatography/mass spectrometry **(**Q-TOF LC/MS) analysis respectively.

4.2. Methodology

4.2.1. Extraction

Aquilaria malaccensis leaf was collected from Telok Kumbar, Penang Island, Malaysia and was wiped clean and air dried before it is powdered. The extract was obtained from the leaf using methanol at room temperature (300 K) and was concentrated using a rotary evaporator at 313 K to yield the leaf extract in the form of paste. The paste was dried in an oven at 308 K until no change in mass was observed.

4.2.2. Fourier transform infra-red (FTIR) analysis

The extract was analyzed using the FT-IR Spectrometer Spectrum 2000 (Perkin Elmer). The extract was mixed with FTIR grade potassium bromide at the ration of 1:20 and

grounded. Then it was compressed into a pellet and the spectra was immediately taken from the range of 4000 to 400 cm^{-1}.

4.2.3. Quadrupole-time of flight liquid chromatography/mass spectrometry (Q-TOF LC/MS) analysis

The analysis of present chemical compounds in the leaf extract was determined by using 6520 Accurate-Mass Q-TOF LC/MS (Agilent Technology, USA). The extract (1000 ppm) were reconstituted using 3% acetonitrile (97 % ultrapure water).

The separation was performed using an Agilent ZORBAX SB-C18 column with a diameter of 0.5 mm, length of 150.0 mm and particle size of 5.0 µm. The operating conditions were: injection volume: 2 µL; mobile phase: (A) distilled water with 0.1 % formic acid, (B) acetonitrile with 0.1% formic acid; flow rate: 20 µL min^{-1} The pump gradient was: 0 min, 3 % B; 3.75 min, 20 % B; 8.75 min, 40 % B; 15-17.5 min, 90 % B; 22.5-32.5 min, 3 % B.

The MS and MS/MS analyses were carried out using positive mode electrospray ionization (ESI) equipped with 1200 series (Agilent Technologies, USA) gradient pump.

For MS analysis, dry gas temperature of 598 K, gas flow rate of 5 L min^{-1}, nebulizer pressure of 30 psi and capillary voltage of 3500 V were used. The acquisition mode was set at the m/z range of 25-1700, with a scan rate of 1 spectra ms^{-1}.

For MS/MS analysis, collision energy of 20 eV was used. The other conditions were the same as MS analysis. The detection limit was at 0.0001 unit.

4.2.4. Database search of the unknown compounds

The results obtained from the Agilent MassHunter Workstation Software – Data Acquisition were processed using the MassHunter Qualitative Analysis software. Molecular feature extraction (MFE) was performed in order to determine the molecular masses. MFE was carried out using the following setting: target data type: small molecules (chromatographic); peak filters: above 10,000 counts (to eliminate the background noise); positive ions: +H, +Na (potential cation adduct that was present in the extract); isotope mode: common organic molecules and charge state: limit assigned charge states to a maximum of 2.

After the MFE search, the mass list was uploaded to the metabolite search using the METLIN Metabolite Database. The mass list was searched against the neutral mass in the database using the accuracy of less than 7 ppm of mass difference. The matched MS/MS spectra of compounds were verified using Mass Frontier^{TM} 6.0. In Mass Frontier analysis, fragments were generated using all possible rules, including aromatic rings, the default limit of 10 000 fragments per iteration, and four iterations. These spectra were compared to the experimental MS/MS spectra. The compound was predicted based on the fragment ions. The identified and proposed compounds were verified using purchased chemical standards from Agros Organics and Sigma-Aldrich with over 95 % purity.

4.3. Results and discussion

4.3.1. Fourier transform infra-red (FTIR) analysis

The extract was analyzed with the FTIR to identify the functional groups present in the leaf extract. The spectrum obtained is shown as Figure 4.1 and the functional groups present in the leaf extract from the spectrum is displayed as Table 4.1. From the spectrum,

the leaf extract may contain several functional groups such as O-H (strong and broad peak at 3363 cm^{-1}), C=C (strong peak at 1622 and 1455 cm^{-1}), C-O (weak adsorption at 1321 cm-1) and C-N (strong peak at 1074 cm^{-1}). All these functional groups could possibly contribute to the better adsorption properties of the compounds present in the *Aquilaria malaccensis* leaf extract.

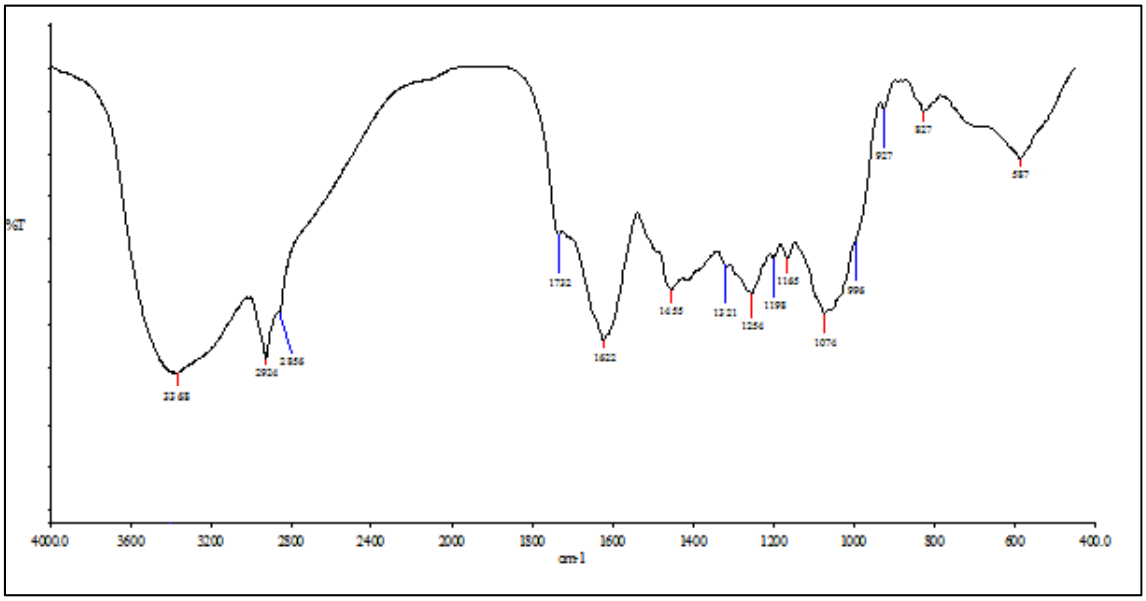

Figure 4.1. FTIR spectrum of *Aquilaria malaccensis* leaf extract.

Table 4.1. Assignment of FTIR spectrum with the functional groups.

Wavelength band (cm^{-1})	**Peak intensity**	**Functional group**
3363	Strong, broad	O-H (stretch)
2926, 2856	medium	C-H (stretch)
1622, 1455	strong	C=C (stretching)
1321	weak	C-O (stretching)
1074	strong	C-N (stretching)
827	weal	C-H (out-of-plane bend)

4.3.2. Q-TOF LC/MS analysis

Five compounds (choline, isoleucine, adenosine, phenylalanine and mangiferin) (Figure 4.2) managed to be purchased as standard chemicals and were confirmed to be present in the leaf extract using Q-TOF by comparing m/z fragments produced, retention time and [M-H]+ mass. The parameters of this analysis is presented as Table 4.1.

Choline

Choline (IUPAC name: 2-Hydroxy-*N,N,N*-trimethylethanamonium) is an essential nutrient that is water soluble and can be found in broccoli, spinach, wheat germ, beans, nuts and other food sources. It is an ammonium salt. In a plant, choline functions as a vital metabolite to synthesise the membrane phospholipid phosphatidylcholine [27, 28].

Isoleucine

Isoleucine (IUPAC name; 2-amino-3-methylpentanoic acid) is an essential amino acid that can be found in some edible seaweed species [29]. In plants, isoleucine plays a role in self-defense mechanism as the conjugate of isoleucine and jasmonate is a major regulator which controls gene expression and production of secondary metabolites after abiotic/ biotic challenges [30]. The investigation on the isoleucine corrosion inhibition activity on nickel in H_2SO_4 has been reported [31].

Adenosine

Adenosine is a plant growth substance that exists in rice [32]. Various forms of adenosine exist also in plants such as adenosine kinase isoforms in tobacco, cyclic adenosine monophosphate in *Arabidopsis thaliana* and adenosine 5'-phosphosulfate reductase in *Physcomitrella patens* [33-35]. Adenosine has been reported to be present in the leaves of *Aquilaria sinensis* [36]. Adenosine has been reported for its application as a corrosion inhibitor for tin-idium alloys in HCl [37] and some good naturally derived inhibitors were reported to contain adenosine [38]. The ESI product ion for adenosine (standard) and adenosine detected from the agarwood extract is presented in Figure 4.3.

Phenylalanine

Phenylalanine (IUPAC name; 2-Amino-3-phenylpropanoic acid) is an amino acid that exists in many foods including soy, certain nuts, seeds and green leaves. Phenylalanine exists as part of the gene fragments and phenylalanine ammonia-lyase (PAL) which has been reported in *Aquilaria malaccensis Lam*. [39]. Phenylalanine has been studied for its corrosion inhibition properties and the examples include the study of phenylalanine as an inhibitor for bronze in Na_2SO_4 [40] and also in synergistical studies with rare earth as corrosion inhibitor for mild steel in HCl [41].

Mangiferin

Mangiferin (IUPAC name; 1,3,6,7-Tetrahydroxy-2-[3,4,5-trihydroxy-6-(hydroxymethyl)oxan-2-yl]xanthen-9-one) is a glucosylxanthone found in many higher

plants such as *Mangifera indica L.* (Anacardiaceae), *Anemarrhena asphodeloides* (Liliaceae family), and *Cyclopia intermedia* (Fabaceae family) [42]. It has shown antioxidant, analgesic and anti-inflammatory properties [32].

From the structure of the compounds, it was observed that the leaf extract contained desirable functional groups and structural properties for corrosion inhibition such as –OH, nitrogen atom and aromatic ring thus it can be predicted that the compounds will be good inhibitors for mild steel corrosion in acidic solution.

Next, a simple weight loss measurement was conducted by immersing mild steel plate of dimension 3 × 1 × 0.06 cm into 1 mol dm^{-3} HCl solutions with and without 0.1 mmol dm^{-3} (this concentration was chosen as mangiferin has low solubility in acidic solution) of each identified compounds for 24 hours. The purpose of this weight loss measurement is to identify the individual best compound at inhibiting corrosion of mild steel in 1 mol dm^{-3} HCl among the identified compounds. The weight loss measurement revealed that adenosine had the best IE % at over 50 % while the remaining compounds had IE % of lower than 15 %.

All the compounds (identified and other unknowns) could have worked synergistically to produce the observed IE % of the leaf extract in chapter 3.

As such, adenosine was chosen for further studies as an individual compound.

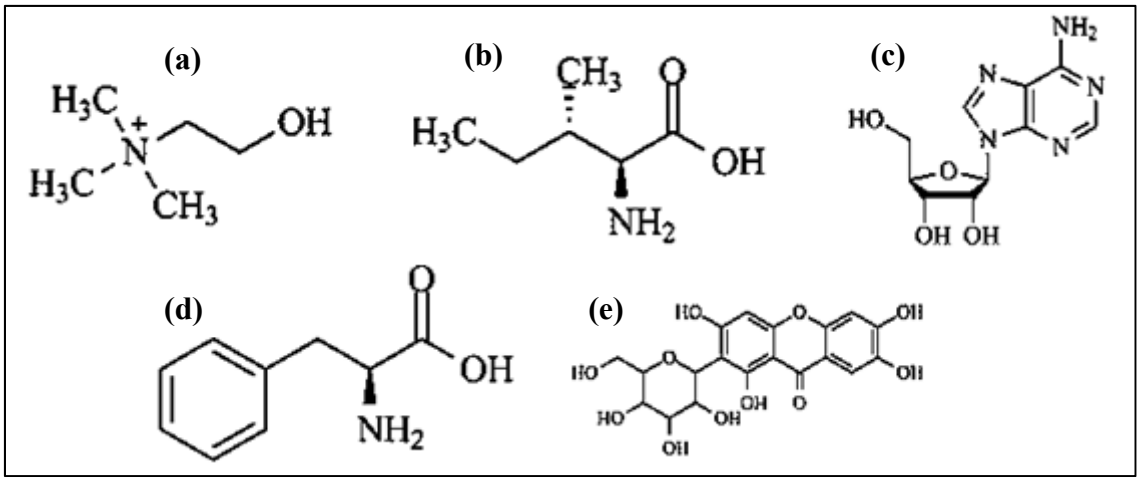

Figure 4.2. Structure of the identified compounds: (a) choline, (b) isoleucine, (c) adenosine, (d) phenylalanine and (e) mangiferin.

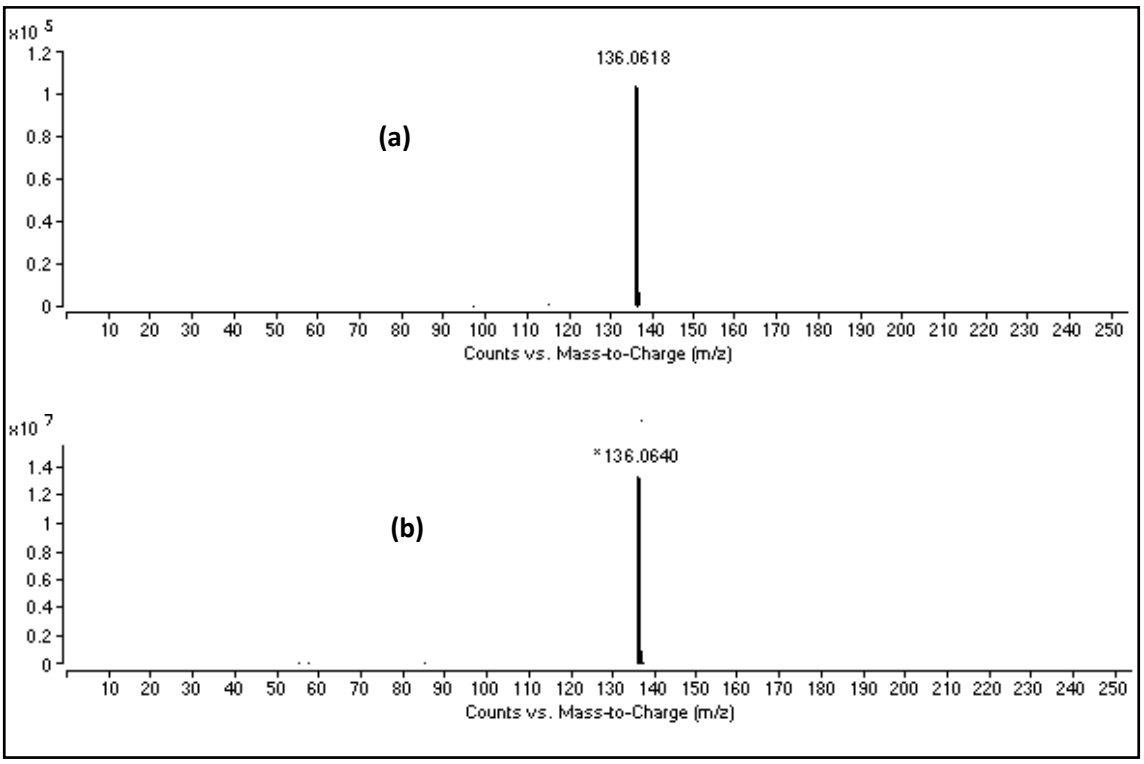

Figure 4.3. ESI product ion for adenosine in (a) agarwood extract (b) standard purchased.

Table 4.1. Compounds' identification in the *Aquilaria malaccensis* leaf extract produced by Q-TOF LC/MS.

Peak	Tentative Identification	Rt (min)	$[M-H]^+$	major fragment ions m/z (% base peak)	MF
1	Choline	1.426	104.1923	60.0817, 104.1078, 45.0362, 58.066	$C_5H_{14}NO$
2	Isoleucine	1.951	132.1965	86.0968, 69.0704, 44.0502, 41.0393	$C_6H_{13}NO_2$
3	Adenosine	2.158	268.2338	136.0635	$C_{10}H_{13}N_5O_4$
4	Phenylalanine	3.278	166.2346	120.0809, 103.0541	$C_9H_{11}NO_2$
5	Tryptophan	9.259	205.0983	146.0595, 118.0652, 144.0803, 188.0712, 160.0397	$C_{11}H_{12}N_2O_2$
6	Iriflophenone 3,5-C-beta diglucoside	11.093	571.1671	433.1112, 469.1145, 403.1007, 355.0825, 367.0824, 457.115, 421.093, 379.0829, 397.0932	$C_{25}O_{15}H_{30}$
7	Iriflophenone-3-C-beta glucoside	11.152	409.1155	195.0285, 313.0709, 231.0287, 219.0287, 271.06, 325.0708	$C_{19}H_{20}O_{10}$
8	Mangiferin	11.83	423.0935	273.0415, 303.0524, 327.0524, 369.0628, 405.0841	$C19_9H_{18}O_{11}$
9	12- oxo phytodienoic acid	16.516	293.2100	107.0846, 81.0696, 275.1997, 133.0992, 119.0856, 105.0701	$C_{18}H_{28}O_3$
10	Genkwanin	19.402	285.0768	285.0781, 286.0811	$C_{16}H_{12}O_5$

4.4. Conclusions

- The leaf extract contained several functional groups that can contribute to the adsorption property of the compounds in the leaf extract.
- Several compounds were tentatively identified and from those, five were successfully identified. From the successfully identified compounds, adenosine was the best inhibitor for mild steel in 1 mol dm^{-3} HCl solution.

References

[1] A. Anejjar, R. Salghi, A. Zarrouk, O. Benali, H. Zarrok, B. Hammouti, S. Al-Deyab, N. Benchat, A. Elaatiaoui, Int. J. Electrochem. Sci, 8 (2013) 11512-11525.

[2] A. El-Etre, Corrosion Science, 45 (2003) 2485-2495.

[3] S. Africa, African Journal of Pure and Applied Chemistry, 2 (2008) 046-054.

[4] M. H. Hussin, A. A. Rahim, M. N. M. Ibrahim, N. Brosse, Measurement, 78 (2016) 90-103.

[5] P. Mourya, S. Banerjee, M. Singh, Corrosion Science, 85 (2014) 352-363.

[6] S. Umoren, U. Eduok, A. Israel, I. Obot, M. Solomon, Green Chemistry Letters and Reviews, 5 (2012) 303-313.

[7] A. S. Yaro, A. A. Khadom, R. K. Wael, Alexandria Engineering Journal, 52 (2013) 129-135.

[8] A. Bouyanzer, B. Hammouti, L. Majidi, Materials Letters, 60 (2006) 2840-2843.

[9] N. Odewunmi, S. Umoren, Z. Gasem, Journal of Industrial and Engineering Chemistry, 21 (2015) 239-247.

[10] M. Deyab, Journal of Industrial and Engineering Chemistry, 22 (2015) 384-389.

[11] G. O. Avwiri, F. Igho, Materials Letters, 57 (2003) 3705-3711.

[12] N. M'hiri, D. Veys-Renaux, E. Rocca, I. Ioannou, N. M. Boudhrioua, M. Ghoul, Corrosion Science, 102 (2016) 55-62.

[13] R. M. Palou, O. Olivares-Xomelt, N. V. Likhanova, in: M. Aliofkhazraei (Ed.) Environmentally Friendly Corroison Inhibitors, InTech, 2014.

[14] S. Şafak, B. Duran, A. Yurt, G. Türkoğlu, Corrosion Science, 54 (2012) 251-259.

[15] P. Morales-Gil, G. Negrón-Silva, M. Romero-Romo, C. Ángeles-Chávez, M. Palomar-Pardavé, Electrochimica Acta, 49 (2004) 4733-4741.

[16] H. Hamani, T. Douadi, M. Al-Noaimi, S. Issaadi, D. Daoud, S. Chafaa, Corrosion Science, 88 (2014) 234-245.

[17] K. Ansari, M. Quraishi, A. Singh, Corrosion Science, 79 (2014) 5-15.

[18] V. Rajeswari, D. Kesavan, M. Gopiraman, P. Viswanathamurthi, K. Poonkuzhali, T. Palvannan, Applied Surface Science, 314 (2014) 537-545.

[19] M. Benabdellah, M. Benkaddour, B. Hammouti, M. Bendahhou, A. Aouniti, Applied Surface Science, 252 (2006) 6212-6217.

[20] A. Hamdy, N. S. El-Gendy, Egyptian Journal of Petroleum, 22 (2013) 17-25.

[21] H. Zhang, D. Wang, F. Wang, X. Jin, T. Yang, Z. Cai, J. Zhang, Desalination, 372 (2015) 57-66.

[22] M. Wahdan, A. Hermas, M. Morad, Materials Chemistry and Physics, 76 (2002) 111-118.

[23] X. Gao, M. Xie, S. Liu, X. Guo, X. Chen, Z. Zhong, L. Wang, W. Zhang, Journal of Chromatography B, 967 (2014) 264-273.

[24] A. Huda, M. Munira, S. Fitrya, M. Salmah, Pharmacognosy Research, 1 (2009) 270.

[25] A. Khalil, A. Rahim, K. Taha, K. Abdallah, Journal of Applied and Industrial Sciences, 1 (2013) 78-88.

[26] H. L. Y. Sin, A. A. Rahim, B. Saad, M. I. Saleh, P. B. Raja, Int. J. Electrochem. Sci, 9 (2014) 830-846.

[27] D. Rhodes, A. Hanson, Annual review of plant biology, 44 (1993) 357-384.

[28] S. D. McNeil, M. L. Nuccio, M. J. Ziemak, A. D. Hanson, Proceedings of the National Academy of Sciences, 98 (2001) 10001-10005.

[29] C. Dawczynski, R. Schubert, G. Jahreis, Food Chemistry, 103 (2007) 891-899.

[30] J. Svoboda, W. Boland, Phytochemistry, 71 (2010) 1445-1449.

[31] A. Aksüt, S. Bilgic, Corrosion Science, 33 (1992) 379-387.

[32] S. Ries, V. Wert, N. O'Leary, M. Nair, Plant Growth Regulation, 9 (1990) 263-273.

[33] Z. Kwade, A. Świaątek, A. Azmi, A. Goossens, D. Inzé, H. Van Onckelen, L. Roef, Journal of Biological Chemistry, 280 (2005) 17512-17519.

[34] T. Van Damme, D. Blancquaert, P. Couturon, D. Van Der Straeten, P. Sandra, F. Lynen, Phytochemistry, 103 (2014) 59-66.

[35] C. E. Stevenson, R. K. Hughes, M. T. McManus, D. M. Lawson, S. Kopriva, FEBS Letters, 587 (2013) 3626-3632.

[36] J. Feng, X. Yang, China journal of Chinese materia medica, 37 (2012) 230-234.

[37] A.-R. El-Sayed, A. M. Shaker, H. M. A. El-Lateef, Corrosion Science, 52 (2010) 72-81.

[38] M. Al-Otaibi, A. Al-Mayouf, M. Khan, A. Mousa, S. Al-Mazroa, H. Alkhathlan, Arabian Journal of Chemistry, 7 (2014) 340-346.

[39] R. Mohamed, M. Wong, The Malaysian Forester, 72 (2009) 45-51.

[40] S. Varvara, I. Rotaru, M. Popa, R. Bostan, M. Glevitzky, L. Muresan.

[41] D.-Q. Zhang, H. Wu, L.-X. Gao, Materials Chemistry and Physics, 133 (2012) 981-986.

[42] J.-J. Jeong, S.-E. Jang, S. R. Hyam, M. J. Han, D.-H. Kim, European Journal of Pharmacology, 740 (2014) 652-661.

5. ANTI-CORROSION BEHAVIOUR OF ADENOSINE ON MILD STEEL IN HCl

5.1. Introduction

The versatile mild steel used in various industries [1] has a problem of being susceptible to corrosion in hydrochloric acid, which is highly corrosive even in low concentrations. The solution to this problem was to incorporate corrosion inhibitors, as this is also one of the most economical methods of corrosion protection [2-5].

A study by our group has confirmed the presence of choline, isoleucine, adenosine, phenylalanine, and mangiferin in the methanol extract of *Aquilaria subintegra* (another agarwood-producing tree) leaves. As mentioned in chapter 4, among the identified compounds, the corrosion study conducted at a single concentration of 0.1 mmol dm^{-3} showed that adenosine is the best corrosion inhibitor for mild steel in 1 mol dm^{-3} HCl. Therefore, this chapter will present the study of adenosine as an individual compound for the corrosion inhibition effect.

There were many studies of corrosion inhibitors that reports the inhibition efficiency using the typical corrosion inhibitor tests including the weight loss study, the potentiodynamic polarization study and the electrochemical impedance spectroscopy measurement and mostly these tests were done in a cell or a container of a beaker shape that does not include any solution motion (hydrodynamic) such as flowing or rotation [6-9].

Although many corrosion inhibitor studies have measured the corrosion inhibition efficiency using stagnant conditions, the effect of hydrodynamic on the corrosion inhibition efficiency was lesser addressed. The study on the effect of hydrodynamic can be used to better describe the adsorption mechanism of the inhibitors onto the surface of

the metal and the processes that could take place in the presence of a flowing solution. This study of adenosine as a corrosion inhibitor will include the measurement of corrosion inhibition in the hydrodynamic condition.

In this chapter, adenosine (Figure 5.1) was used as a corrosion inhibitor for mild steel in 1 mol dm^{-3} HCl solution. The purpose of this study is to clarify the inhibition mechanism of adenosine. Adenosine was evaluated for its anti-corrosion activity on mild steel in 1 mol dm^{-3} HCl by the weight loss method and the electrochemical methods in stagnant and hydrodynamic conditions. The adsorption isotherm model was used to describe the adsorption of adenosine at a single temperature. Finally, the adsorption of adenosine is discussed from its HOMO structure.

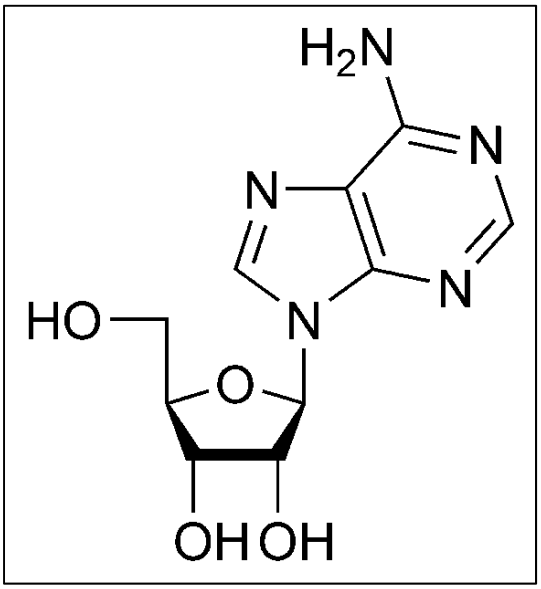

Figure 5.1. Chemical structure of adenosine.

5.2. Methodology

5.2.1. Sample source and solution preparation

Adenosine was purchased from Nacalai Tesque (Japan) and used for this study. 1 mol dm^{-3} HCl was prepared by diluting 37 % concentrated HCl of AR grade in Milli-Q water. Adenosine was diluted to suitable concentrations using the prepared HCl solution.

5.2.2. Specimen preparation

Mild steel with the composition of C, 0.08%; Mn, 1.26%; Si, 0.01%; P, 0.02%; Fe, 98.63%; was used for the surface morphology and electrochemical studies. The mild steel was successively polished with emery papers of grades 240, 400, 800, 1200 and degreased with acetone before it was rinsed with Milli-Q. It was then lightly towel-dried and left to dry at room temperature before use.

5.2.3. Weight loss study

The weight loss study was conducted using mild steels of dimension 1×3×0.06 cm. The initial weight of the mild steel was taken before immersion in 50 mL of the HCl solution. After 24 hours, the mild steel was removed, rinsed with distilled water and left to dry at room temperature before the final weight of the mild steel was taken. The weight loss was obtained from the difference of the weight at final and initial of the study. The IE of the inhibitor (in this chapter, adenosine) was calculated by the formula:

$$\text{IE } \% = \frac{(W_2 - W_1)}{W_2} \times 100$$

Where W_1 is the weight loss of the specimen immersed in HCl with the inhibitor (g) and W_2 is the weight loss of the specimen immersed in HCl without the inhibitor (g).

5.2.4. Electrochemical measurement methods

The electrochemical measurements were carried out using an Electrochemical Analyzer model 660A (ALS/ HCH instruments) with a three-electrode cell. Platinum was used as the counter electrode, Ag/AgCl was used as the reference electrode and the mild steel with exposure area of 2.55 cm^2 was used as the working electrode. The open circuit potential (OCP) was run for 30 minutes to obtain stabilization as previously reported [10, 11] before the electrochemical measurements were conducted. All the experiments were conducted at a temperature of 300 ± 2 K.

5.2.4.1. Potentiodynamic polarization measurement

The measurement was conducted at the scan rate of 1 mVs^{-1} (an anodic-to-cathodic sweep) over a potential range of ±300 mV with reference to E_{corr}. The linear segments of the anodic and cathodic curves were extrapolated to E_{corr} to obtain the corrosion current densities (I_{corr}). The IE of the inhibitor was calculated using the equation [12]:

$$\text{IE } \% = \left(\frac{I_2 - I_1}{I_2}\right) \times 100 \qquad (1)$$

Where I_1 is the current density of the specimen with the inhibitor (μA cm^{-2}) and I_2 is the current density of the blank specimen (μA cm^{-2}).

5.2.4.2 Electrochemical impedance spectroscopy (EIS) measurement

The measurement was conducted at the corrosion potential (E_{corr}) of the HCl solution with various concentrations of adenosine, which was within the range of -450 to -428 mV, with frequencies from 100, 000 to 0.1 Hz at an amplitude of 10 mV and a scan rate of 10 points per decade. The electrode potential was OCP (after 30 minutes). The results were represented in Nyquist diagrams and the electrical equivalent circuit for the system was obtained along with the charge transfer resistance (R_{ct}) value. The IE was calculated using the equation [12]:

$$\text{IE } \% = \frac{R_{ct(1)} - R_{ct(2)}}{R_{ct(1)}} \times 100 \qquad (2)$$

Where $R_{ct(1)}$ is the charge transfer resistance of the specimen with the inhibitor ($\Omega.cm^2$) and $R_{ct(2)}$ is the charge transfer resistance of the blank specimen ($\Omega.cm^2$).

5.2.4.3. Hydrodynamic condition study using channel-flow setup

The hydrodynamic condition of flowing medium and its effect on corrosion inhibition was studied using a channel-flow cell connected to a flowmeter (FC development Co. Ltd.) and Electrochemical Analyzer model 660 A (ALS/ HCH instruments). The electrodes used were similar to the stagnant cell condition, but with a working electrode with size of the area of exposure of 0.03 cm^2.

5.3. Results and discussion

5.3.1. Weight loss study

Table 5.1 shows the weight loss measurement for mild steel in 1 mol dm^{-3} HCl with and without adenosine at various concentrations. The table shows that adenosine has successfully inhibits corrosion in its presence with an increasing IE at increasing concentration of adenosine used. The IE increased until 78.88 % at the concentration of 1×10^{-3} mol dm^{-3} adenosine. Consequently, the corrosion rate decreased with the increase in the concentration of adenosine. The increasingly successful corrosion inhibition due to the increase in concentration of adenosine could be attributed to the increased area of the surface of mild steel that becomes protected by the adsorbed adenosine to shield the surface of mild steel from the corrosive medium.

Table 5.1. Weight loss measurement for mild steel in 1 mol dm^{-3} HCl with and without adenosine at various concentrations.

Concentration (mmol dm^{-3})	**IE %**	**Corrosion rate (mpy)**
Blank	-	509
0.1	57.44	217
0.3	61.85	194
0.6	73.58	135
1.0	78.88	107

5.3.2. Potentiodynamic polarization measurement

The potentiodynamic polarization measurement can determine the corrosion inhibition behavior across a specific range of potentials. The result is represented as Tafel plots in Figure 5.2. The parameters presented in Table 5.2 were obtained from the Tafel plots.

From Figure 5.2, the presence of adenosine caused the current density (I_{corr}) to decrease more than that of the blank, indicating a successful corrosion inhibition. Inhibitors can be categorized as anodic or cathodic inhibitors from the 85 mV change in E_{corr} with respect to the blank [13]. Adenosine did not display such a behavior, thus, it functions by inhibiting both the hydrogen gas evolution (cathodic reaction) and the metal dissolution (anodic reaction). Adenosine seems to be a mixed-type inhibitor, inhibiting both the anodic and the cathodic reaction, but adenosine predominantly works as an anodic inhibitor as the E_{corr} shifted slightly towards the anodic potential and B_a (anodic Tafel plot slope) apparently decreased more. The unchanged Tafel curve shape indicated that the corrosion mechanism was not altered with the addition of adenosine. The parallel lines of the cathodic reaction observed with increasing concentrations could indicate that the hydrogen evolution mechanism was not altered by the addition of adenosine, but it was activation-controlled [14]. The IE calculated from the I_{corr} of the Tafel curves increased as a result of the increase in the concentration of adenosine. The highest percentage of IE was at 75 % at the concentration of 1 mmol dm^{-3}.

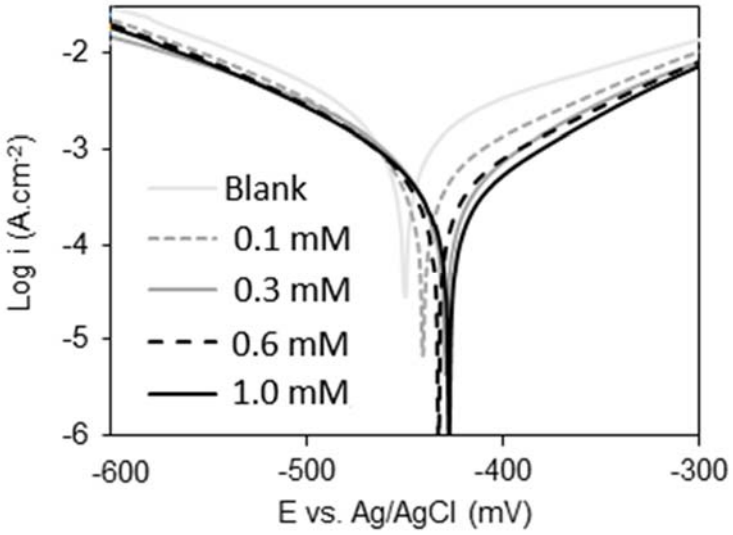

Figure 5.2. Tafel plot for mild steel in 1 mol dm^{-3} HCl with and without adenosine at various concentrations (mol dm^{-3}).

Table 5.2. Tafel plot parameters for mild steel in 1 mol dm^{-3} HCl with and without adenosine at various concentrations.

Specimen	**Concentration (mmol dm^{-3})**	I_{corr} **(mA cm^{-2})**	E_{corr} **(mV)**	B_a	$-B_c$	***IE %***
Blank	-	1.585	-450	98	66	-
Adenosine	0.1	0.794	-441	57	42	50
	0.3	0.501	-430	54	68	68
	0.6	0.398	-433	49	39	75
	1.0	0.398	-428	48	40	75

B_a = anodic Tafel plot slope, B_c = cathodic Tafel plot slope

5.3.3. Electrochemical impedance spectroscopy (EIS) measurement

EIS is a non-destructive electrochemical measurement that is reliable and valuable for analyzing reactions occurring on a surface [15]. For this study, the result was represented

as Nyquist plots. Constant phase element (CPE) was utilized to describe the data due to the depressed shape of the obtained semicircles [16]. Deviations from the ideal semicircle shape are characteristic of the dispersion in frequency and attributed to physical phenomena such as roughness and nonhomogeneity of solid surfaces during corrosion [17]. The presence of only a single capacitive loop for all the measurements indicated the corrosion process to be mainly charge-transfer-controlled [18]. The decrease in *n* values with the presence of adenosine inicated the increase in non-homogeneity of the surface due to the adsorption of the extract molecule [19,20]. The obtained experimental data were fitted to a 'Randles' type equivalent circuit model (Figure 5.3 inset) to obtain the parameters of the Nyquist plots.

The impedance of CPE is expressed by [21-23]:

$$Z_{CPE} = \frac{1}{Y_o(j\omega)^n} \quad (3)$$

Where Y_o is the frequency dependent magnitude of a pseudo-capacitance, j is $-1^{1/2}$, ω is the angular frequency and $-1 \leq n \leq 1$.

For this experiment, the CPE was obtained by fitting the experimental result into the equivalent circuit (Figure 5.3 inset). The CPE values of adenosine at various concentrations were less than that of the blank specimen. Reduction of the local dielectric constant and/or increase in the thickness of the electrical double layer might be the cause of the decrease in the CPE. This could suggest adsorption of the inhibitor molecules at the metal-solution interphase [24].

The diameters of the capacitive loops represent R_{ct}, and the IE was calculated from the R_{ct} value. From Figure 5.3, the presence of adenosine increased the diameter of the loop compared to the blank specimen. The increase in diameter indicated a resistance to charge

transfer; thus, the corrosion inhibition on mild steel by adenosine was successful. Supporting the finding in the potentiodynamic polarization measurement, the shapes of the loops were similar at all concentrations indicating that the corrosion mechanism was unchanged with the addition of adenosine. From Table 5.3, as the concentrations of adenosine increased, the IE also increased. The highest percentage of IE was at 63.1 % at the concentration of 1 mmol dm^{-3}.

From several reports, individual compounds that were discovered from plant extracts have IE that are less than the IE of the plant extract [25-27]. Possibly, the compounds in the extract, worked synergistically to produce the observed IE of the plant extract [28]. The corrosion IE of *Aquilaria malaccensis* extract, which contains some amount of adenosine, was reported to show IE of over 90 % at 1500 ppm [29]. Here, the weight loss study of adenosine as an individual compound showed an IE of close to 80 % at the concentration of 1 mmol dm^{-3}.

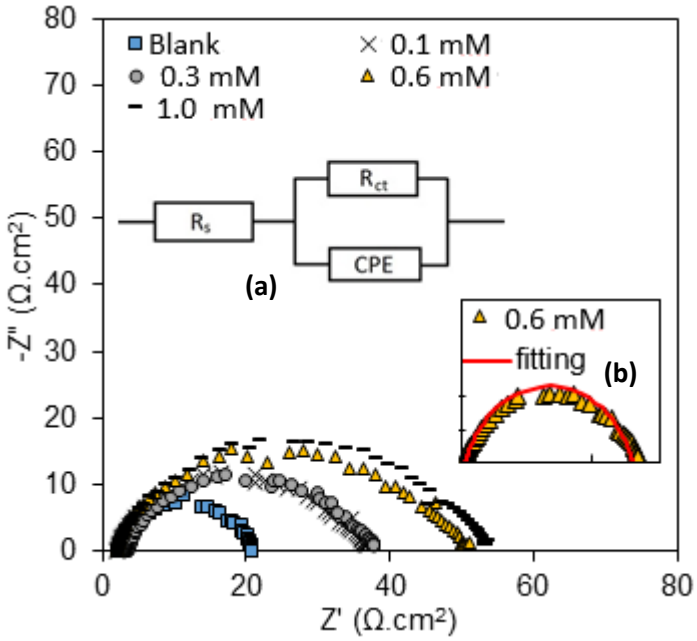

Figure 5.3. Nyquist plot for mild steel in 1 mol dm^{-3} HCl with adenosine at various concentrations (mol dm^{-3}), inset: (a) Equivalent circuit model, (b) Equivalent circuit fitting with Nyquist plot plot for mild steel in 1 mol dm^{-3} HCl with 0.6 mmol dm^{-3} adenosine.

Table 5.3. Nyquist plot parameters for mild steel in 1 mol dm^{-3} HCl with and without adenosine at various concentrations (stagnant condition).

Specimen	**Concentration (mmol dm^{-3})**	***R_s*** **($\Omega.cm^2$)**	**CPE ($\mu F/cm^2$)**	***n***	***R_{ct}*** **($\Omega.cm^2$)**	***IE %***
Blank	-	2.69	230	0.9482	17.66	-
Adenosine	0.1	2.61	190	0.8810	32.13	45.0
	0.3	3.72	233	0.8420	32.58	45.8
	0.6	2.51	176	0.8682	44.83	60.6
	1.0	2.57	178	0.8659	47.85	63.1

R_s = solution resistance, CPE = constant phase element, R_{ct} = charge transfer resistance.

5.3.4. Effect of hydrodynamic condition

Many inhibitors have been studied for their inhibition effect using the stagnant condition of a non-flowing cell, however, the performance of the inhibitors in hydrodynamic conditions are seldom explored. The hydrodynamic effects on the inhibition of adenosine on mild steel in 1 mol dm^{-3} HCl were studied using the channel flow setup. The channel-flow setup is able to control the flow rate of the medium in the cell and the inhibition effect of 1 mmol dm^{-3} adenosine was studied at the flow rate of 50 and 150 cm^3 min^{-1}. Due to the physical setup of the cell, potentiodynamic polarization analysis was deemed less suitable thus the EIS measurement was conducted. From the EIS measurement, the depressed semi-circle shape of the Nyquist curves was fitted into the 'Randles' equivalent circuit, which is the same equivalent circuit used to describe the inhibition of adenosine in the stagnant cell. The Nyquist plot (Figure 5.4) for the blank specimen and the specimen with adenosine on mild steel in 1 mol dm^{-3} HCl are presented in Table 5.4. The increase in flow rate has the effect of decreasing the resistance of both the blank specimen and specimen with adenosine, still, however, the resistance of the specimen with adenosine was higher than the blank specimen at all flow rates. The IE of adenosine at 50 cm^3 min^{-1} was 52.6 % and the IE of adenosine at 150 cm^3 min^{-1} slightly decreased to 48.0 %. The IE of adenosine at both flow rates were lower than the IE of adenosine at the stagnant condition (63.1 %) for the same concentration.

There are several effects during the hydrodynamic condition that could affect the inhibition [30] (illustrated as Figure 5.5):

a) The increase in flow increased the mass transport of the inhibitor molecules to the surface of the mild steel.

b) The Fe^{2+} ion from the dissolution of the mild steel surface was mass transported to the bulk solution, causing lesser [Fe^{2+}-Inhibitor] complex on the surface of the electrode.

c) The high flow velocity causes high shear stress and, in turn, causes the adsorbed inhibitor to desorb from the surface of the mild steel.

Effect (a) causes the increase of coverage on the surface by the inhibitor, thus improving the IE. Effect (b) and (c) causes the acceleration of the rate of corrosion. At hydrodynamic condition, the flowing medium may have increased the Fe^{2+} ion that was mass transported to the bulk solution, thus accelerating the corrosion. However, when the flow rate was increased to 150 cm^3 min^{-1}, the high velocity of the HCl solution caused sheer stress and more adenosine molecules desorbed from the surface of mild steel into the bulk solution, thus the IE decreased more at this flow rate. Thus, adenosine is a better inhibitor in a stagnant condition and the IE decreases with the presence of flow condition, especially at 150 cm^3 min^{-1}.

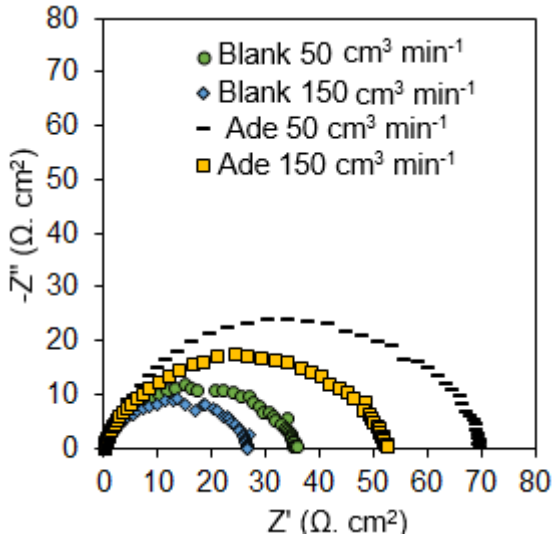

Figure 5.4. Nyquist plot for mild steel in 1 mol dm^{-3} HCl without and with adenosine at 1 mmol dm^{-3} (hydrodynamic condition).

Table 5.4. E Nyquist plot parameters for mild steel in 1 mol dm^{-3} HCl with and without adenosine at 1 mmol dm^{-3} (hydrodynamic condition).

Flow rate (cm^3 min^{-1})	**Specimen**	***R_s* ($\Omega.cm^2$)**	**CPE ($\mu F/cm^2$)**	***n***	***R_{ct}* ($\Omega.cm^2$)**	***IE %***
50	Without adenosine	0.24	218	0.8481	32.09	-
	With adenosine	0.15	288	0.8282	67.65	52.6
150	Without adenosine	0.05	254	0.8062	26.18	-
	With adenosine	0.13	178	0.8305	50.35	48.0

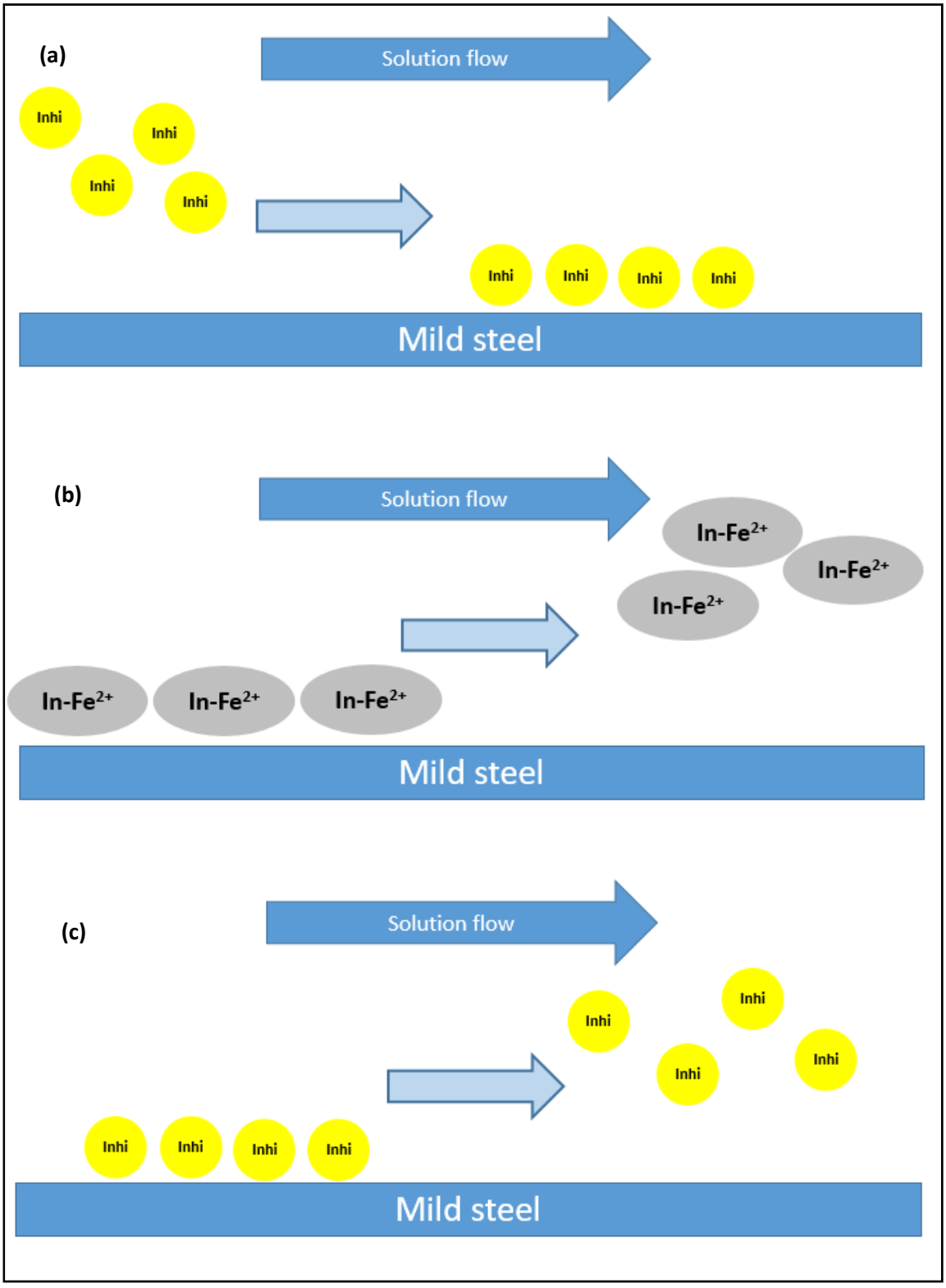

Figure 5.5. The effect of hydrodynamic condition: a) Flow condition brings in more inhibitor from the bulk solution, b) flow condition causes mass transportation of Fe^{2+}-Inhibitor complex away from the mild steel and c) flow condition causes sheer stress to adsorbed inhibitors.

5.3.5. Adenosine adsorption mechanism

Corrosion inhibition can be attributed to many mechanisms, and a widely accepted mechanism is the adsorption of inhibitors on the metal surface. The basis for this mechanism is that the adsorbed inhibitor molecules will prevent direct contact with the corrosive media on adsorbed (active) sites while the corrosion reaction normally occurs at non-adsorbed sites [31].

The adsorption of the inhibitors at a single temperature can be detailed using the adsorption isotherm models, and the two main types of adsorption are chemisorption and physisorption. For the purpose of this part, the IE data obtained from the weight loss measurement, EIS measurement and the potentiodynamic polarization of the stagnant condition was used to obtain the surface coverage (IE %/ 100 = θ) [32,33] and fitted into several adsorption isotherm models. It was found to best fit the Langmuir adsorption isotherm model, as was supported by the plotting of θ against concentration (Figure 5.6), yielding a typical shape of the curve that is best described by the Langmuir adsorption isotherm model.

The Langmuir adsorption isotherm model assumes that the adsorbed molecules only occupy one site and do not interact with other molecules. This is expressed by the following formula [32,33]:

$$\frac{c}{\theta} = \frac{1}{K_{ads}} + c \qquad (4)$$

Where C is the concentration (mol dm^{-3}), Θ is the surface coverage and K_{ads} is the adsorption constant.

Plotting C/Θ against C yields a linear curve in which the K_{ads} can be obtained from the slope of the linear curve.

Calculation of the Gibbs free energy is important to determine the type of adsorption for inhibitors and explain the inhibition mechanism. K_{ads} is reported to be related to the Gibbs free energy at a single temperature as follows [32, 33]:

$$\Delta G_{ads} = -RT \ln(K_{ads} \times A) \quad (5)$$

where ΔG_{ads} is the change in Gibbs free energy/standard adsorption free energy, K_{ads} is the adsorption equilibrium constant, R is the universal gas constant (8.314 J K^{-1} mol^{-1}), T is the absolute temperature (K) and A is the concentration of water (55.5 mol dm^{-3}) [32, 33]

A ΔG_{ads} value of -40 kJ mol^{-1} and more negative is associated with adsorption by a chemisorption process while a ΔG_{ads} value of -20 kJ mol^{-1} and less negative is associated with adsorption by a physisorption process [34]. The chemisorption process is attributed to charge transfer or sharing between the metal and inhibitor molecule while physisorption is attributed to electrostatic interactions between the charged metal and ions. The calculated ΔG_{ads} for the adsorption of adenosine for the weight loss measurement, EIS measurement and the potentiodynamic polarization measurement were -33.25, -32.99 and -34.26 kJ mol^{-1} respectively, thus, the likely adsorption mechanism is a mixed-type adsorption by both the physorption and chemisorption processes.

By comparing the Tafel plot (Figure 5.2) and the surface coverage, it was observed that at 0.1 mmol dm^{-3} adenosine, the surface coverage was at 0.5, the cathodic reaction (hydrogen evolution) inhibition was minimal and the anodic reaction (Fe dissolution) inhibition was the lowest among all tested concentrations. However, as the concentration of adenosine increased to 1 mmol dm^{-3}, the anodic reaction inhibition apparently increased more than the cathodic reaction inhibition, even when the surface coverage has

increased by 50 % at 0.75. This could indicate that the arrangement of adenosine molecules on the surface of mild steel was loosely packed, causing small ions of H^+ to be able to pass through the loosely packed barrier (created by the adsorption of the adenosine molecules) to obtain an electron for forming hydrogen gas. However, due to the Fe atom's larger size, the adsorptions of adenosine molecules were able to better inhibit the metal dissolution, as shown by the Tafel curve at Figure 5.2. From the Gibbs free energy of adenosine, the adenosine molecule can undergo adsorption by the physisorption and chemisorption process. In an acidic environment, the surface of the mild steel is positively charged. This caused the Cl^- ions to be attracted to the surface of the mild steel. In an acidic solution, the adenosine molecules are protonated and are adsorbed (by the physisorption process) onto the surface of mild steel with the Cl^- ion as a linking bridge [35]. Likewise the chemisorption adsorption process can be achieved by donating electrons from its electron-dense aromatic ring, O and N atoms of adenosine to the empty d-orbitals of the Fe atom to form a coordinating type of covalent bond with the Fe atom.

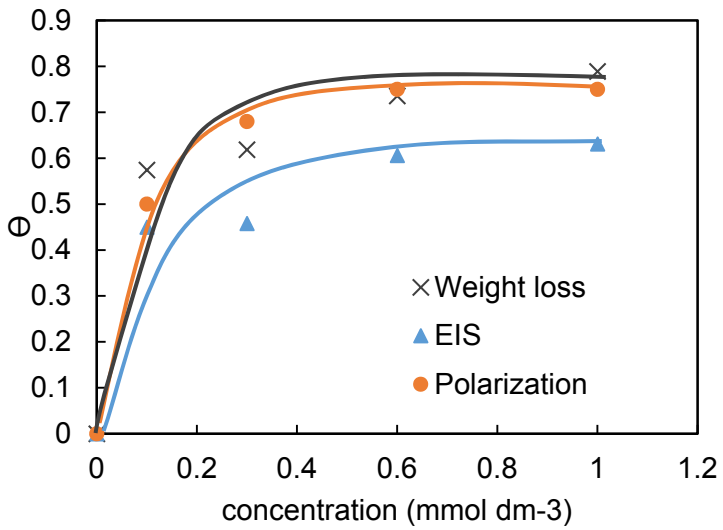

Figure 5.6. Relationship of surface coverage and the concentration of adenosine for weight loss, EIS and potentiodynamic polarization method.

5.4. Conclusions

- Adenosine has successfully inhibited the corrosion of mild steel in 1 mol dm^{-3} HCl and increasing the concentration of adenosine increased the IE up to 78.88 % at the concentration of 1 mmol dm^{-3}.
- Adenosine was more efficient as a corrosion inhibitor in the stagnant condition rather than the hydrodynamic condition.
- Adenosine acted as a mixed-type inhibitor (acting both as an anodic and cathodic inhibitor) but predominantly as an anodic inhibitor according to the potentiodynamic polarization measurement.
- Adenosine adsorbed onto the surface of the mild steel in 1 mol dm^{-3} HCl by the mixed-type process (by both the physisorption and chemisorption process) according to the calculated Gibbs free energy.

References

[1] M. Migahed, A. Abdul-Raheim, A. Atta, W. Brostow, Materials Chemistry and Physics, 121 (2010) 208-214.

[2] A. A. Khadom, A. Y. Musa, A. A. H. Kadhum, A. B. Mohamad, M. S. Takriff, Portugaliae Electrochimica Acta, 28 (2010) 221-230.

[3] K. Boumhara, M. Tabyaoui, C. Jama, F. Bentiss, Journal of Industrial and Engineering Chemistry, 29 (2015) 146-155.

[4] S. Umoren, U. Eduok, A. Israel, I. Obot, M. Solomon, Green Chemistry Letters and Reviews, 5 (2012) 303-313.

[5] A. A. Khadom, A. S. Yaro, Russian Journal of Physical Chemistry A, 85 (2011) 2005-2012.

[6] M. A. Amin, S. S. Abd El-Rehim, E. E. F. El-Sherbini, R. S. Bayoumi, Electrochimica Acta, 52 (2007) 3588-3600.

[7] J. Aljourani, K. Raeissi, M. A. Golozar, Corrosion Science, 51 (2009) 1836-1843.

[8] M. Lagrenée, B. Mernari, M. Bouanis, M. Traisnel, F. Bentiss, Corrosion Science, 44 (2002) 573-588.

[9] M. El Azzouzi, A. Aouniti, S. Tighadouin, H. Elmsellem, S. Radi, B. Hammouti, A. El Assyry, F. Bentiss, A. Zarrouk, Journal of Molecular Liquids, 221 (2016) 633-641.

[10] M. H. Hussin, M. J. Kassim, Materials Chemistry and Physics, 125 (2011) 461-468.

[11] F. Bentiss, M. Traisnel, M. Lagrenee, Corrosion Science, 42 (2000) 127-146.

[12] Y. Yan, W. Li, L. Cai, B. Hou, Electrochimica Acta, 53 (2008) 5953-5960.

[13] E. S. Ferreira, C. Giacomelli, F. C. Giacomelli, A. Spinelli, Materials Chemistry and Physics, 83 (2004) 129-134.

[14] B. Xu, Y. Liu, X. Yin, W. Yang, Y. Chen, Corrosion Science, 74 (2013) 206-213.

[15] D. Jayaperumal, Materials Chemistry and Physics, 119 (2010) 478-484.

[16] Y. Tang, X. Yang, W. Yang, R. Wan, Y. Chen, X. Yin, Corrosion Science, 52 (2010) 1801-1808.

[17] H. H. Hassan, Electrochimica Acta, 53 (2007) 1722-1730.

[18] S. Şafak, B. Duran, A. Yurt, G. Türkoğlu, Corrosion Science, 54 (2012) 251-259.

[19] A. Popova, E. Sokolova, S. Raicheva, M. Christov, Corrosion Science, 45 (2003) 33-58.

[20] W.-H. Li, Q. He, S.-T. Zhang, C.-L. Pei, B.-R. Hou, Journal of Applid Electrochemistry, 38 (2007) 289-295

[21] L. Chauhan, G. Gunasekaran, Corrosion Science, 49 (2007) 1143-1161.

[22] H. Ashassi-Sorkhabi, D. Seifzadeh, M. Hosseini, Corrosion Science, 50 (2008) 3363-3370.

[23] R. De Levie, Journal of electroanalytical chemistry and interfacial electrochemistry, 261 (1989) 1-9.

[24] A. O. Yüce, G. Kardaş, Corrosion Science, 58 (2012) 86-94.

[25] P. B. Raja, A. K. Qureshi, A. A. Rahim, H. Osman, K. Awang, Corrosion Science, 69 (2013) 292-301.

[26] N. M'hiri, D. Veys-Renaux, E. Rocca, I. Ioannou, N. M. Boudhrioua, M. Ghoul, Corrosion Science, 102 (2016) 55-62.

[27] A. A. Rahim, E. Rocca, J. Steinmetz, M. Kassim, R. Adnan, M. S. Ibrahim, Corrosion Science, 49 (2007) 402-417.

[28] R. M. Palou, O. Olivares-Xomelt, N. V. Likhanova, in: M. Aliofkhazraei (Ed.) Environmentally Friendly Corroison Inhibitors, InTech, 2014.

[29] H. L. Y. Sin, A. A. Rahim, C. Y. Gan, B. Saad, M. I. Salleh, M. Umeda, in: Measurement, 2016.

[30] X. Jiang, Y. Zheng, W. Ke, Corrosion Science, 47 (2005) 2636-2658.

[31] L. L. Shereir, Corrosion, Newnes-Butterworths, London, 1977.

[32] M. H. Hussin, A. A. Rahim, M. N. M. Ibrahim, N. Brosse, Measurement, 78 (2016) 90-103.

[33] R. Fuchs-Godec, V. Doleček, Colloids and Surfaces A: Physicochemical and Engineering Aspects, 244 (2004) 73-76.

[34] K. Krishnaveni, J. Ravichandran, A. Selvaraj, Ionics, 20 (2014) 115-126.

[35] R. Solmaz, G. Kardaş, M. Culha, B. Yazıcı, M. Erbil, Electrochimica Acta, 53 (2008) 5941-5952.

6. SURFACE MORPHOLOGY OF CORROSION OF MILD STEEL, EQCM STUDY AND QUANTUM CHEMICAL STUDIES

6.1. Introduction

Aside from the corrosion studies such as weight loss studies and the electrochemical studies, the effect of the addition of inhibitors into the corrosive medium can also be observed from the surface morphology of the mild steels. In general, the protective function of the inhibitors would serve to preserve the surface of the mild steel better and thus would have a smoother surface than the mild steel that was immersed in a corrosive medium without any inhibitor. The mechanism of the attack of HCl onto the mild steel occurs in such a way that pitting usually does not exist, it is mostly a uniform attack on the surface of the mild steel. The study of the surface morphology would thus provide a physical evidence of the inhibitors effect on the mild steel, and it is especially useful if it is observed continuously from the same site.

Adenosine is a purine nucleoside and that occurs in several plants including rice and agarwood trees. From our previous study, adenosine was found to be an excellent corrosion inhibitor of mild steel in HCl solution [1]. However, the real-time adsorption and desorption activity of adenosine during corrosion inhibition was not thoroughly studied and thus not fully understood. A quartz crystal microbalance (QCM) is an excellent instrument to study highly sensitive changes of interfacial processes, thus, it would be a suitable instrument to study the real-time adsorption and desorption activity of adenosine. This is due to the thin layer of electrodes used for the QCM studies which allows for thin layer film studies [2]. When paired with an electrochemical cell, it is referred to as an electrochemical quartz crystal microbalance (EQCM) and it allows for *in-situ* observation in the change of frequency of the surface of the working electrode

during the electrochemical measurement. From the Sauerbrey equation, the measured frequency change can be used to calculate the mass change (Δm) of the surface of the working electrode [3]. There were previous studies on the adsorption of various compounds [73-76] and corrosion tests [8,9] conducted using the QCM. However, despite the popularity of researches into corrosion inhibitors for iron and its alloys (mild, carbon and stainless steels) in HCl solution [10-14], the real-time adsorption of those inhibitor on a corroding surface of an iron working electrode in HCl solution was relatively unaddressed, especially using QCM.

In this chapter, the surface morphology of the mild steels immersed in 1 mol dm^{-3} HCl with and without the *Aquilaria malaccensis* leave extract and adenosine was observed using the laser scanning microscopy. Also, the real-time adsorption of adenosine was studied on an electrode sputtered with iron in 1 mmol dm^{-3} HCl, to simulate an acidic condition but which does not corrode the thin iron film (approximately 100 microns) too quickly. This study will be useful to understand the involvement of adenosine and the simultaneous effect of corrosion on the adsorption of adenosine on the surface of iron.

6.2. Methodology

6.2.1. Surface morphology

The surface morphology of the mild steel was monitored using a laser scanning microscope OLS 1200 (Olypmpus) at the magnification of 20×. The polished mild steels were immersed in 1 mol dm^{-3} HCl at the temperature of 300 ± 2 K, with and without 1000 ppm leaf extract and) 1×10^{-3} mol dm^{-3} adenosine and removed every 12 hours, dried and analyzed using the laser scanning microscope (LSM) on the same spot. The

mild steels were then re-immersed until the next analysis. These steps were repeated for 48 hours.

6.2.2. EQCM and QCM measurement system

A quartz crystal microbalance QCM 922A (Seiko EG&G) was used to measure the frequency change from the quartz electrode while a potentiostat VersaSTAT 4 (Princeton Applied Research, AMETEK®) was used for the electrochemical measurements. An Ag/AgCl electrode (saturated KCl electrolyte, platinum wire as salt bridge) [15] was used as the reference electrode, platinum was used as the counter electrode and an AT cut quartz-gold coated electrode sputtered with iron (Seiko EG & G) (Figure 6.1) was used as the working electrode. The setup for the experiment was as Figure 2.7 (chapter 2). All experiments were conducted at atmosphere condition and temperature of 294 ± 2 K. Prior to each measurement, the working electrode was cleaned by polarizing at -800 mV vs. Ag/AgCl for 300 s. The 1 mmol dm^{-3} HCl solution was prepared using AR grade 37 % concentrated HCl and diluted using double distilled water. Adenosine was purchased from Nacalai Tesque and diluted using the prepared HCl solution to suitable concentrations.

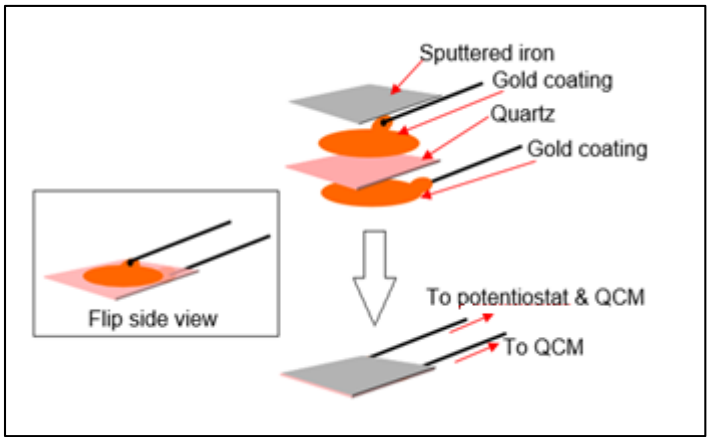

Figure 6.1. AT cut quartz-gold coated electrode sputtered with iron.

6.2.3. Quick microgravimetric analysis

After the cell setup, the frequency was recorded when the cell contained ten mL of 1 mmol dm^{-3} HCl (time is 0 s). The cell was allowed to stabilize until time was 300 s, then the first aliquot of concentrated adenosine (two mL) was added to achieve 1 mmol dm^{-3} of adenosine. The frequency was allowed to stabilize until time was 600 s. The steps of adding the concentrated adenosine and allowing the frequency to stabilize for another 300 s was repeated until the final concentration of 4 mmol dm^{-3} of adenosine was achieved.

6.2.4. Extended time microgravimetric analysis

After the cell setup, the frequency was recorded when the cell contained 18 mL of 1 mmol dm^{-3} HCl (time is 0 s). The cell was allowed to stabilize until time was 300 s, then the aliquot of concentrated adenosine (two mL) was added to achieve the final concentration of 2 or 3.74 mmol dm^{-3} adenosine. The frequency was observed for over 7000 s.

6.2.5. Linear sweep voltammetry (LSV) with simultaneous QCM measurement

20 mL of the 1 mmol dm^{-3} HCl solution with adenosine at various concentration was used. After the cathodic cleaning step, the open circuit potential (OCP) was recorded for 15 s. The LSV measurement was conducted at a sweep rate of 5 mVs^{-1} within a range of OCP ± 250 mV vs. Ag/AgCl.

6.3. Results and discussion

6.3.1. Surface morphology

To obtain the same spot laser analysis, the surface of the mild steel was etched to form a straight line (for aligning purposes) and a tiny dot above it, then the image was taken at a fixed distance from the dot for every analysis. From Figure 6.1, the mild steel surface immersed in 1 mol dm^{-3} HCl only was rougher than the surface of the mild steel immersed in 1 mol dm^{-3} HCl with the leaf extract or adenosine for all recorded durations. Thus, the leaf extract and adenosine have successfully retarded the corrosion of the mild steel in 1 mol dm^{-3} HCl solution. The observation was further supported by the surface roughness (R_a) obtained (Table 6.1), as the difference in R_a (0 hour and 48 hours) of the surface of mild steel for the leaf extract and adenosine was 0.305 and 0.573 μm, respectively, while that for the blank specimen was 1.768 μm. This condition of the obviously smoother surface of the mild steel specimen immersed in 1 mol dm^{-3} HCl shows that both the leaf extract and adenosine are a corrosion inhibitors that forms a protective thin film over the surface of the mild steel. Therefore, the corrosion inhibitors can be used as a low cost and effective inhibitor of mild steel in 1 mol dm^{-3} HCl.

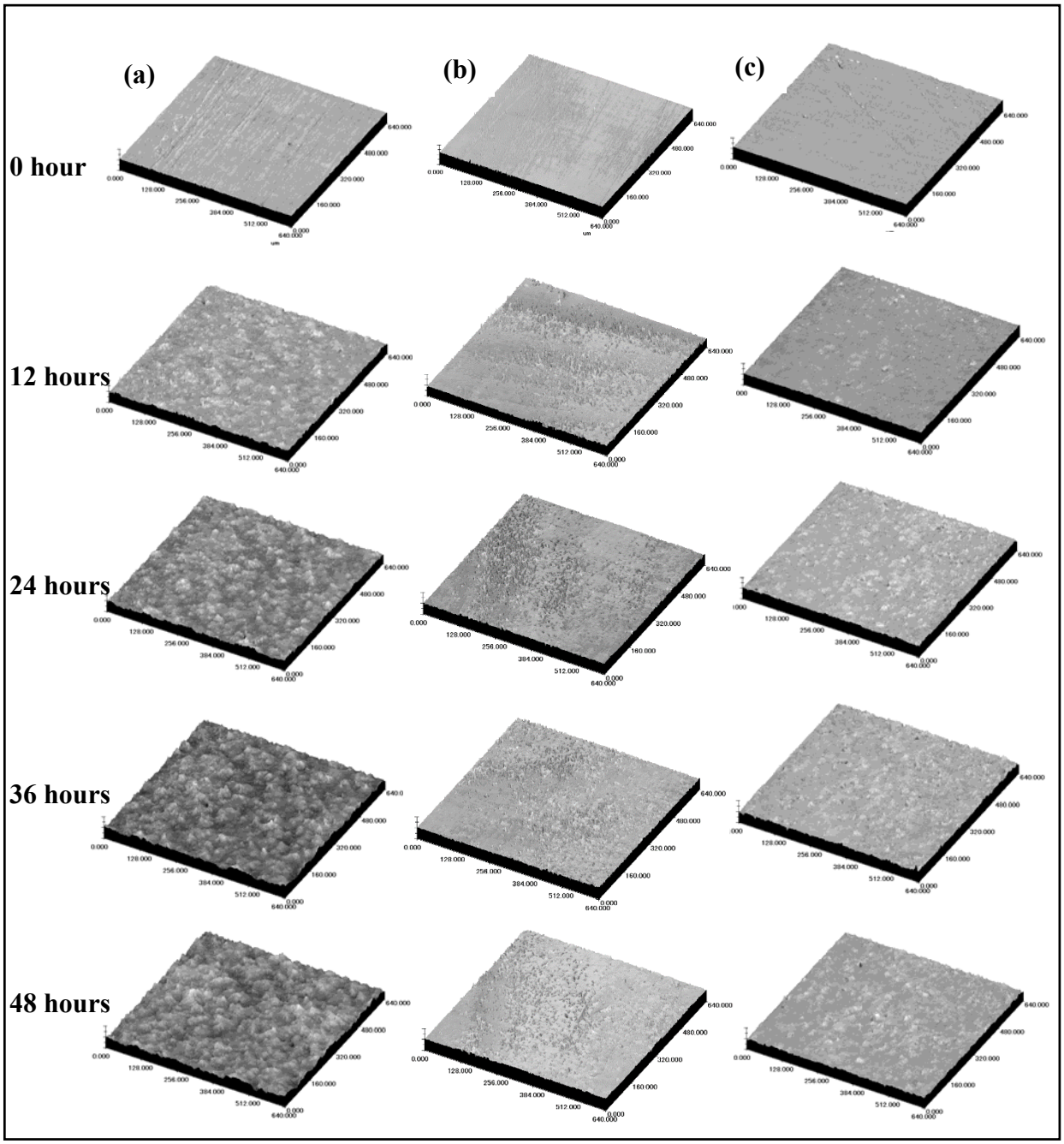

Figure 6.1. Surface morphology of mild steel immersed in a) 1 mol dm^{-3} HCl only, b) 1 mol dm^{-3} HCl with 1000 ppm *Aquilaria malaccensis* leaf extract, c) 1×10^{-3} mol dm^{-3} adenosine.

Table 6.1. Difference in R_a (0 hour and subsequent time) for mild steel in 1 mol dm^{-3} HCl with and without 1000 ppm *Aquilaria malaccensis* leaf extract and 1×10^{-3} mol dm^{-3} adenosine.

Specimen	**Δ*R*a (μm)**			
	12 hours	**24 hours**	**36 hours**	**48 hours**
Blank	0.939	1.334	1.686	1.768
With leaf extract	0.023	0.205	0.263	0.305
With adenosine	0.309	0.517	0.631	0.573

where ΔR_a = Difference in R_a at 0 hour and subsequent time

6.3.2. Quick microgravimetric analysis

The calculation to obtain Δ*m* from the frequency change using the Saurbrey equation is [3]:

$$\Delta f = \frac{2f_0^2}{A\sqrt{\rho_q \mu_q}} \Delta m \quad (1)$$

where Δ*f* is the frequency change observed (Hz), f_0 is the resonant frequency (Hz), A is the piezzoelectrically active crystal area (cm^2), ρ_q is the density of quartz (2.648 g cm^2), μ_q is the shear modulus of quartz for AT-cut crystal (2.947×10^{11} g cm^{-1} s^{-2}) and Δ*m* is the mass change (g).

The calculated Δ*m* against time with the gradual addition of concentrated adenosine into 1 mmol dm^{-3} HCl solution on the quartz electrode is shown in Figure 6.2. From the calculated Δ*m*, negative value of Δ*m* indicates the mass loss of the surface of the Fe sputtered electrode. At 0 s, the cell contained ten mL of 1 mmol dm^{-3} HCl and the constant mass decrease of the surface of the quartz electrode was caused by the dissolution of the iron into the bulk solution by the corrosive solution. After 300 s, the appropriate aliquots

(to achieve 1, 2, 3, 3.74, 4 mmol dm^{-3} adenosine) were added at every 300 s interval. At the beginning of after each addition of concentrated adenosine aliquots, the mass decreased apparently for the first 30 s. The apparent mass decrease was not caused by the dissolution of the surface of iron but was caused by the displacement of the pre-adsorbed water molecules on the surface of the iron by the adsorption of the adenosine molecules [16]. The corrosion potential was observed to shift to more positive direction with the increase of the concentration of adenosine and this indicated an anodic-type control inhibition by adenosine [17]. For 1 to 3 mmol dm^{-3} adenosine, after the initial 30 s of their respective addition, the mass continued to decrease but at a lower rate than the pre-addition of the respective aliquots, thus the addition of the aliquots successfully decreased the rate of iron dissolution (successful corrosion inhibition activity). However for 3.74 and 4 mmol dm^{-3} adenosine, after the initial 30 s of their respective addition, the mass begun to increase steadily. The mass gain could be caused by the adsorption of a layer, believed to be an adenosine-iron complex.

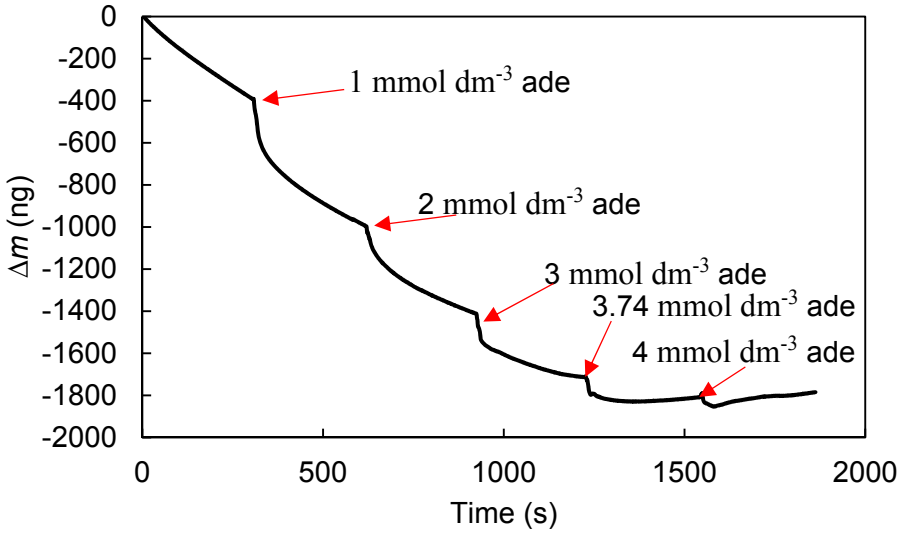

Figure 6.2. Mass change against time with the gradual addition of concentrated adenosine into 1 mmol dm^{-3} HCl solution on the quartz electrode at OCP. The concentration pointed by the red arrows indicates the total concentration of the solution at when the aliquot was added.

6.3.3. Extended time microgravimetric analysis

The long-term observation of the adsorption of the adenosine molecules/complex from the microgravimetric analysis was then conducted. In this experiment, the frequency was recorded from time 0s when the cell contained 18 mL of 1 mmol dm^{-3} HCl. After 300s, the appropriate aliquots were added into the cell to obtain concentrations 2 or 3.74 mmol dm^{-3} adenosine and the Δm was observed over an extended period. Figure 6.3 shows the result of the mass change of the surface of the quartz electrode against time after the addition of the aliquots. From Figure 6.3, the mass loss was at a constant rate for the surface of the quartz electrode when the blank aliquot was added as the corrosion process was not interrupted with the addition. When 2 or 3.74 mmol dm^{-3} adenosine was added, the mass of the surface more apparently decreased until 1500 s and this could be caused

by the displacement of water molecules due to the adsorption of the adenosine molecules. From 1500 s onwards, for 2 mmol dm^{-3} adenosine, mass gained slightly until 3000 s and finally decreased in mass at a constant but lower rate than blank from 3000 s onwards. This indicated that 2 mmol dm^{-3} adenosine decreased the iron dissolution. From 1500 s onwards, for 3.74 mmol dm^{-3} adenosine, mass increased at an almost constant rate until the end of the experiment. It is proposed that the mass gain until 3000 s for 2 mmol dm^{-3} and 3.74 mmol dm^{-3} was caused by the adsorption of a layer. As the adsorption of the layer reaches equilibrium, the nett reaction after 3000 s was the iron dissolution (at exposed sites) as the mass continues to decrease steadily. For 3.74 mmol dm^{-3} adenosine after 3000 s, the layer adsorption probably have not reached equilibrium, thus the continuous mass gain. During the adsorption of the layer, some of the adsorbed layer species might desorb from the surface, however, the equilibrium could be shifted to favour more adsorption than desorption, thus the increase in the mass of the surface. Visual observations suggest that iron continuously dissolves as the gold under-coat became more exposed. Therefore, it is believed that as the iron continuously dissolves into Fe^{2+}, adenosine could form complexes with Fe^{2+} [18] and adsorb as a layer.

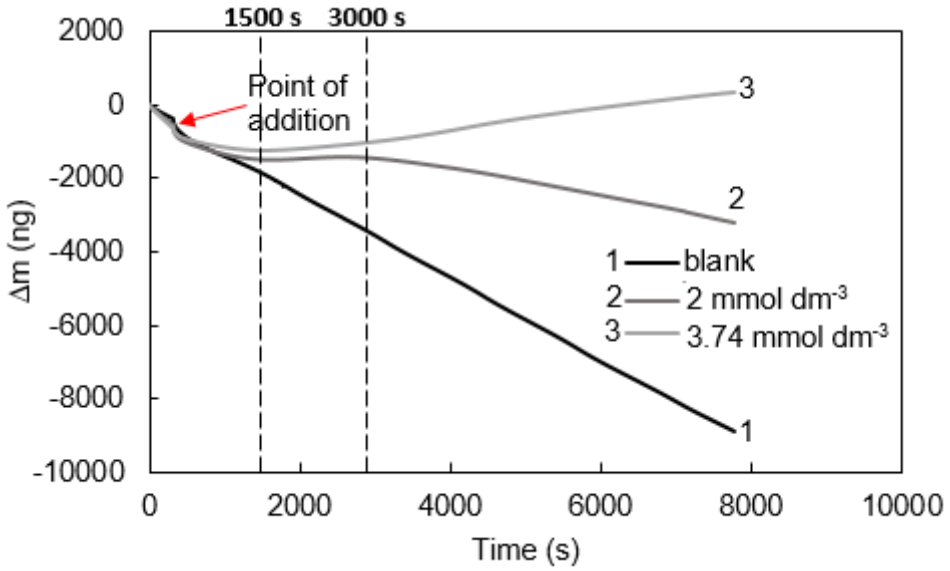

Figure 6.3. Mass change against time after the addition of concentrated adenosine into 1 mmol dm^{-3} HCl solution on the quartz electrode at OCP.

6.3.4. Linear sweep voltammetry (LSV) with simultaneous QCM measurement

A simultaneous experiment on LSV and QCM was carried out to observe the real-time mass change of the electrode when it is scanned (polarized) from the anodic to cathodic region within the range of OCP ± 250 mV and the result is shown in Figure 6.4. The scan was conducted across the regions to simulate reported electrochemical studies and also the electrochemical studies in our group regarding the anti-corrosion activities of adenosine [1, 19-21]. A lower current density (less deviation from 0 A for Figure 6.4 a) indicates higher resistance. A higher resistance indicates a better corrosion inhibition activity and subsequently less mass loss by iron dissolution. Therefore, the resistance should be negatively related to the mass loss by iron dissolution. From Figure 6.4 (a), the resistance of the quartz electrode seems to be in an increasing order of blank< 2 mmol dm^{-3} ade< 3.74 mmol dm^{-3} ade. However, the QCM study (Figure 6.4 b) showed the mass

loss was in an increasing order of blank<2 mmol dm^{-3} ade< 3.74 mmol dm^{-3} ade, which is positively related to the resistance. Scanning from the anodic region to OCP, for blank, the mass loss accounts for the anodic reaction of the blank which was the iron dissolution. However, since the anodic polarization with the presence of adenosine showed more mass loss than blank, it is proposed that the anodic reaction with the presence of adenosine could consist of iron dissolution as well as the direct participation of the inhibitors [22] in the form of desorption of the pre-adsorbed adenosine molecules/complex (formed and adsorbed at the beginning of the measurement). For blank, as it was polarized towards the cathodic region, the rate of mass loss becomes lower until it was almost plateau, indicating that there were no more mass loss as the cathodic reaction takes place. However, in the presence of adenosine, there were slight mass gain on the surface of the electrode when it was polarized to the cathodic region. The mass gain could be caused by the re-adsorption of the adenosine molecules/complex onto the surface of the electrode. The known cathodic reaction of iron in HCl solution is hydrogen evolution. Since blank did not show more mass increase during the cathodic reaction although the cathodic reaction of blank should produce more hydrogen (than 1 and 3.741 mmol dm^{-3} ade) as the cathodic reaction of blank was not inhibited, the hydrogen reaction was believed to not affect the mass change as the hydrogen produced probably escaped immediately and did not participate in the adsorption.

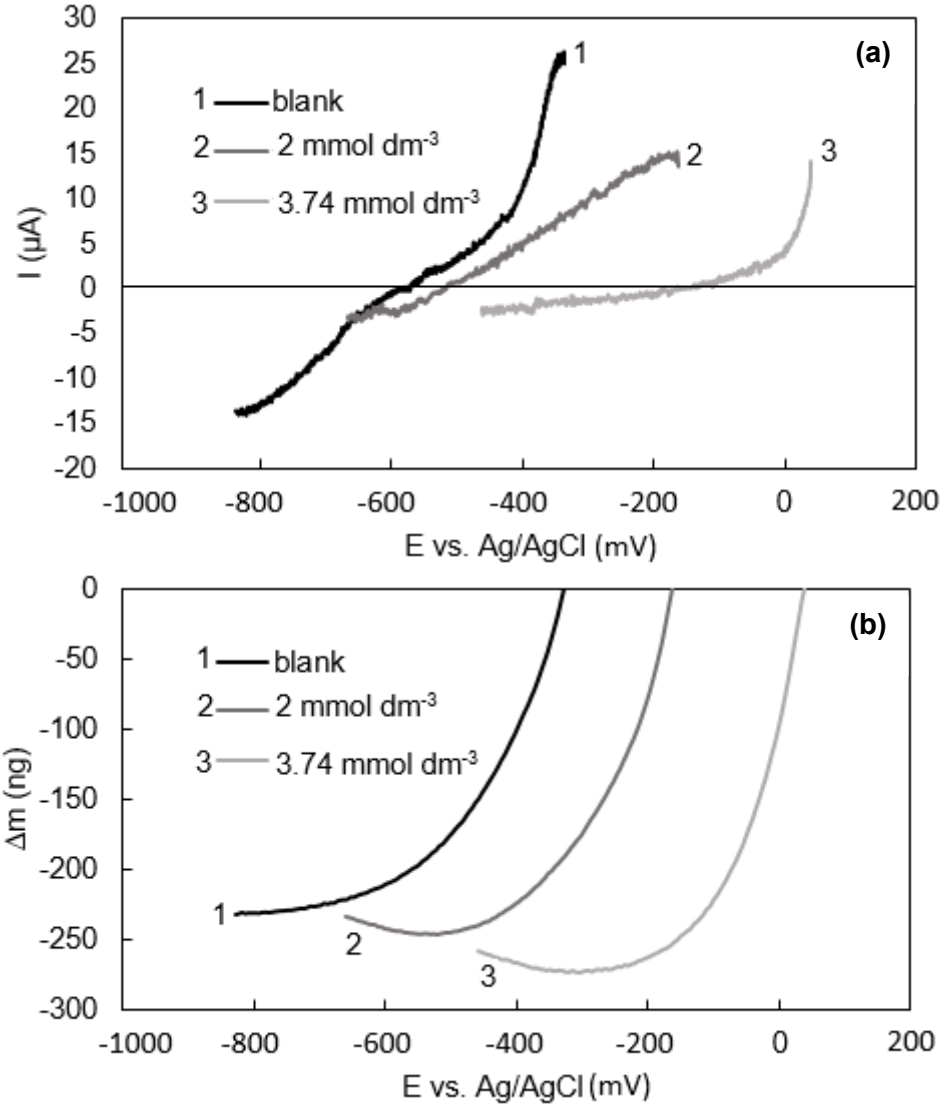

Figure 6.4. (a) LSV measurement in 1 mmol dm^{-3} HCl with adenosine at different concentration and (b) the simultaneous mass change.

Figure 6.5 demonstrates the considerations of the processes that could have caused the observed mass changes of the surface of iron in HCl solution. The three processes that could affect the mass change of the iron surface are the water molecules displacement by the adsorption of adenosine molecules/complex (Figure 6.5a), the iron dissolution and

adenosine molecules/complex desorption for the anodic reaction (Figure 6.5b) and adenosine molecules/complex re-adsorption for the cathodic reaction (Figure 6.5c).

The most probable reaction for each processes are:

for Figure 6.5(a), $Ade_{(sol)} + H_2O_{(ads)} \longrightarrow Ade_{(ads)} + H_2O_{(sol)}$ (2)

for Figure 6.5(b), $[Ade]_{(ads)} \longrightarrow [Ade]_{(sol)}$ (3)

$Fe \longrightarrow Fe^{2+} + 2e$ (4)

for Figure 6.5(c), $[Ade]_{(sol)} \longrightarrow [Ade]_{(ads)}$ (5)

At OCP, the mass gain could be caused by the displacement of the water molecules due to the adsorption of adenosine (Figure 6.5a), as shown by the microgravimetric analyses when adenosine was first introduced into the corroding system of iron in HCl solution. The QCM successfully allowed for the real-time observation of mass gain on the corroding surface of iron in the presence of adenosine which was probably caused by the adsorption of an adenosine-iron complex layer. While the microgravimetric analyses allows for mass change observation of the surface of iron at OCP, where both the anodic and cathodic reactions takes place, the LSV analysis allows for the observation of the mass changes due to the anodic and cathodic reactions separately. The electrochemical measurement showed that the adenosine molecules/complex could undergo desorption when it was polarized through the anodic region (Figure 6.5 b) and adsorption when it was polarized to the cathodic region (Figure 6.5 c). While many previous studies of corrosion inhibitors [10-14] had discussed the iron dissolution and hydrogen evolution for iron (or steels) corrosion in HCl solution, the EQCM has allowed for the observation of the direct participations of the inhibitors during the corrosion inhibition process. While these discoveries unravel the process in a new viewpoint, there are several aspects of these

discoveries that could not be completely explained yet, such as the continuous mass gain of 3.74 mmol dm^{-3} adenosine exhibited in the extended microgravimetric measurement and the behaviour of the adsorption and desorption of adenosine when polarized from the anodic to the cathodic region. Although the comparison of the results with a blank solution could negate the effects of other ions that similarly exist in the blank and solutions with adenosine, the mass gain process could still be attributed with the adsorption of other ions or molecules species present in the cell aside from the adenosine molecules/complex, such as water molecules that could be trapped within the layers of adsorbed adenosine molecules/complex [23]. More studies could be proposed in the future to understand these phenomena.

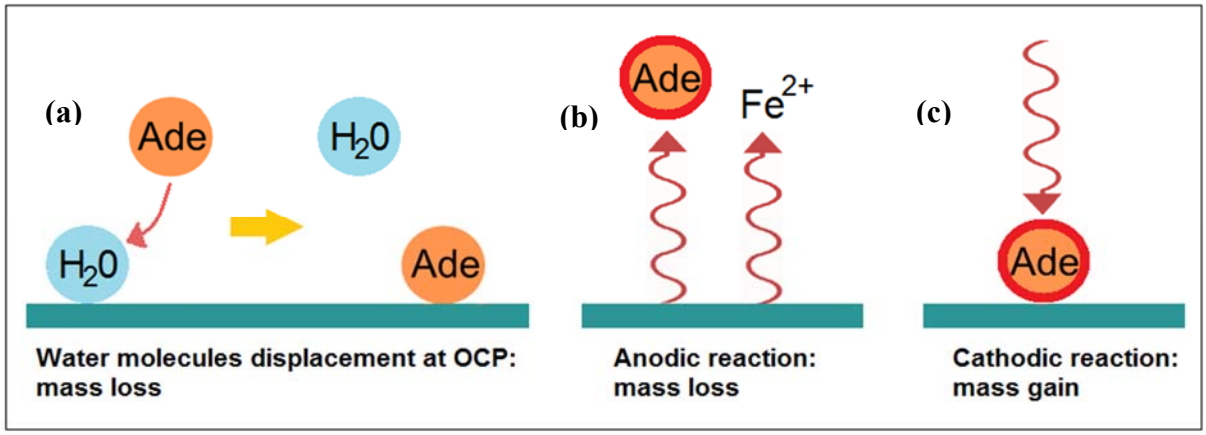

Figure 6.5. Schematic illustration of the processes that could have caused the observed mass changes of the surface of iron in HCl solution: (a) water molecules displacement by adenosine adsorption at OCP (mass loss), (b) desorption of adenosine molecules/complex and iron dissolution for the anodic reaction (mass loss) and (c) adenosine molecules/complex adsorption for the cathodic reaction (mass gain).

6.3.5. Quantum chemical studies

Since there could be two possible mechanisms of adsorption (physisorption and chemisorption) for adenosine from the calculated Gibbs free energy, adenosine could be adsorbed by electrostatic attraction (physisorption) and charge transfer (chemisorption). In this work, the chemisorption mechanism, which is possibly the main contributor for the IE of adenosine, as shown from the ΔG_{ads} values that were closer to -40 kJ mol^{-1} (in chapter 5), will be further explored using the quantum chemical studies. The possible sites of electron exchange can be obtained using the quantum chemical studies and thus the orientation of the adenosine molecule for adsorption onto the surface of the mild steel can be proposed. The calculated HOMO and LUMO spatial distributions and the Fukui function would be able to determine the most probable sites of adsorption from the distribution of the electron density. For this purpose, the structure of the neutral and the most possible protonated structure of adenosine [24] was evaluated (Figure 6.6). The spatial distributions of the HOMO and LUMO and the Fukui indices were obtained ugsing Winmostar(LA) V6.015 (Winmostar by Delphi) and MOPAC2016 Version 16.146W (by Prof. James J. P. Stewart, Stewart Computational Chemistry, HTTP://OpenMOPAC.net). All structures were calculated based on the PM7 method, and the solvent effect was taken into account by the software by including the solvent (water) dielectric constant and calculated using the conductor-like screening model (COSMO) method. Figures 6.7, 6.8 and 6.9 show the HOMO and LUMO spatial distribution and the Fukui indices of the neutral adenosine and the protonated adenosine. HOMO is associated with electron donating ability and LUMO is associated with the electron accepting ability [25,26]. As the Quantum calculation accounts from the viewpoint of chemisorption interaction, a good inhibitor for chemisorption interaction would have a low LUMO-HOMO gap. The

calculated LUMO-HOMO gap for the neutral and the protonated adenosine is 8.5078 and 8.6363 eV, indicating that the neutral adenosine would be more suitable for a chemisorption interaction. The Fukui indices can be used to predict the reaction selectivity of the atoms at the adenosine molecules [27,28]. From Figures 6.7 and 6.8, the possible sites of electron exchange from HOMO and LUMO spatial distribution and the Fukui functions were in agreement for both the neutral and the protonated adenosine. The most possible sites of the electron exchange on the adenosine molecule were the aromatic rings including $–NH_2$. Thus, it was proposed that the adenosine molecule (both neutral and protonated) would most likely approach the surface of mild steel with the aromatic rings flatly facing the surface of the mild steel, with the aliphatic ring/chain pointing away from the surface of the mild steel, to obtain maximum coverage by the electron dense aromatic rings as Figure 6.9.

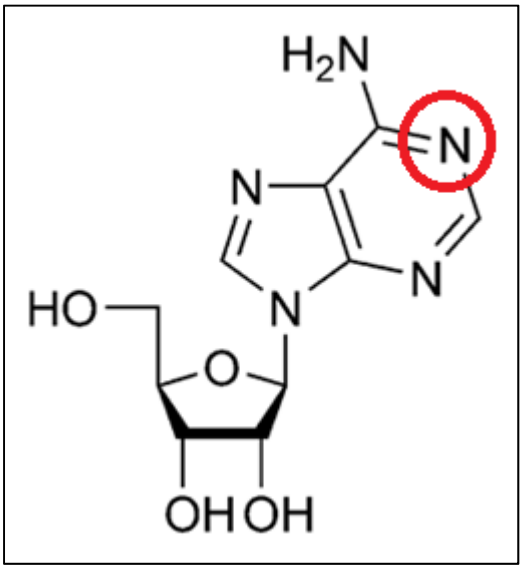

Figure 6.6. Chemical structure of adenosine and most possible site of protonation (red circle)

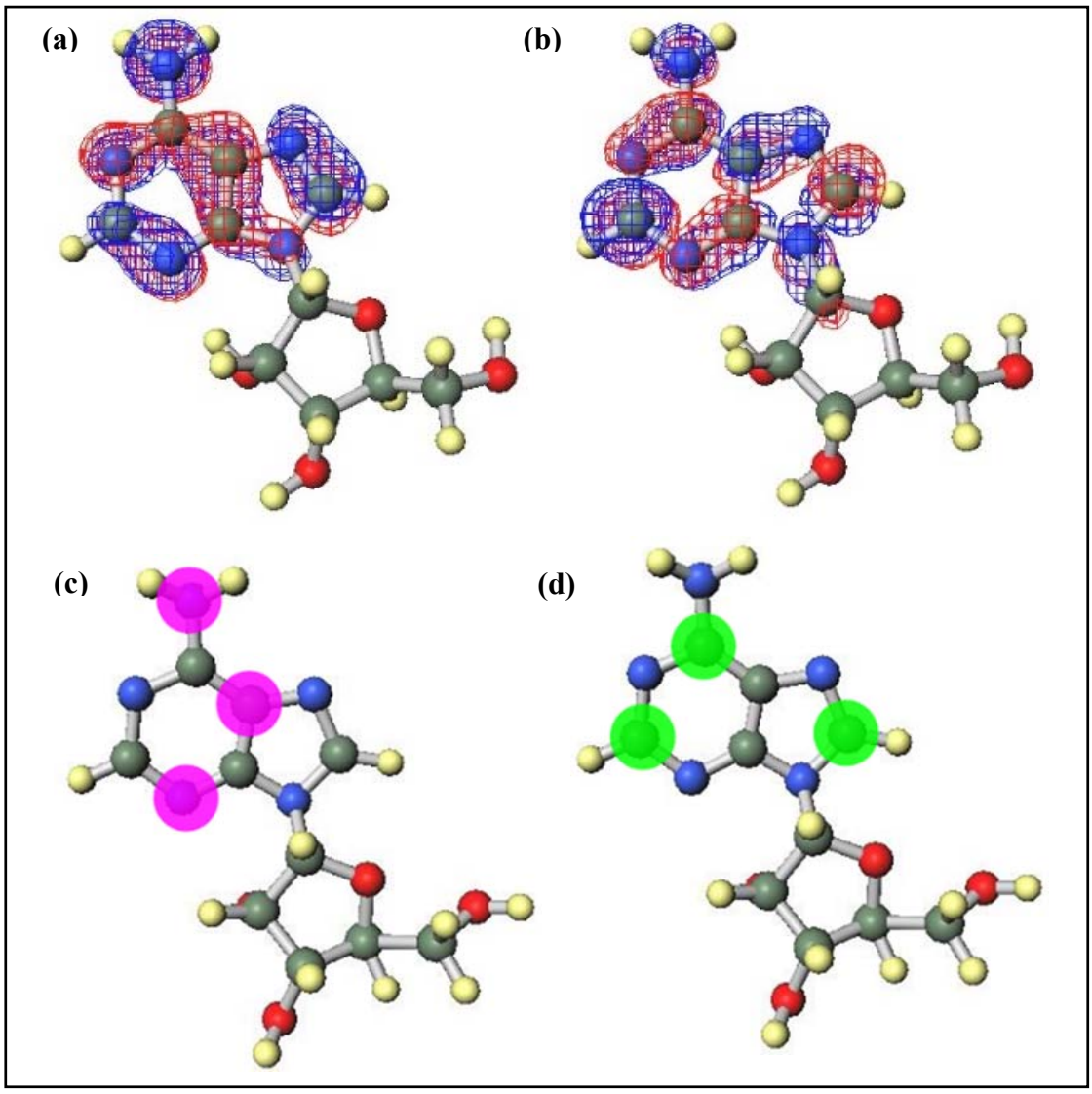

Figure 6.7. (a) HOMO spatial distributions, (b) LUMO spatial distributions, (c) f- isosurfaces of Fukui functions and (d) f+ isosurfaces of Fukui functions for neutral adenosine.

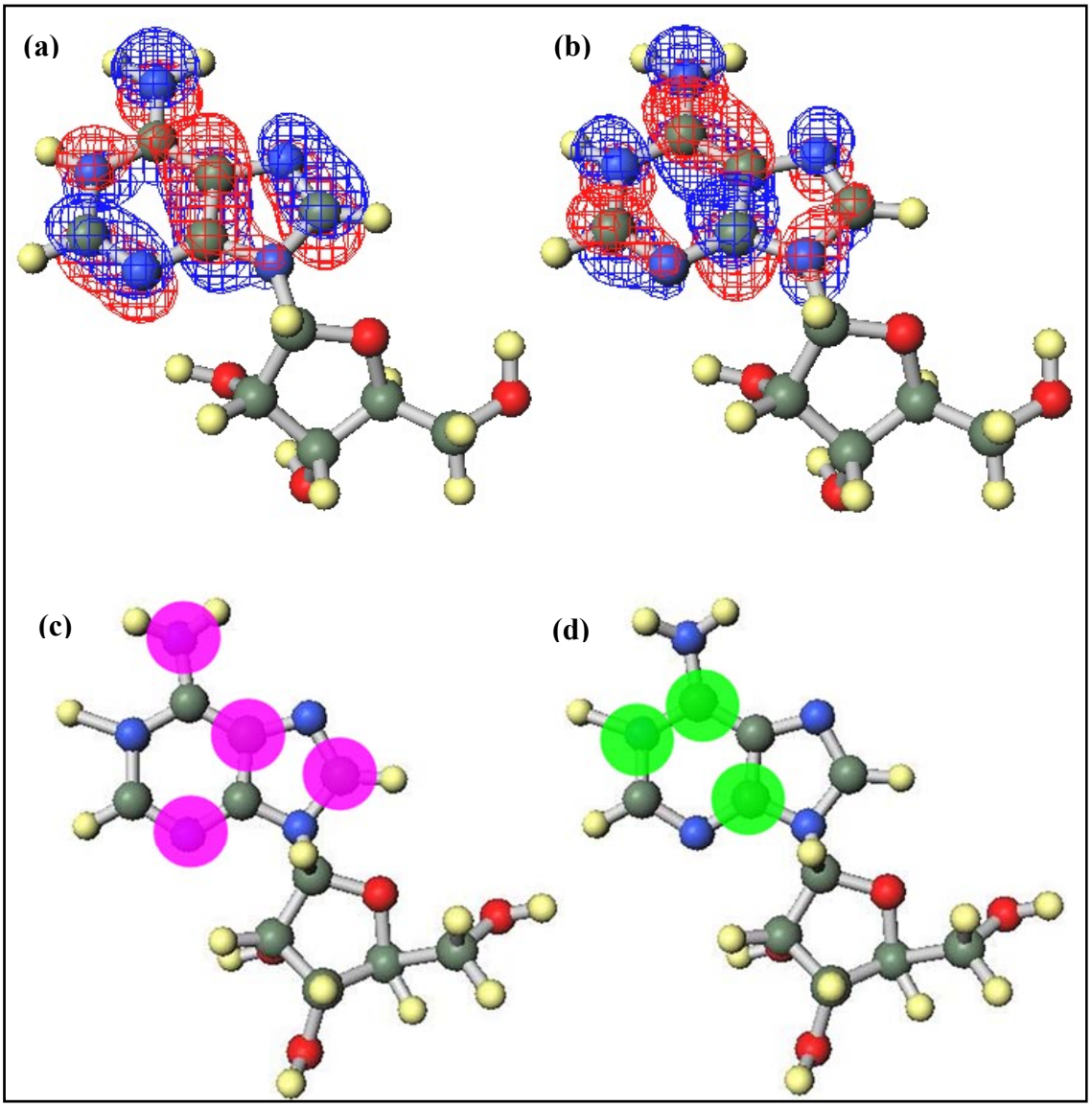

Figure 6.8. (a) HOMO spatial distributions, (b) LUMO spatial distributions, (c) f- isosurfaces of Fukui functions and (d) f+ isosurfaces of Fukui functions for protonated adenosine.

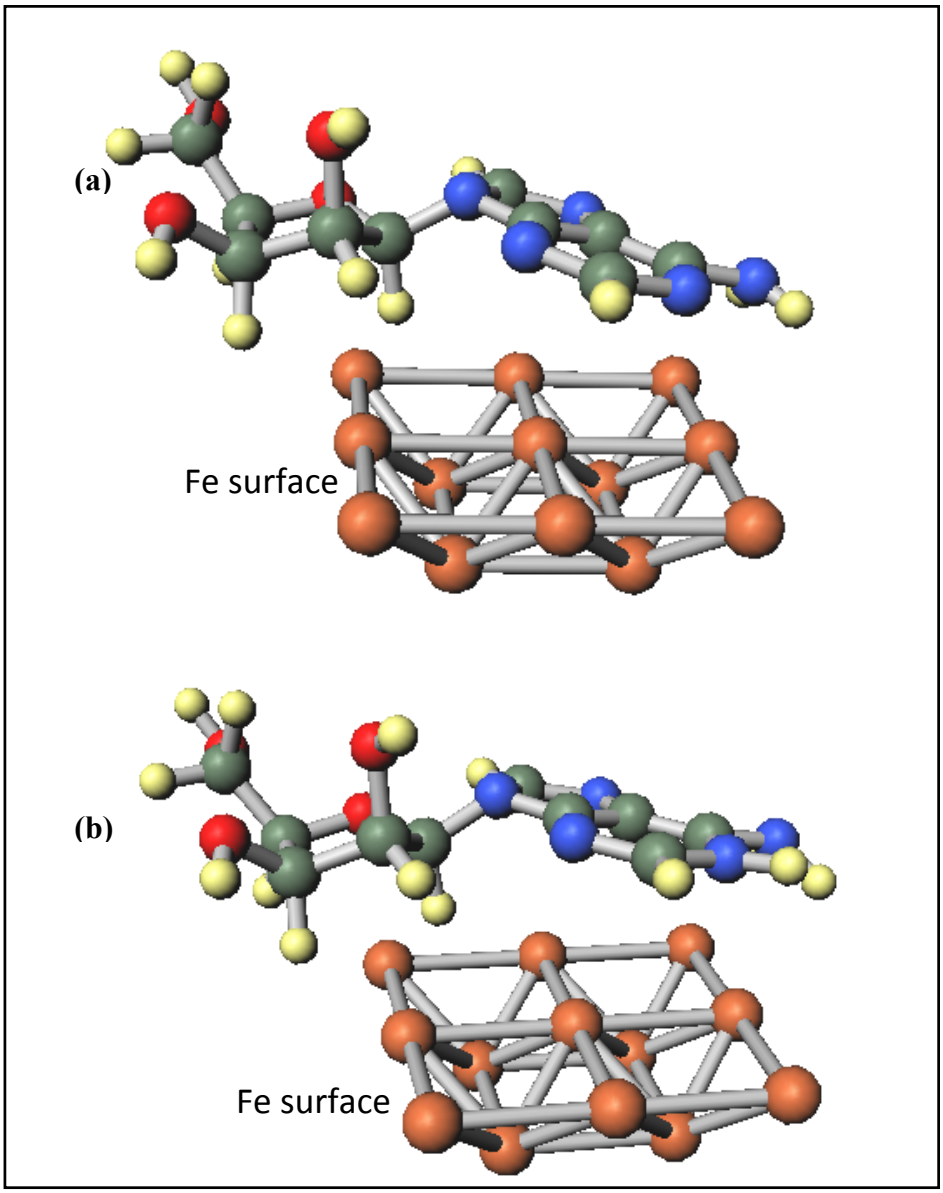

Figure 6.9. Optimized orientation of a) neutral adenosine, b) protonated adenosine when adsorbed onto the surface of the mild steel (distance of adenosine from Fe surface was set at 4 Å)

6.4. Conclusions

- From the surface morphology analysis, the surface of the mild steel immersed in 1 mol dm^{-3} HCl with inhibitors (adenosine or leaf extract) showed a smoother surface than the mild steel immersed in 1 mol dm^{-3} HCl only. This was observed at every 12 hours interval up to 48 hours.
- The average surface roughness data was in agreement with the visual observation of the surface morphology.
- The real-time mass change of a corroding surface of iron in 1 mmol dm^{-3} HCl when adenosine was introduced into the system was successfully observed with the QCM.
- For the QCM technique, in an OCP corroding system freshly introduced with adenosine, the adsorption process of adenosine molecules/complex could happen along with the iron dissolution process.
- From the EQCM technique, adenosine molecules/complex could desorb from the surface of iron when electrically polarized from the anodic region and adenosine could re-adsorb onto the surface when polarized towards the cathodic region.
- From the quantum chemical studies, the HOMO-LUMO energy gap suggested that the non-protonated adenosine is the better structure for adsorption by chemisorption.
- The protonated and non-protonated adenosine are likely to approach the surface of the metal by the aromatic rings and N atoms with the aliphatic ring/chain away from the surface of the metal.

References

[1] H. L. Y. Sin, M. Umeda, S. Shironita, A. A. Rahim, B. Saad, Research on Chemical Intermediates, Accepted (2016).

[2] P. Thanapackiam, S. Rameshkumar, S. S. Subramanian, K. Mallaiya, Materials Chemistry and Physics, 174 (2016) 129-137.

[3] K. Marcisz, M. Karbarz, Z. Stojek, Journal of Solid State Electrochemistry, (2016) 1-8.

[4] K. Kubiak, Z. Adamczyk, M. Cieśla, Colloids and Surfaces B: Biointerfaces, 139 (2016) 123-131.

[5] G. Fan, J. Liu, Y. Cao, L. Feng, H. Xu, Physicochemical Problems of Mineral Processing, 52 (2016) 597-608.

[6] J. Kou, S. Xu, Colloids and Surfaces A: Physicochemical and Engineering Aspects, 490 (2016) 110-120.

[7] L. Wang, I. Siretanu, M. H. G. Duits, M. A. C. Stuart, F. Mugele, Colloids and Surfaces A: Physicochemical and Engineering Aspects, 494 (2016) 30-38.

[8] A. Shaban, G. Vastag, A. Pilbáth, I. Kék, L. Nyikos, Journal of Materials and Environmental Science, 7 (2016) 2572-2582.

[9] R. J. Wilbraham, C. Boxall, Electrochemistry Communications, 62 (2016) 52-55.

[10] D. Seifzadeh, V. Valizadeh-Pashabeigh, A. Bezaatpour, Chemical Engineering Communications, (2016).

[11] N. Soltani, H. Salavati, N. Rasouli, M. Paziresh, A. Moghadasi, Chemical Engineering Communications, 203 (2016) 840-854.

[12] R. Mehdaoui, A. Khelifa, A. Khadraoui, O. Aaboubi, A. H. Ziane, F. Bentiss, A. Zarrouk, Research on Chemical Intermediates, 42 (2016) 5509-5526.

[13] R. Y. Khaled, A. Abdel-Gaber, H. Holail, International Journal of Electrochemical Science, 11 (2016) 2790-2798.

[14] M. Shabani-Nooshabadi, M.-S. Ghandchi, Metallurgical and Materials Transactions A, 46 (2015) 5139-5148.

[15] D. J. G. Ives, G. J. Janz, Reference Electrode Theory and Practice, Academic Press, New York and London, 1961.

[16] P. Kern, D. Landolt, Journal of the Electrochemical Society, 148 (2001) B228-B235.

[17] F. Bentiss, M. Lagrenee, M. Traisnel, J. C. Hornez, Corrosion Science, 41 (1999) 789-803.

[18] E. E. Oguzie, Y. Li, F. H. Wang, Journal of Colloid and Interface Science, 310 (2007) 90-98.

[19] C. O. Akalezi, E. E. Oguzie, C. E. Ogukwe, E. A. EJele, International Journal of Industrial Chemistry, 6 (2015) 273-284.

[20] N. A. Odewunmi, S. A. Umoren, Z. M. Gasem, S. A. Ganiyu, Q. Muhammad, Journal of the Taiwan Institute of Chemical Engineers, 51 (2015) 177-185.

[21] M. H. Hussin, M. J. Kassim, Materials Chemistry and Physics, 125 (2011) 461-468.

[22] A. Davenport, Corrosion (General), Electrochemical Society, 2008.

[23] J. J. R. Stålgren, J. Eriksson, K. Boschkova, Journal of Colloid and Interface Science, 253 (2002) 190-195.

[24] L. E. Kapinos, B. P. Operschall, E. Larsen, H. Siegel, Chemistry-A Europena Journal, 17 (2011) 8156-8164.

[25] F. Zhang, Y. Tang, Z. Cao, W. Jing, Z. Wu, Y Chen, Corrosion Science, 61, (2012) 1-9.

[26] S. Zor, M. Saracoglu, F. Kandemirli, T. Arslan, Corrosion, 67, (2011) 125003-1-125003-11.

[27] C. Zuriaga-Monroy, R. Oviedo-Roa, L. E. Montiel-Sánchez, A. Vega-Paz, J. Marín-Cruz, J.-M. Martínez-Magadán, Industrial and Engineering Chemistry Research, 55, (2016) 3506-3516.

[28] R. Parthasarathi, V. Subramanian, P. Chattaraj, Chemical Physics Letters, 382, (2003) 48-56.

7. GENERAL CONCLUSIONS

The leaf extract of *Aquilaria malaccensis* was shown to be a successful corrosion inhibitor for mild steel in 1 mol dm^{-3} HCl and the subsequently identified compound of adenosine from the leaf extract was also shown to be a successful corrosion inhibitor for mild steel in 1 mol dm^{-3} HCl. Both the leaf extract and adenosine showed good corrosion inhibition activity from several anti-corrosion assessments and the mechanism of corrosion inhibition was proposed.

Chapter 3. Anti-corrosion behaviour of *Aquilaria malaccensis* leaves extract on mild steel in 1 mol dm^{-3} HCl

- The *Aquilaria malaccensis* leaf extract successfully inhibited the corrosion of mild steel in 1 mol dm^{-3} HCl up to 94.49 % at the concentration of 1500 ppm.
- The leaf extract acted as a mixed-type, but predominantly cathodic inhibitor based on the potentiodynamic polarization measurement.
- The leaf extract best fits the Langmuir adsorption isotherm and was adsorbed by a mixed-type, but predominantly physisorption process based on the Gibbs free energy calculation.

Chapter 4. *Aquilaria malaccensis* leaves extracts content analysis

- The leaf extract contained several functional groups that can contribute to the adsorption property of the compounds in the leaf extract.

- Several compounds were tentatively identified and from those, five were successfully identified. From the successfully identified compounds, adenosine was the best inhibitor for mild steel in 1 mol dm^{-3} HCl solution.

Chapter 5. Anti-corrosion behaviour of adenosine on mild steel in 1 mol dm^{-3} HCl

- Adenosine has successfully inhibited the corrosion of mild steel in 1 mol dm^{-3} HCl and increasing the concentration of adenosine increased the IE up to 78.88 % at the concentration of 1 mmol dm^{-3}.
- Adenosine was more efficient as a corrosion inhibitor in the stagnant condition rather than the hydrodynamic condition.
- Adenosine acted as a mixed-type inhibitor (acting both as an anodic and cathodic inhibitor) but predominantly as an anodic inhibitor according to the potentiodynamic polarization measurement.
- Adenosine adsorbed onto the surface of the mild steel in 1 mol dm^{-3} HCl by the mixed-type process (by both the physisorption and chemisorption process) according to the calculated Gibbs free energy.

Chapter 6. Surface morphology of corrosion of mild steel, EQCM study and quantum chemical calculation

- From the surface morphology analysis, the surface of the mild steel immersed in 1 mol dm^{-3} HCl with inhibitors (adenosine or leaf extract) showed a smoother surface than the mild steel immersed in 1 mol dm^{-3} HCl only. This was observed at every 12 hours interval up to 48 hours.

- The average surface roughness data was in agreement with the visual observation of the surface morphology.
- The real-time mass change of a corroding surface of iron in 1 mmol dm^{-3} HCl when adenosine was introduced into the system was successfully observed with the QCM.
- For the QCM technique, in an OCP corroding system freshly introduced with adenosine, the adsorption process of adenosine molecules/complex could happen along with the iron dissolution process.
- From the EQCM technique, adenosine molecules/complex could desorb from the surface of iron when electrically polarized from the anodic region and adenosine could re-adsorb onto the surface when polarized towards the cathodic region.
- From the quantum chemical studies, the HOMO-LUMO energy gap suggested that the non-protonated adenosine is the better structure for adsorption by chemisorption.
- The protonated and non-protonated adenosine are likely to approach the surface of the metal by the aromatic rings and N atoms with the aliphatic/chain ring away from the surface of the metal.

LIST OF PUBLICATIONS

1. Helen Lee Yun Sin, Minoru Umeda, Sayoko Shironita, Afidah Abdul Rahim, Bahruddin Saad, *Aquilaria malaccensis* as a green Corrosion Inhibitor for Mild steel in HCl Solution, International Journal of Electrochemical Science, 11, 7562-7575 (2016)

2. Helen Lee Yun Sin, Minoru Umeda, Sayoko Shironita, Afidah Abdul Rahim, Bahruddin Saad, Adenosine as a green corrosion inhibitor for mild steel in hydrochloric acid solution, Research on Chemical Intermediates, DOI 10.1007/s11164-016-2739-9

3. Helen Lee Yun Sin, Minoru Umeda, Sayoko Shironita, Afidah Abdul Rahim, Bahruddin Saad, Quartz crystal microbalance study of adenosine as inhibitor for corrosion in HCl solution, Electrochemistry, 84, 959-962 (2016)

Reference publication

Helen Lee Yun Sin, Afidah Abdul Rahim, Bahruddin Saad, Muhammad Idris Salleh, Pandian Bothi Raja, International Journal of Electrochemical Science, 9, 830-846 (2014)